Fate and Transformation Model of 17α-Ethinylestradiol in

Activated Sludge Treatment Processes

Mariko J. Lust

A dissertation

submitted in partial fulfillment of the

requirements for the degree of

Doctor of Philosophy

University of Washington

2014

Reading Committee:

H. David Stensel, Chair

Stuart Strand

Heidi Gough

Program Authorized to Offer Degree:

Civil and Environmental Engineering

University of Washington

Abstract

Fate and Transformation Model of 17α-Ethinylestradiol

in Activated Sludge Treatment Processes

Mariko J. Lust

Chair of the Supervisory Committee:
Professor H. David Stensel
Civil and Environmental Engineering

The discharge of the synthetic estrogen, 17α-ethinylestradiol (EE2), in wastewater treatment

plant (WWTP) effluents is an environmental concern as this compound can alter the reproductive

system of aquatic wildlife at low ng/L concentrations. The impact of EE2 at such low

concentrations indicates the need to identify activated sludge (AS) process designs that minimize

WWTP effluent EE2 concentrations. An EE2 fate and transformation model was developed

based on the following mechanisms: (1) EE2 production from deconjugation of EE2-3-sulfate

(EE2-3S), a conjugated form excreted from humans, (2) EE2 removal from biodegradation by

heterotrophic biomass growing on other substrates, and (3) EE2 removal from sorption to

activated sludge. These mechanisms were incorporated into the International Water Association

(IWA) Activated Sludge Model No. 2d (ASM2d) to model the fate of EE2 across aerobic and

biological nutrient removal (BNR) AS systems. The model was successfully calibrated and evaluated using lab-scale aerobic and BNR AS sequencing batch reactors (SBRs) fed primary effluent. A sensitivity analysis predicted effluent EE2 concentrations were most sensitive to the biodegradation rate coefficient, the feed biodegradable chemical oxygen demand (bCOD) to EE2 ratio, and the aerobic SRT and were less sensitive to the deconjugation rate coefficient and the solid-liquid partitioning coefficient.

EE2 biodegradation kinetics were further investigated using lab-scale SBRs at 20°C fed synthetic wastewater. Three sets of reactor experiments were conducted using different municipal AS plant seed sources and with solids retention times (SRTs) ranging from 8 to 13 days. Significant EE2 biodegradation occurred only under aerobic conditions. Pseudo first-order biodegradation rate coefficients (k_b) normalized to the reactor volatile suspended solids (VSS) concentration ranged from 4 to 22 L/g VSS-d, 4 to 19 L/g VSS-d, and 3 to 20 L/g VSS-d for aerobic, anaerobic/aerobic, and anoxic/aerobic AS processes, respectively. Enriched denitrifying communities selected by anoxic-only operation did not degrade EE2 under anoxic or aerobic conditions. The variation in EE2 k_b values suggests there is a high degree of uncertainty in this value when predicting process performance.

Experiments were conducted with an EE2-degrading isolate, *Rhodococcus equi*, to examine its biodegradation kinetics, EE2 degradation inhibition, and application of a transposon mutagenesis technique to identify genes involved in EE2 degradation. *R. equi* degraded EE2 during exponential growth on glucose with a relatively low k_b of 3.4 L/g VSS-d at 27°C, and did not degrade EE2 during the stationary growth phase. Clotrimazole inhibited EE2 degradation,

suggesting a cytochrome p450 mono-oxygenase may be involved in EE2 degradation. Transposome mutagenesis coupled with a yeast estrogen screen (YES) assay to screen mutants was successfully applied to isolate an *R. equi* mutant with lost EE2-degrading ability. This technique and/or mutant may be useful for future research aimed at elucidating the EE2 degradation pathway(s).

Table of Contents

List of Figures

v

List of Tables

List of Abbreviations

ACN	acetonitrile
AOB	ammonia oxidizing bacteria
APCI	atmospheric pressure chemical ionization
AS	activated sludge
ASM	activated sludge model
ATCC	American Type Culture Collection
ATP	adenosine triphosphate
ATU	allylthiourea
bCOD	biodegradable chemical oxygen demand
BNR	biological nutrient removal
BOD	biochemical oxygen demand
CAS	conventional activated sludge
COD	chemical oxygen demand
CSTR	completely stirred tank reactor
CYP	cytochrome P450 mono-oxygenase
DNA	deoxyribonucleic acid
E1	estrone
E1-3G	estrone-3-glucuronide
E1-3S	estrone-3-sulfate
E2	17β-estradiol
E2-3G	17β-estradiol-3-glucuronide
E2-3S	17β-estradiol-3-sulfate
EE2	17α-ethinylestradiol
EE2-3G	17α-ethinylestradiol-3-glucuronide
EE2-3S	17α-ethinylestradiol-3-sulfate
EBPR	enhanced biological phosphorus removal
EDC	endocrine disrupting compound
ESI	electrospray ionization
HRT	hydraulic retention time
IWA	International Water Association
LB	Luria Bertani
LC	liquid chromatography
LOD	limit of detection
LOQ	limit of quantification
MAR-FISH	microautoradiography-fluorescence in situ hybridization
MBR	membrane bioreactor
MDL	method detection limit
MeOH	methanol
MLSS	mixed liquor suspended solids
MLVSS	mixed liquor volatile suspended solids
MS/MS	tandem mass spectrometry
ND	non-detect
OD	optical density

PAO	polyphosphate accumulating organism
PCR	polymerase chain reaction
PHA	polyhydroxy-alkanoates
PP	polyphosphate
RAS	return activated sludge
rRNA	ribosomal ribonucleic acid
sbCOD	soluble biodegradable chemical oxygen demand
SBR	sequencing batch reactor
sCOD	soluble chemical oxygen demand
SPE	solid phase extraction
SRT	solids retention time
TKN	total Kjeldahl nitrogen
TRFLP	terminal restriction fragment length polymorphism
TSS	total suspended solids
VFA	volatile fatty acid
VSS	volatile suspended solids
WWTP	wastewater treatment plant
YES	yeast estrogen screen

Acknowledgements

Chapter 1: Introduction

The discharge of estrogens in wastewater treatment plant (WWTP) effluents is an environmental concern as these compounds can alter the reproductive systems of aquatic wildlife at low ng/L concentrations. Of particular concern is the synthetic estrogen used in oral contraceptives, 17α-ethinylestradiol (EE2), as this compound is the most potent and the hardest to degrade relative to the natural estrogens. Identification of activated sludge (AS) designs that minimize effluent EE2 concentrations is therefore important. EE2 is removed during AS treatment primarily from biodegradation but also from sorption to wasted solids. Also of consideration is the production of EE2 from conjugated EE2, as estrogens are primarily excreted from the body in a conjugated form with either a glucuronide or sulfate moiety. Conjugated estrogens can be hydrolyzed by microbial activity in sewers and WWTPs, producing the biologically active free estrogen. Currently, varied EE2 removal efficiencies across WWTPs result in its discharge into the environment at levels that can impact downstream aquatic wildlife.

An EE2 fate and transformation model provides a platform for assessing estrogen production and removal mechanisms and ultimately could serve as a tool for designing AS systems with high EE2 removal performance. As EE2 removals are due to biodegradation by heterotrophic biomass and sorption to solids, heterotrophic biomass and solids productions should be modeled based on site specific operating conditions, process configuration, and wastewater characteristics. Knowledge of biodegradation and deconjugation kinetics and how these kinetics are affected by operating conditions is also needed for such a model to be useful. In addition, the impact of redox conditions on these kinetics should be included as a growing number of WWTPs

are incorporating anoxic and anaerobic zones in AS treatment for biological nutrient removal (BNR).

A model was developed as part of this research for predicting the fate and transformation of EE2 across activated sludge systems. The model includes: (1) EE2 production from deconjugation of its conjugated form, (2) EE2 biodegradation by heterotrophic bacteria, and (3) sorption of EE2 to activated sludge. Heterotrophic biomass and solids production were modeled using the International Water Association (IWA) Activated Sludge Model No. 2 (ASM2d). Chapter 3, "Extension of ASM2d to Model the Fate of 17α-Ethinylestradiol in Activated Sludge Systems," describes the development and application of this model. Predicted effluent EE2 concentrations were most sensitive to the EE2 biodegradation rate coefficient, but limited studies have measured this kinetic parameter in activated sludge. EE2 biodegradation kinetics in aerobic and BNR AS processes are investigated in Chapter 4, "Biodegradation kinetics of 17α-Ethinylestradiol in Activated Sludge Treatment Processes." EE2 biodegradation by denitrifying bacteria is further explored in Chapter 5, "Estrogen Degradation by Enriched Denitrifying Communities."

A current limitation in modeling EE2 biodegradation is predicting how operational conditions affect the biodegradation kinetics of activated sludge either by promoting growth of EE2-degrading biomass and/or altering their biodegradation kinetics. Identification of microbial genes involved in EE2-degradation could provide useful probes for monitoring the growth of EE2-degrading biomass in activated sludge and their expression of EE2-degrading genes. In an effort to identify genes involved in EE2 degradation, transposome mutagenesis was performed in an EE2-degrading culture of *Rhodococcus equi* and a mutant with hindered EE2-degrading

2

ability was identified using the yeast estrogen screen (YES) assay. Chapter 6 describes the isolation of this mutant as well as experimental results investigating the kinetics and inhibition of EE2 biodegradation by *R. equi*.

Chapter 2 is a literature review of research relevant to free estrogen production and removal mechanisms during activated sludge treatment and existing estrogen models. Chapter 7 summarizes conclusions from the presented research and identifies future research needs. Appendix I, "A Mechanistic Model for Fate and Removal of Estrogens in Biological Nutrient Removal Activated Sludge Systems," is a published paper describing an estrogen fate and transformation model integrated with the IWA ASM No. 1. Appendix II provides the mathematical derivation of an equation for modeling estrogen biodegradation by biomass during exponential growth.

Chapter 2: Literature Review

The following provides background information that supports the need for the research presented here and a summary of prior work on estrogen transformation and removal in wastewater treatment. Topics discussed are: (1) environmental impacts of estrogens discharged in wastewater treatment plant (WWTP) effluents, (2) forms and occurrence of estrogens in WWTPs, (3) estrogen production from deconjugation, (4) estrogen removal by biodegradation and partitioning to activated sludge (AS), and (5) estrogen fate and transformation models.

2.1 Significance of Estrogens Discharged in WWTP Effluents

WWTPs receive a broad spectrum of chemicals of both domestic and industrial origin, some of which can act as hormone receptor agonists or antagonists disrupting normal endocrine system activity in animals (Mills and Chichester, 2005; Ternes et al., 2004). WWTP effluents are therefore point sources of endocrine disrupting compounds (EDCs) discharged into the environment. Of particular concern are EDCs impacting the reproductive systems of aquatic wildlife. Field studies on native fish populations have documented a consistent increase in feminized male fish collected downstream of WWTP outfalls compared to reference sites (Bjerregaard et al., 2006; Bjorkblom et al., 2013; Hashimoto et al., 2000; Jobling et al., 2006; Tetreault et al., 2011; Vajda et al., 2008; Woodling et al., 2006; Xie et al., 2010). For example, Vajda et al. (2008) reported about 20 percent of the white suckers collected downstream of the Boulder, Colorado WWTP outfall were intersex, with oocytes present in their testicular tissue, while no intersex fish were observed upstream of the discharge point. These field studies

4

indicate estrogenic compounds discharged in WWTP effluents are likely inducing abnormal morphological changes in aquatic wildlife.

Reproductive consequences in the environment from exposure to estrogenic compounds are unclear, but studies on wild roach have shown an association between the severity of fish feminization, indicated by the number of oocytes present in the testes, and a reduction in the production of offspring. Jobling et al. (2002) observed a reduction in sperm production, motility and fertilization success in wild intersex roach, which correlated to the degree of feminization. Competitive breeding experiments using DNA microsatellites to track offspring showed reproductive performance was reduced up to 76 percent for severely intersex roach (Harris et al., 2011) and could be completely hindered for sex-reversed males (Lange et al., 2011). These studies highlight the potential for reproductive consequences or reduction in genetic diversity in waterways receiving large inputs of estrogenic compounds.

The natural estrogens, estrone (E1) and 17β-estradiol (E2), and the synthetic estrogen, 17α-ethinylestradiol (EE2), are major contributors to the estrogenic activity of WWTP effluents (Korner et al., 2001; Miege et al., 2009; Nakada et al., 2004; Snyder et al., 2001; Vega-Morales et al., 2013). Estrogenic activity is commonly determined using bioassays that measure estrogen receptor controlled expression of reporter genes (such as luciferase or β-galactosidase), proliferation of cancel cells, or induction of vitellogenin, a precursor protein of egg yolk. The estrogenic activity of E2 and EE2 is four to six orders of magnitude greater than xenoestrogens, such as bisphenol-A, alkylphenols, and alkylphenol-ethoxylates (Campbell et al., 2006; Gutendorf and Westendorf, 2001; Murk et al., 2002; Van den Belt et al., 2004). Numerous

laboratory studies have shown estrogenic effects on fish occur at E1, E2 and EE2 concentrations in the ng/L range including reduced egg production, reduced testicular growth, delayed maturation, development of ova-testes in males, and development of populations with skewed female to male ratios (Mills and Chichester, 2005). Predicted no-effect concentrations of E1, E2, and EE2 in surface waters are 6, 2, and 0.1 ng/L, respectively (Caldwell et al., 2012).

2.2 Forms and Occurrence of Estrogens in WWTPs

Prior to elimination from humans, estrogens are generally conjugated with either a glucuronide or sulfate moiety making the estrogen more water soluble and therefore easier to excrete. Chemical structures of E1, E2, EE2, and conjugated EE2 are shown in Figure 2-1. Conjugation often occurs at the hydroxyl group located on the aromatic ring (carbon 3 based on the steroid numbering convention) favoring the formation of the glucuronide conjugates estrone-3-glucuronide (E1-3G), 17β-estradiol-3-glucuronide (E2-3G), and 17α-ethinylestradiol-3-glucuronide (EE2-3G) and the sulfate conjugates estrone-3-sulfate (E1-3S), 17β-estradiol-3-sulfate (E2-3S), and 17α-ethinylestradiol-3-sulfate (EE2-3S) (Gomes et al., 2005). Conjugated estrogens are biologically inactive and can be converted to the biologically active free estrogen by enzymatic hydrolysis of the conjugated moiety. Estrogens excreted with urine are predominantly in the form of estrogen glucuronides (Johnson and Williams, 2004). Conjugated estrogens in the bile, however, may undergo deconjugation prior to excretion as evidenced by the significant fraction of free estrogens in feces (Adlercreutz and Jarvenpaa, 1982).

estrone (E1) 17β-estradiol (E2) 17α-ethinylestradiol (EE2)

17α-ethinylestradiol-3-glucuronide (EE2-3G) 17α-ethinylestradiol-3-sulfate (EE2-3S)
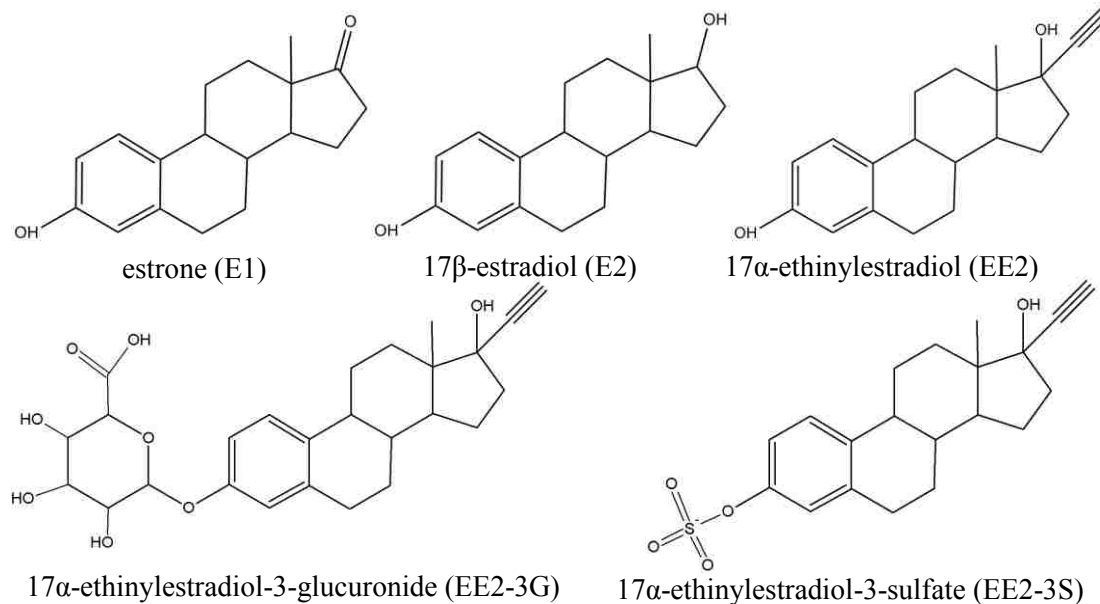
Figure 2-1. Chemical structures of free estrogens E1, E2, and EE2 and conjugated estrogens EE2-3G and EE2-3S

Occurrence of free and conjugated estrogens in WWTPs

Free estrogens are measured at ng/L concentrations with varied removal efficiencies reported among WWTPs. A summary of free estrogen concentrations measured in WWTP influents and effluents is provided in Table 2-1. In addition, free estrogen removal efficiencies based on composite samples or frequent sampling events over the course of the day are also shown. Influent concentrations range from non-detect (ND) to 670 ng/L for E1, 162 ng/L for E2, and 330 ng/L for EE2 with removals ranging from -55 to 99 percent for E1, 18 to 99 percent for E2, and 34 to 98 percent for EE2. Production of E1 during wastewater treatment, as indicated by negative removals, can be from oxidation of E2 to E1 and/or deconjugation of conjugated E1 (Servos et al., 2005). EE2 removals could not be quantified for two WWTPs as similar influent and effluent EE2 concentrations were measured (Johnson et al., 2000; Ternes et al., 1999b), but these studies indicate extremely low EE2 removals are occurring at some WWTPs.

Table 2-1. Reported free estrogen influent and effluent concentrations (ng/L) and removals (percent) at WWTPs

Reference	Location	E1 Influent	E1 Effluent	E1 Removal	E2 Influent	E2 Effluent	E2 Removal	EE2 Influent	EE2 Effluent	EE2 Removal
Atkinson et al. (2012)	Canada	13.1 - 104	11.2 - 370		ND - 66.9	ND - 26.7		ND - 5.7	ND - 9.8	
Cicek et al. (2007)	Canada	72.3	4.9	93	26.5	4.4	83	30.4	7.6	75
Servos et al. (2005)	Canada	19 - 78	1 - 96	-55 - 98	2.4 - 26	0.2 - 14.7	40 - 99			
Chimchirian et al. (2007)	USA	57.8 - 83.3	6.3 - 49.1		ND - 161.6	ND - 5.4		ND - 1.2	ND - 0.6	
Drewes et al. (2005)	USA	26.3 - 80.3	<0.6 - 50.4		7 - 24.5	<0.6 - 6		<0.7 - 14.4	<0.7 - 4.1	
Gunatilake et al. (2013)	USA	ND - 178.7	ND - 5.2		ND - 76.7	ND - 6.2		ND - 4.7	ND	
Reddy et al. (2005)	USA	24.2	0.7		7.6	0.2				
Clara et al. (2005)	Austria	29 - 670	ND - 72		14 - 125	ND - 30		3 - 70	ND - 5	
Pauwels et al. (2008)	Belgium	10.1 - 25.6						4.2 - 86.3		
Gomes et al. (2005)	England	21			43			ND		
Koh et al. (2007)	England	15	3		5	0.7		1.2	1	
Koh et al. (2009)	England	54 - 71	1.9 - 9	89 - 91	9 - 20	ND - 2.2	94 - 96	2	ND - 1.3	60 – 68
Kumar et al. (2011)	England	51			43			2		
Johnson et al. (2000)	Europe	ND -140	ND - 54	10 - >98	ND - 48	ND - 12	18 - 99	ND - 10	ND - 4.5	ND - >98
Cargouet et al. (2004)	France	9.6 - 17.6	4.3 - 7.2	44 - 59[a]	11.1 - 17.4	4.5 - 8.6	43 - 60[a]	4.9 - 7.1	2.7 - 4.5	34 - 45[a]
Andersen et al. (2003)	Germany	54.9 - 76.6	<1		12.2 - 19.5	<1		6.2 - 10.1	<1	
Schlusener and Bester (2008)	Germany	53 - 130	2 - 91	-72[b] - 92	9 - 68	4 - 19	-53[b] - 75			
Ternes et al. (1999b)	Germany, Brazil	27 - 45	6.8 - 25	10 - 83	15 - 21	<0.4 - 5.4	64 - 99	2.4 - 4.2	0.9 - 2.4	ND – 78
Can et al. (2014)	Istanbul	7 - 34	1.5 - 27		8 - 34	2.2 - 8		34 - 68	2.2 - 17	
Baronti et al. (2000)	Italy	25 - 132	2.5 - 82.1	61	4 - 22	0.4 - 3.5	87	0.4 - 13	ND - 1.7	85
D'Ascenzo et al. (2003)	Italy	44	17		11	1.6				
Gentili et al. (2002)	Italy	100	5		2	ND		20	5	
Vethaak et al. (2005)	Netherlands	20 - 130	<0.3 - 11		17 - 150	<0.8		<0.3 - 5.9	<0.3 - 2.6	
Joss et al. (2004)	Switzerland	7.3 - 75	0.5 - 8.6	49 - ≥99	4.9 - 11	<0.5 - 1	88 - ≥98	0.7 - 5.2	≤0.5	69 – 94
Nie et al. (2012)	China	51.7	12.7		7.7	ND		77.7	ND	
Ye et al. (2012)	China	42.2 - 110.7	3.8 - 30.4		7.4 - 32.7	ND - 1.9		8.6 - 44.6	ND	
Zhang et al. (2011)	China	10.2 - 34.9	8.3 - 14	50	46.6 - 93	8.7 - 32.4	69	ND - 11.5	ND	-
Zhou et al. (2012)	China	11.6 - 110	ND - 140		3.7 - 140	ND - 8.4		ND - 330	ND - 5.8	
Komori et al. (2004)	Japan	10 - 57	ND - 180		ND - 21	ND - 11				
Kumar et al. (2009b)	Japan	22.6	36.4		77.2	4.3		ND		
Liu et al. (2011)	Japan	32.7	31.7		13	ND				

a. Based on average of 6 grab samples

b. WWTP had anomalous E1, E2, E1-3S, and E2-3S removals of -72, -53, -360, and -74 percent, respectively

8

Influent E1-3S and E2-3S concentrations are often of similar magnitude as free estrogens, while influent E1-3G and E2-3G concentrations are generally lower. Reported conjugated estrogen concentrations in WWTP influents and effluents are summarized in Table 2-2. Given that estrogens are primarily excreted as glucuronide conjugates, the low concentrations of estrogen glucuronides arriving at WWTPs indicate that deconjugation occurs during sewer conveyance. Results of Komori et al. (2004) showed significantly higher influent concentrations of conjugated estrogens compared to the other studies. These higher concentrations may be a result of low deconjugation activity during conveyance, short conveyance retention times, or analytical inaccuracies associated with low reported method recoveries of these compounds (9 to 15 percent) in their study.

Concentrations of EE2-3G and EE2-3S in WWTP influents have not been widely reported. One study sampled the influent of two WWTPs in the United Kingdom for EE2, EE2-3G, and EE2-3S, and all of these compounds were below their detection limits of 1.8, 5.7, and 3.5 ng/L, respectively (Gomes et al., 2005). Adler et al. (2001) reported a median EE2 concentration of 7 ng/L in German WWTP influents. Following treatment with glucuronidase and arylsulfatase, the median EE2 concentration was 9.5 ng/L, indicating conjugated forms of EE2 comprised about 26 percent of the EE2 loading.

Table 2-2. Reported conjugated estrogen concentrations (ng/L) in WWTP influents and effluents

Reference	Location	E1-3S		E2-3S		E1-3G		E2-3G	
		Influent	*Effluent*	*Influent*	*Effluent*	*Influent*	*Effluent*	*Influent*	*Effluent*
Reddy et al. (2005)	USA	34.1	0.3	3.2	ND	0.4	ND	0.3	ND
Gomes et al. (2005)	England	12				ND			
Koh et al. (2007)	England	10	12						
Koh et al. (2009)	England	7 - 19	0.8 – 7.7						
Kumar et al. (2009a)	England	1.5 - 1.9	ND - 0.4	61.5 - 97.4	ND - 1.3	<0.6	ND	<0.6	ND
Kumar et al. (2011)	England	24	6	16	4	5	ND	4	ND
Schlusener and Bester (2008)	Germany	4 - 26	2 - 47	ND - 79	5 - 141				
D'Ascenzo et al. (2003)	Italy	25	9	3.3	ND	4.3	0.7	5.2	ND
Gentili et al. (2002)	Italy	8	3			6	3		
Komori et al. (2004)[a]	Japan	12 - 170	7.5 - 34	26 - 410	27 - 94	ND - 88	31 - 140	5.3 - 100	47 - 210
Kumar et al. (2009b)	Japan	18	11.8	3.6	0.4	ND	ND	8.1	ND
Liu et al. (2011)	Japan	7.7	0.7	ND	ND	ND	ND	ND	ND

a. Reported method recoveries were low at 9 to 15 percent for influent and 22 to 51 percent for effluent

10

Conjugated estrogen removals across AS systems are useful for understanding the magnitude of free estrogen production. The fate of conjugated EE2 across WWTPs is unknown. E1-3S removals based on composite sampling ranged from 53 to 91 percent across five WWTPs (Koh et al., 2009; Liu et al., 2011; Schluesener and Bester, 2008); E2-3S removals of 13 and 41 percent were calculated for two of these WWTPs with E2-3S either not being detected or measured at the other three plants. Glucuronide conjugates were either not detected or not measured. Anomalous removals of -72 percent for E1, -53 percent for E2, -360 percent for E1-3S and -74 percent for E2-3S were reported across one WWTP (Schluesener and Bester, 2008) and were therefore not included in the above ranges. Based on the magnitude of sulfated estrogens entering WWTPs and their observed removals, deconjugation of sulfated estrogens may be a source of free estrogens during wastewater treatment.

2.3 Estrogen Production by Deconjugation

Increases in natural estrogens have been measured during wastewater treatment (Andersen et al., 2003; Atkinson et al., 2012; Fernandez et al., 2008; Nie et al., 2012; Servos et al., 2005; Ternes et al., 1999b), suggesting estrogen production is occurring. Estrogen production can occur when deconjugation releases free estrogens and should be considered when modeling the fate and transformation of estrogens during AS treatment.

11

Microbial deconjugation of conjugated estrogens

While the enzyme β-glucuronidase originating from *Escherichia coli* can hydrolyze steroid glucuronides (Shackleton, 1986) and its activity has been measured in AS (Ternes et al., 1999a), the prevalence of arylsulfatase activity in raw sewage and AS is less certain. Arylsulfatase activity is commonly measured in soils where it is involved in sulfate ester hydrolysis for sulfur assimilation (Knauff et al., 2003). Although arylsulfatase activity has been measured in multiple genera, including *Pseudomonas, Klebsiella, Enterobacter, Salmonella*, *Proteus, Streptomyces, Microbacterium*, and *Rhodococcus* (Beil et al., 1995; Cregut et al., 2013; Murooka et al., 1990; Yamada et al., 1978), the identity of microbial populations actively deconjugating sulfated estrogens in AS are unknown.

Strictly anaerobic bacteria have been isolated from human feces that are able to deconjugate E1-3S and E2-3S. These isolates were *Eubacterium cylindroides, Peptococcus niger, Clostridium clostridioforme,* and several *Bacteroides* strains (Vaneldere et al., 1991, 1988, 1987) and could generally be separated into two groups. The first group reduced sulfur compounds to obtain energy, with deconjugation occurring during exponential growth and coinciding with production of hydrogen sulfide. The second group appeared to exhibit arylsulfatase activity for sulfur assimilation, with deconjugation occurring during the stationary growth phase which was repressed by cysteine (Vaneldere et al., 1991, 1988, 1987). Although anaerobic sulfate reduction would not be expected in AS, deconjugation of estrogen sulfates for sulfur assimilation may be occurring in AS.

Deconjugation modeling and kinetics

Deconjugation has been modeled as a pseudo first-order rate as a function of a pseudo first-order deconjugation rate coefficient (k_{deconj}, L/g TSS-d), the soluble conjugated estrogen concentration (E_{conj}, ng/L), and the mixed liquor suspended solids concentration (X, g TSS/L) (Joss et al., 2004):

$$\frac{dE_{conj}}{dt} = -k_{deconj}E_{conj}X \qquad \textbf{(1)}$$

Results from aerobic batch tests with raw wastewater show estrogen glucuronides are deconjugated about 30 times faster than estrogen sulfates. E1-3G and E2-3G k_{deconj} values were both 325 L/g TSS-d at 22°C; E1-3S and E2-3S k_{deconj} values were 9.4 and 11.3 L/g TSS-d, respectively, following a 12 hour lag phase (Kumar et al., 2012). These k_{deconj} values support previous inferences that deconjugation of estrogen glucuronides likely takes place during conveyance to WWTPs based on their low concentrations in WWTP influents. A E1-3S k_{deconj} value of 30.9 L/g TSS-d was observed with AS collected from a municipal WWTP (Kumar et al., 2012), indicating deconjugation rates may be sufficient during AS treatment for production of E1.

Deconjugation kinetics obtained with AS collected from a laboratory bioreactor fed synthetic wastewater were slower. E1-3G and EE2-3G k_{deconj} values were about 2 L/g TSS-d at 17°C while less than 10 percent of E1-3S and EE2-3S were deconjugated after eight hours contact with the AS (Gomes et al., 2009). Although these kinetics were obtained at a lower temperature than those determined by Kumar et al. (2012), the discrepancy between the E1-3S behavior with this laboratory AS fed synthetic wastewater versus the WWTP AS described above suggests

13

these deconjugation kinetics may not be representative of those seen at WWTPs with a continual seed source.

Impact of redox conditions on deconjugation

Redox conditions can impact deconjugation rates and transformation pathways of the conjugated natural estrogens (Zheng et al., 2012). This impact was demonstrated in batch tests with 1 percent dairy wastewater that showed E2-3S removals of 25 percent in the absence of oxygen compared to 95 percent with oxygen over the course of 9 days (Zheng et al., 2012). It was not reported whether the lack of oxygen resulted in anoxic or anaerobic conditions. In this same study, E1-3S was the primary transformation product in batch tests with E2-3S under aerobic conditions, while E2 was the primary transformation product in the absence of oxygen. No studies were found addressing the impact of redox conditions on deconjugation with domestic wastewater or AS. Moreover, the transformation of EE2-3S under reduced redox conditions is unknown.

2.4 Estrogen Removal by Biodegradation

As greater than 90 percent of estrogen removals are due to biodegradation during AS treatment (Andersen et al., 2003; Joss et al., 2004; Muller et al., 2008; Zhou et al., 2012), this is the most important mechanism to model when predicting the fate and transformation of estrogens during wastewater treatment.

Estrogen-degrading bacteria

Multiple bacteria have been identified that can oxidize E2 to E1, and some of these can grow on E1 and E2 as the sole carbon source (Kurisu et al., 2010; Yoshimoto et al., 2004; Yu et al., 2007). Cultures able to oxidize E2 to E1 without further transformation of E1 have been documented from the genera *Brevundimonas*, *Escherichia*, *Flavobacterium*, *Microbacterium*, *Nocardioides, Rhodococcus, Sphingomonas* and *Bacillus* (Jiang et al., 2010; Yu et al., 2007). Pure cultures able to degrade E1 and E2 as a sole carbon source include bacteria from the genera *Novosphingobium* (Fujii et al., 2002; Hashimoto et al., 2010)*, Rhodococcus* (Kurisu et al., 2010; Yoshimoto et al., 2004)*, Sphingomonas* (Kurisu et al., 2010; Yu et al., 2007)*, Sphingobacterium* (Haiyan et al., 2007)*, Aminobacter* (Yu et al., 2007), and *Bacillus* (Jiang et al., 2010). In addition, *Denitratisoma oestradiolicum* gen. nov., sp. nov. and *Steroidobacter denitrificans* gen. nov., sp. nov., can degrade E1 and E2 using the estrogen as the sole carbon source while denitrifying nitrate in the absence of oxygen (Fahrbach et al., 2008, 2006).

Although these estrogen-degrading isolates belong to multiple taxonomic classes, *Alphaproteobacteria* have been identified as important in E1 degradation during AS treatment. Hashimoto et al. (2010) documented correlation between concentrations of the estrogen-degrading Alphaproteobacterium, *Novosphingobium* sp. Strain JEM-1, and E1 removal efficiencies in two WWTPs using real-time PCR.   Additionally, Thayanukul et al. (2010) used microautoradiography-fluorescence in situ hybridization (MAR-FISH) to document that 96 percent of E1-assimilating bacteria were *Alphaproteobacteria* at an E1 concentration of 540 ng/L, while the *Betaproteobacteria* or *Gammaproteobacteria* were more important at 200

15

μg/L E1, suggesting that *Alphaproteobacteria* may contribute to E1 degradation at the ng/L concentrations typically found in WWTPs.

Fewer bacteria have been identified that degrade EE2. *Sphingobacterium* sp. JCR5, a bacterium isolated from an oral contraceptive factory WWTP, was reported to grow on EE2 as the sole carbon source (Haiyan et al., 2007). Yoshimoto et al. (2004) isolated Rhodococci, *R. zopfii* and three *R. equi* strains, from municipal AS able to grow on EE2. Other heterotrophic bacteria have been reported to degrade EE2 while growing on other substrates. For example, Pauwels et al. (2008) isolated bacteria from the genera *Phyllobacterium*, *Ralstonia*, *Pseudomonas* and *Acinetobacter* able to cometabolize EE2 while metabolizing E1 and E2. *Rhodococcus*, *Pseudomonas*, and *Bacillus* cultures, *R. zopfii*, *R. equi*, *R. erythropolis*, *R. rhodochrous*, *P. aeruginosa*, *P. putida*, and *B. subtillis*, degraded EE2 while growing on ethanol (Larcher and Yargeau, 2013) while *R. equi* and *R. erythropolis* were also shown to degrade EE2 while growing on glucose and adipic acid, respectively (O'Grady et al., 2009).

EE2 removals with pure cultures of ammonia oxidizing bacteria (AOB) have been reported at high ammonia and/or EE2 concentrations, but batch tests with AOB cultures at environmentally relevant concentrations showed no EE2 transformation. Original batch tests by Shi et al. (2004) showed EE2 removal with a pure culture of *Nitrosomonas europaea* at 280 mg/L NH_4-N and 400 μg/L EE2. However, EE2 removals at high NH_4-N concentrations (200 to 500 mg/L) with AOB cultures, as observed by Shi et al. (2004), were later shown to be the result of abiotic nitration in the presence of high nitrite concentrations, which would not occur under normal conditions found in WWTPs (Gaulke et al., 2008). Khunjar et al. (2011) reported an EE2 biotransformation

16

rate by *N. europaea* of 13.6 L/g biomass as COD-d at 15 mg/L NH_4-N, but these results were obtained at a high EE2 concentration of 200 μg/L. Experiments at environmentally relevant concentrations of 500 ng/L EE2 and 10 mg/L NH_4-N showed no EE2 removal with this same strain and with another AOB culture of *Nitrosospira multiformis* (Gaulke et al., 2008), suggesting these AOBs would not significantly contribute to EE2 removals during AS treatment.

Studies have tried to elucidate the roles of AOBs and heterotrophs in nitrifying AS (NAS). Bagnall et al. (2012) monitored AOB concentrations and the degradation performance of E1, E2 and EE2 in lab-scale reactors fed synthetic wastewater. Following replacement of ammonia with nitrate in the synthetic feed, they observed no significant change in estrogen degradation even though the AOB concentration was reduced by 99 percent. Khunjar et al. (2011) monitored metabolites using radiolabeled EE2 in flow through reactors cultivating a pure culture of *N. europaea* and an enriched heterotrophic community with inhibited nitrification activity. The metabolites with the AOB culture were obtained under unrealistically high NH_4-N feed conditions (700 mg/L) and resulted in nitrated EE2 metabolites (12% of the radioactivity), sulfated EE2 (4%), 4-hydroxy EE2 (6%), and no mineralization. The AOB culture therefore resulted in minor transformation of EE2 as the nitrated EE2 metabolites would not be formed under environmentally relevant conditions. The enriched heterotrophic community fed acetate, on the other hand, was able to mineralize EE2 (55% of radioactivity) with minor metabolites (2%). Although inhibition of EE2 degradation by NAS has been observed with allylthiourea (ATU), an AOB inhibitor (Khunjar et al., 2011; Maeng et al., 2013), Maeng et al. (2013) showed addition of ATU reduced adenosine triphosphate (ATP) production by about 50 percent and hindered removal of dissolved organic carbon. Addition of ATU therefore impacts

17

heterotrophic communities, making interpretation of these results more ambiguous. These former studies support hypotheses that heterotrophs are the key estrogen degraders in AS.

Estrogen degradation pathways

E2 is commonly oxidized to E1 (Dytczak et al., 2008; Kurisu et al., 2010; Ternes et al., 1999a; Yu et al., 2007) with subsequent degradation possibly involving oxidation of the A, B, and D-rings. Lee and Liu (2002) proposed oxidation of E1 at the D-ring producing a lactone structure while Kurisu et al. (2010) proposed oxidation at the aromatic A-ring producing 4-hydroxyestrone. In addition, Kurisu et al. (2010) hypothesized another degradation pathway with attack of the saturated B-ring, yielding metabolites keto-estradiol and keto-estrone. Li et al. (2012) further hypothesized that E1 was converted to tyrosine following cleavage of a saturated ring.

Detected EE2 metabolites suggest EE2 degradation pathways may involve oxidation of the ethynyl group or hydroxylation of the aromatic ring. Haiyan et al. (2007) proposed an EE2 degradation pathway for *Sphingobacterium* sp. JCR5 in which EE2 is oxidized to E1 followed by cleavage of the B ring and the A ring. Intermediate metabolites are the unsaturated acids 2-hydroxy-2,4-dienevaleric acid and 2-hydroxy-2,4-diene-1,6-dioic acid which are ultimately mineralized to CO_2 and water. O'Grady et al. (2009) detected a metabolite from EE2 transformation by *R. erythropolis* with a proposed chemical structure involving oxidation of the ethynyl group to an acetic acid moiety. EE2 metabolites involving hydroxylation of the A ring, producing 2-hydroxy-EE2, as well as cleavage of the A ring have been reported for nitrifying AS (Yi and Harper, 2007).

18

Biodegradation modeling and kinetics

Estrogen biodegradation has been modeled as a pseudo first-order rate as a function of the soluble estrogen concentration and the mixed liquor total or volatile suspended solids concentration (Gaulke et al., 2009; Joss et al., 2004; Ternes et al., 2004):

$$\frac{dE_T}{dt} = -k_b E_S X \tag{2}$$

E_T is the total estrogen concentration (ng/L), t is the time (d), k_b is the pseudo first-order estrogen biodegradation coefficient (L/g VSS-d or L/g TSS-d), E_S is the soluble estrogen concentration (ng/L), and X is the mixed liquor concentration (g/L) either as volatile suspended solids (VSS) or total suspended solids (TSS). Pseudo first-order estrogen biodegradation rate (k_b) constants obtained from batch degradation tests conducted at ng/L concentrations are summarized in Table 2-3.

Table 2-3. Pseudo first-order estrogen biodegradation rate (k_b) constants in literature from batch estrogen degradation tests conducted at ng/L estrogen concentrations

Activated sludge source[a]	SRT (d)	Temp (°C)	k_b E1	k_b E2	k_b EE2	Units	Ref
Aerobic Conditions							
CAS WWTP, USA	3	20	NA[b]	NA	1.6 ± 0.3	L/g VSS-d	1
A/O MBR WWTP, USA	30 – 40	20	229 ± 64	432 ± 20	1.7 ± 0.1	L/g VSS-d	1
CAS WWTP, United Kingdom	NA	14.8	19[c]	NA	3.6[c]	L/g TSS-d	2
CAS WWTP, United Kingdom	NA	20.5	12[c]	NA	4.3[c]	L/g TSS-d	2
A[2]O pilot-scale MBR, Switzerland	30	16	430 ± 55	950 ± 120	6 ± 1	L/g TSS-d	3
A/O CAS WWTP, Switzerland	12	16	162 ± 25	350 ± 42	8 ± 2	L/g TSS-d	3
Lab-scale MBR, Mexico	40	28	79 ± 5	207 ± 6	12.4 ± 2	L/g VSS-d	4
Anoxic Conditions							
A[2]O pilot-scale MBR, Switzerland	30	16	115 ± 30	280 ± 50	3 ± 2[d]	L/g TSS-d	3
A/O CAS WWTP, Switzerland	12	16	30 ± 10	460 ± 60	1.2 ± 0.3[d]	L/g TSS-d	3
Anaerobic Conditions							
A[2]O pilot-scale MBR, Switzerland	30	16	28 ± 3	500 ± 200	1.5 ± 0.5[d]	L/g TSS-d	3
A/O CAS WWTP, Switzerland	12	16	10 ± 1	175 ± 10	-	L/g TSS-d	3

1 Gaulke et al., 2009; 2 Xu et al., 2009; 3 Joss et al., 2004; 4 Estrada-Arriaga and Mijaylova, 2010

a. CAS - conventional activated sludge; A/O - anoxic/aerobic; MBR - membrane bioreactor; A[2]O – anaerobic/anoxic/aerobic
b. NA - not available
c. k_b values calculated from reported first-order degradation rate constant (k), mixed liquor suspended solids concentration (X) and estrogen solids-liquid partitioning coefficient (K_P)
d. Values in the range of the quantification limit of 1 ± 0.5 L/g TSS-d

E2 is readily transformed with the highest k_b values, roughly double those of E1, while EE2 is the most difficult to degrade, with k_b values generally being one or two orders of magnitude less than those for the natural estrogens. These k_b values suggest estrogen biodegradation kinetics are variable between WWTPs, with aerobic k_b values ranging by a factor of about 35 for E1, 5 for E2 and 8 for EE2.

Impact of redox conditions on biodegradation

Compared to aerobic conditions, the majority of studies indicate EE2 degradation under anoxic and anaerobic conditions is insignificant. Joss et al. (2004) reported EE2 degradation kinetics measured in batch tests with AS (Table 2-3) were significant only under aerobic conditions as the anoxic and anaerobic k_b values were in the range of the quantification limit based on abiotic controls. EE2 degradation was not observed in anoxic basins of full-scale WWTPs (Andersen et al., 2003; Zhang et al., 2011) or during the anoxic period of a batch test conducted with lab-scale anoxic/aerobic SBR mixed liquor (Dytczak et al., 2008). Li et al. (2011), however, reported EE2 degradation occurred in the anoxic compartment of a lab-scale anaerobic/anoxic/aerobic complete mix reactor, resulting in a 10 percent removal; no EE2 degradation occurred in the anaerobic compartment. Enriched denitrifying communities grown in anoxic laboratory reactors have also been shown to degrade EE2 under anoxic conditions, but the anoxic degradation rates were slow with EE2 k_b values of 0.4 L/g TSS-d (Suarez et al., 2010) and 0.6 L/g TSS-d (Zeng et al., 2009).

Under anoxic conditions, three types of reactions have been observed with the natural estrogens: (1) oxidation of E2 to E1, (2) reduction of E1 to E2, and (3) degradation of E1 and E2 to

21

unknown byproducts (Hashimoto and Murakami, 2009). Batch tests with E1 showed k_b values were reduced by 73 to 81 percent under anoxic conditions compared to aerobic conditions while high E2 k_b values were observed regardless of the redox condition (Table 2-3). Anoxic transformation and degradation of these natural estrogens has also been observed at full-scale WWTPs. E2 removals of 57 percent and E1 increases of 30 percent occurred across an anoxic basin at a Chinese WWTP (Zhang et al., 2011) while the majority of both E1 and E2 removals took place in the anoxic basins at a German WWTP (Andersen et al., 2003).

Under anaerobic conditions, the following reactions have been observed with the natural estrogens: (1) reduction of E1 to E2, (2) no degradation of E2, and (3) degradation of E2 to unknown byproducts. In anaerobic batch tests with AS taken from an oxidation ditch, E1 was initially reduced to E2 with no subsequent estrogen degradation (Mes et al., 2008). However, anaerobic batch tests conducted by Joss et al. (2004) showed E1 was reduced to E2 which was subsequently degraded. E1 k_b values were reduced by 67 to 76 percent under anaerobic conditions compared to anoxic conditions while high E2 k_b values were still observed under anaerobic conditions (Table 2-3).

2.5 Estrogen Removal by Solids Partitioning

Though 10 percent or less of the estrogen removal in an AS system is due to sorption to waste solids (Andersen et al., 2003; Joss et al., 2004; Muller et al., 2008; Zhou et al., 2012), this removal mechanism needs to be included in an estrogen fate and transformation model to more accurately predict AS process effluent estrogen concentrations.

22

Sorption modeling and kinetics

Estrogen partitioning to AS follows a linear sorption isotherm for estrogen concentrations in the ng/L to μg/L range (Andersen et al., 2005; Gomes et al., 2011) which can be characterized by a solid-liquid partitioning (K_p) coefficient (L/g TSS):

$$K_P = \frac{E_X}{E_S \cdot X} \tag{3}$$

E_X is the sorbed estrogen concentration (ng/L), E_S is the soluble estrogen concentration (ng/L), and X is the mixed liquor suspended solids concentration (g TSS/L). K_P values are greatest for EE2 followed by E2 and then E1, corresponding to their log K_{ow} values of 4.15, 3.94, and 3.43 for EE2, E2 and E1, respectively (Lai et al., 2000). EE2 K_P values for AS range from 0.2 to 0.7 L/g TSS (Andersen et al., 2005; Clara et al., 2004; Estrada-Arriaga and Mijaylova, 2010; Gomes et al., 2011; Xu et al., 2008). E1 K_P values are 0.43 to 0.69 of corresponding EE2 K_P values while E2 K_P values are 0.65 to 0.82 of those for EE2 (Andersen et al., 2005; Estrada-Arriaga and Mijaylova, 2010; Gomes et al., 2011). Varied K_p values between WWTPs are likely due to varying floc properties such as organic carbon content and particle size (Lai et al., 2000).

Estrogen sorption/desorption to AS has been modeled as a function of an adsorption rate coefficient (k_{sor}, L/g TSS-d), E_S, E_X, X, and K_P (Joss et al., 2004):

$$\frac{dE_S}{dt} = -k_{sor}\left(E_S \cdot X - \frac{E_X}{K_P}\right) \tag{4}$$

Based on sorption batch tests with radioactive EE2, a k_{sor} of greater than 40 L/g TSS-d was determined based on near complete sorption occurring within 30 minutes (Joss et al., 2004). Rapid E1, E2, and EE2 sorption to AS within 10 to 30 minutes has also been observed by others (Andersen et al., 2005; Ren et al., 2007).

Impact of redox conditions on estrogen partitioning

Greater K_P values have been observed in anaerobic compartments of AS systems compared to anoxic and aerobic conditions. For a laboratory anaerobic-anoxic-oxic flow through AS system, the apparent EE2 K_P values determined for the anoxic and aerobic compartments based on steady-state operation were about 0.85 of the K_P value for the anaerobic compartment (Li et al., 2011; Zeng et al., 2013). Similarly, the E2 K_P value for the anoxic compartment was about 0.75 of that observed for the anaerobic compartment. E2 K_P values could not be determined for the aerobic compartment due to its degradation below detection limits.

2.6 Estrogen Fate and Transformation Models

Both Joss et al. (2004) and Monteith et al. (2008) have applied estrogen fate and transformation models to predict the fate of E1, E2 and EE2 across WWTPs. Joss et al. (2004) included: (1) production of estrogens from deconjugation (estrogen glucuronides and sulfates were combined into one variable), (2) biodegradation using a pseudo first-order reaction rate based on mixed liquor suspended solids (MLSS) and (3) sorption/desorption of conjugated estrogens. The estrogen fate model and the reactor configurations for existing full-scale WWTPs were implemented in the Aquasim 2.0 software. There was no report of modeling the MLSS

concentration using an activated sludge model (ASM). Estrogen degradation rate constants were measured by conducting batch tests with AS from the WWTPs under aerobic, anoxic and anaerobic conditions (results shown in Table 2-3). Deconjugation and adsorption rate constants were obtained from data available in the literature. The estrogen fate model was applied to model the fate of E1, E2 and EE2 across BNR processes in full-scale WWTPs and pilot plants. They did not, however, apply the model to actual conjugated estrogen data. Rather, they assumed a fraction of the influent estrogen was in a conjugated form.

Integration of an estrogen fate model with an ASM was performed by Monteith et al. (2008) using GPS-X software, however, no details were provided on the ASM used. The estrogen fate model included: (1) biodegradation using a pseudo first-order reaction rate based on mixed liquor VSS and (2) instantaneous sorption to solids using an estrogen solids-liquid partitioning coefficient. A WWTP was configured in GPS-X consisting of primary sedimentation and secondary AS treatment (anaerobic, anoxic and aerobic bioreactors in series). Estrogen degradation rate constants were chosen to achieve estrogen removals deemed typical based on literature values. Estrogen solids-liquid partitioning values were estimated from octanol-water partitioning coefficients. The model was then used to predict effluent E1, E2 and EE2 concentrations of three existing WWTPs.

2.7 Research Objectives

The discharge of estrogens in WWTP effluents is an environmental concern as these compounds are affecting the reproductive systems of fish in downstream populations. High estrogen removals during wastewater treatment are desirable to protect aquatic habitats, however, highly

varied estrogen removals are reported across WWTPs. Of particular concern is the synthetic estrogen, EE2, as this compound is the most potent and the hardest to degrade relative to the natural estrogens.

Estrogens are primarily excreted from the body in a conjugated form, and deconjugation of these compounds may be a source of biologically active free estrogens during wastewater treatment. Based on studies with the natural estrogens, the relatively low concentrations of estrogen glucuronides in WWTP influents as well as their high deconjugation kinetics observed with raw sewage suggest these compounds are being readily deconjugated en route to WWTPs. Estrogen sulfates, on the other hand, appear to be entering WWTPs at concentrations such that their deconjugation could result in production of free estrogens. There is a lack of research examining whether deconjugation is an important EE2 production mechanism during wastewater treatment. No study has explored EE2-3S deconjugation kinetics with AS fed real wastewater or applied a deconjugation model to EE2-3S data.

Biodegradation by heterotrophic biomass is the primary estrogen removal mechanism during AS treatment, although sorbed estrogens are also removed with waste AS. Current estrogen models could be improved by basing biodegradation on the active heterotrophic biomass rather than on the mixed liquor total and volatile suspended solids concentrations. This can be accomplished by integrating the EE2 fate and transformation model with a comprehensive ASM, which facilitates modeling the impacts of wastewater characteristics and operational conditions on EE2 removals. Measurements of estrogen biodegradation rate coefficients of AS are limited and their values are variable across WWTPs. Microbial genes involved in EE2 degradation are unknown.

26

If identified, these genes could serve as useful probes to understand the variability in EE2 biodegradation kinetics.

An EE2 fate and transformation model provides a platform for assessing estrogen production and removal mechanisms and ultimately could serve as a tool for designing AS systems with high EE2 removal performance. Research objectives aimed at expanding our ability to model the fate of EE2 across AS systems were:

- Develop an EE2 fate and transformation model integrated with a comprehensive ASM based on the following mechanisms: (1) EE2 production from deconjugation of EE2-3S, (2) EE2 removal from biodegradation by heterotrophic biomass, and (3) EE2 removal from sorption to AS

- Calibrate the EE2 fate and transformation model to free and conjugated EE2 data and test the model under different operating conditions

- Explore EE2 biodegradation kinetics in AS systems

- Test a transposon mutagenesis technique to isolate mutants with hindered EE2-degrading ability in an effort towards identifying EE2-degradation genes

Chapter 3: Extension of ASM2d to Model the Fate of 17α-Ethinylestradiol in Activated Sludge Systems

Prepared for submittal to Water Research

3.1 Abstract

The discharge of the synthetic estrogen, 17α-ethinylestradiol (EE2), in wastewater treatment plant (WWTP) effluents is an environmental concern as this compound can alter the reproductive system of aquatic wildlife at low ng/L concentrations. Identification of activated sludge (AS) process designs that minimize effluent EE2 concentrations is therefore important. An EE2 fate and transformation model was developed based on the following mechanism: (1) EE2 production from deconjugation of EE2-3-sulfate (EE2-3S), a conjugated form excreted from humans, (2) EE2 removal from biodegradation by heterotrophic biomass growing on other substrates, and (3) EE2 removal from sorption to activated sludge. These mechanisms were incorporated into the International Water Association (IWA) Activated Sludge Model No. 2d (ASM2d) to model the fate of EE2 across aerobic and biological nutrient removal (BNR) AS systems. The model was calibrated and evaluated for mixed liquor solids, nutrients, and EE2 using lab-scale aerobic and BNR AS reactors fed primary effluent and amended with ng L^{-1} estrogen concentrations. Deconjugation kinetics indicate EE2 production from EE2-3S occurs during AS treatment. A sensitivity analysis predicted effluent EE2 concentrations were most sensitive to the biodegradation rate coefficient, the influent biodegradable chemical oxygen demand (bCOD) to EE2 ratio, and the aerobic SRT and were least sensitive to the deconjugation rate coefficient and the solid-liquid partitioning coefficient.

3.2 Introduction

The synthetic estrogen, 17α-ethinylestradiol (EE2), is a potent endocrine disrupting compound discharged in municipal wastewater treatment plant (WWTP) effluents with a predicted no-effect concentration of 0.1 ng/L in surface waters (Caldwell et al., 2012). EE2 is partially removed during activated sludge (AS) treatment by biodegradation and sorption to waste solids with biodegradation accounting for most of the removal (Andersen et al., 2003; Joss et al., 2004; Muller et al., 2008; Zhou et al., 2012). Reported EE2 influent concentrations and removal efficiencies vary widely for AS treatment facilities; from 0.4 to 330 ng/L and 34 to 98 percent, respectively (Baronti et al., 2000; Clara et al., 2005; Johnson et al., 2000; Joss et al., 2004; Koh et al., 2009; Servos et al., 2005; Vethaak et al., 2005; Zhang et al., 2011; Zhou et al., 2012). The variation in performance may be due to differences in wastewater characteristics, process configuration, and operating conditions.

AS process models are commonly used to relate the effect of wastewater characteristics, process design, and operating conditions on the system's biomass and removal of important wastewater constituents. Incorporating EE2 removal mechanisms into such models provides a means to evaluate and identify process designs that minimize effluent EE2 concentration. This study incorporated the fate and transformation of EE2 into the International Water Association (IWA) Activated Sludge Model No. 2d (ASM2d) (Henze et al., 1999). The IWA ASM2d models biomass and solids production for AS processes incorporating anaerobic and/or anoxic zones for enhanced biological phosphorus removal (EBPR) and/or biological nitrogen removal. Selection of the IWA ASM2d therefore allowed the fate of EE2 to be modeled across both aerobic and biological nutrient removal (BNR) AS processes. Ideally, activated sludge models (ASMs)

29

accounting for the fate of EE2 should include the free and conjugated forms in the influent

wastewater, the EE2 biological degradation kinetics, the concentration of the EE2-degrading

organisms, the solids-liquid partitioning, and the effect of redox condition.

EE2 enters WWTPs in both conjugated and free forms. Prior to elimination from the body,

estrogens are generally conjugated with either a glucuronide or sulfate moiety making the

estrogen more water soluble and therefore easier to excrete. Conjugation generally occurs at the

hydroxyl group located on the aromatic ring (carbon 3 based on the steroid numbering

convention) favoring the formation of 17α-ethinylestradiol-3-glucuronide (EE2-3G) and 17α-

ethinylestradiol-3-sulfate (EE2-3S) (Gomes et al., 2005). Conjugated estrogens are biologically

inactive, but they can be deconjugated to the biologically active free estrogen by microbial

activity during sewage collection and conveyance. Deconjugation is generally not completed

prior to arrival of sewage to the WWTP as illustrated in a study by Adler et al. (2001) which

found conjugated EE2 comprised about 26 percent of the total influent EE2 based on median free

and conjugated EE2 concentrations for a number of German treatment facilities. Batch tests with

raw wastewater showed almost complete deconjugation of EE2-3G in 8 hours with only minor

conversion of EE2-3S (Gomes et al., 2009), which is likely attributable to the glucuronidase

activity of intestinal bacteria such as *Escherichia coli*. These results suggest that sulfated EE2

may be the predominant conjugated form in WWTP influents which has been observed for the

natural estrogens in WWTP sampling campaigns (D'Ascenzo et al., 2003; Gomes et al., 2005;

Kumar et al., 2011, 2009a; Liu et al., 2011; Reddy et al., 2005).

30

There has been no reported work adequately examining EE2 production from deconjugation of EE2-3S by AS. Gomes et al. (2009) observed less than 10 percent removal of EE2-3S over 8 hours with AS obtained from a laboratory reactor fed synthetic wastewater. However, a more rapid half-life of 0.2 hours was observed for conjugated sulfates of the natural estrogens in batch tests with municipal WWTP AS (Kumar et al., 2012), which suggests potential for appreciable EE2 production from EE2-3S during AS treatment. Previous models on the fate of EE2 in AS treatment have not accounted for EE2-3S deconjugation kinetics. Joss et al. (2004) applied an estrogen fate model to free estrogen data collected from 48-hour sampling campaigns at two full-scale biological nutrient removal (BNR) facilities. Although the model included relationships for deconjugation, biodegradation, and sorption to solids, deconjugation was based on reported kinetics for estrogen glucuronides and conjugated estrogen model predictions were not confirmed with analytical data. Lust et al. (2012, paper shown in Appendix I) included estrogen biodegradation and sorption removal mechanisms with the IWA ASM No. 1 (ASM1) (Henze et al., 1987). They did not, however, include deconjugation in developing model fits for EE2 removal in short-term tests with laboratory sequencing batch reactors and reported free estrogen measurements at a German full-scale WWTP. The model presented here expands on this earlier work by including deconjugation kinetics for transformation of EE2-3S to free EE2.

Estrogen biodegradation has been described by a pseudo first-order model based on the soluble estrogen concentration and the AS total suspended solids (TSS) concentration by Joss et al. (2004) or the AS heterotrophic biomass concentration by Lust et al. (2012, paper shown in Appendix I). Estrogen degradation is considered to be done by bacteria growing on other wastewater substrates in view of the ng/L influent estrogen concentrations (Tan et al., 2013).

31

Though EE2 biodegradation in municipal WWTPs has been considered possible by cometabolic degradation by ammonia-oxidizing bacteria (AOB) and by cosubtrate utilization by heterotrophic bacteria, more recent studies suggest that the heterotrophic bacteria account for most if not all of the EE2 degraded in AS (Bagnall et al., 2012; Racz et al., 2012). Bagnall et al. (2012) monitored AOB concentrations and the degradation performance of EE2 in lab-scale reactors fed synthetic wastewater amended with EE2 concentrations at 38 to 570 ng/L. Following replacement of ammonia with nitrate in the synthetic feed, they observed no significant change in EE2 degradation even though the AOB concentration was reduced by 99 percent. Conclusions with studies on AOB degradation have been less reliable due to feed conditions resulting in high nitrite concentrations and often unrealistically high EE2 concentrations compared to relevant ng/L concentrations. Gaulke et al. (2008) showed that early batch studies with AOB at NH_4-N concentrations of 200 mg/L or more produced high NO_2-N concentrations resulting in EE2 removal by nitration instead of cometabolic degradation. Khunjar et al. (2011) reported an EE2 transformation rate of 13.6 L/g biomass as COD-d by *N. europaea* at 200 µg/L EE2 and 15 mg/L NH_4-N; however, Gaulke et al. (2008) observed no EE2 removal by this same strain of *N. europaea* nor with another AOB culture of *Nitrosospira multiformis* at environmentally relevant concentrations of 500 ng/L EE2 and 10 mg/L NH_4-N. These studies suggest that heterotrophs are the primary EE2 degraders in AS. Thus, the model presented here bases the EE2 biodegradation kinetics on the heterotrophic bacteria concentration. If needed, the model can be modified to include an incremental removal of EE2 by AOB.

Incorporation of anaerobic and anoxic zones in AS treatment trains for BNR introduce different redox conditions which can impact biodegradation and deconjugation kinetics. Joss et al. (2004)

reported significantly reduced EE2 degradation kinetics in anaerobic and anoxic batch tests with municipal BNR AS in the range of the abiotic control. Zeng et al. (2009) and Li et al. (2011) found no EE2 degradation under anaerobic conditions in laboratory reactors, but they did report EE2 degradation occurred under anoxic conditions. Anoxic degradation by enriched denitrifying communities, however, was extremely slow with pseudo first-order EE2 biodegradation rate coefficients normalized to the reactor TSS of 0.4 L/g TSS-d (Suarez et al., 2010) and 0.6 L/g TSS-d (Zeng et al., 2009). These rates likely result in insignificant EE2 removal during anoxic zones which has been reported for a laboratory anoxic/aerobic AS reactor (Dytczak et al., 2008) and for anoxic basins of full-scale WWTPs (Zhang et al., 2011). Although the impact of redox conditions on deconjugation of EE2-3S is unknown, batch tests with dairy wastewater showed 17β-estradiol-3-sulfate (E2-3S) removal rates were reduced in the absence versus the presence of oxygen (Zheng et al., 2012). The estrogen fate and transformation model presented here incorporates functions for different biodegradation and deconjugation kinetics under aerobic and reduced redox conditions.

In contrast to other model calibration efforts with limited field data collection, modeling in this study was calibrated and tested using data collected long term from aerobic and BNR lab-scale reactors. These reactors were fed domestic wastewater primary effluent and supplemented with free and conjugated estrogens at ng/L concentrations.

3.3 Methods

Model development

The IWA ASM2d was applied to simulate mixed liquor biomass growth and solids production in AS systems. The ASM2d was modified to model nitrate (S_{NO3}, mg N L^{-1}) and nitrite (S_{NO2}, mg

N L^{-1}) as separate variables. Details of modifications made to the ASM2d including two-step nitrification and denitrification are provided in supplemental information at the end of the chapter.

The following processes were added to the ASM2d to account for the fate of EE2: (1) deconjugation of EE2-3S with production of EE2, (2) biodegradation of EE2 to an unknown metabolite, and (3) sorption/desorption of EE2 with AS. Three model components were introduced: conjugated EE2-3S (S_{CE}, ng L^{-1}), soluble EE2 (S_E, ng L^{-1}), and sorbed EE2 (X_E, ng L^{-1}); sorbed EE2-3S was assumed to be negligible. Deconjugation of EE2-3G was not included as prior studies suggest that estrogen glucuronides are readily deconjugated en route to WWTPs. EE2 losses due to volatilization were assumed to be negligible based on its low Henry's Law constant of 7.9 x 10^{-12} atm m^3 mol^{-1} (Silva et al., 2012). Mathematical equations and the stoichiometric matrix of the EE2 fate and transformation model are presented in Table 3-1. Parameter definitions are provided in Table 3-4.

Table 3-1. Process equations and stoichiometric matrix of the EE2 fate and transformation model

Process	Equation	S_{CE}	S_E	X_E
		Component		
Aerobic Biodegradation	$\left(\dfrac{S_{O2}}{K_{O2,bio}+S_{O2}}\right)S_E\left(k_{bio,H}X_H+k_{bio,PAO}X_{PAO}\right)$		-1	
Anoxic Biodegradation	$\eta_{anox}\left(\dfrac{K_{O2,bio}}{K_{O2,bio}+S_{O2}}\right)\left(\dfrac{S_{NO3}+S_{NO2}}{K_{NOx,bio}+S_{NO3}+S_{NO2}}\right)S_E\left(k_{bio,H}X_H+k_{bio,PAO}X_{PAO}\right)$		-1	
Anaerobic Biodegradation	$\eta_{anaer}\left(\dfrac{K_{O2,bio}}{K_{O2,bio}+S_{O2}}\right)\left(\dfrac{K_{NOx,bio}}{K_{NOx,bio}+S_{NO3}+S_{NO2}}\right)S_E\left(k_{bio,H}X_H+k_{bio,PAO}X_{PAO}\right)$		-1	
Aerobic Deconjugation	$\left(\dfrac{S_{O2}}{K_{O2,cle}+S_{O2}}\right)S_{CE}\left(k_{cle,H}X_H+k_{cle,PAO}X_{PAO}\right)$	-1	0.7873	
Anoxic/ Anaerobic Deconjugation	$\eta_{cle}\left(\dfrac{K_{O2,cle}}{K_{O2,cle}+S_{O2}}\right)S_{CE}\left(k_{cle,H}X_H+k_{cle,PAO}X_{PAO}\right)$	-1	0.7873	
Adsorption	$k_{ads}S_E X_{VSS}$		-1	1
Desorption	$\dfrac{k_{ads}}{K_P}X_E$		1	-1

a. S_{CE} – conjugated EE2-3S; S_E – soluble EE2; X_E – sorbed EE2; X_H – heterotrophic biomass; X_{PAO} – polyphosphate accumulating organism biomass; X_{VSS} – mixed liquor volatile suspended solids; S_{O2} – dissolved oxygen; S_{NO3} – nitrate; S_{NO2} – nitrite; η_{anox} – anoxic reduction factor for biodegradation; η_{anaer} – anaerobic reduction factor for biodegradation; $K_{O2,bio}$ – oxygen half-saturation coefficient for biodegradation; $K_{NOx,bio}$ – nitrate/nitrite half-saturation coefficient for biodegradation; $k_{bio,H}$ - biodegradation rate coefficient of X_H; $k_{bio,PAO}$ - biodegradation rate coefficient of X_{PAO}; η_{cle} – anoxic/anaerobic reduction factor for deconjugation; $K_{O2,cle}$ – oxygen half-saturation coefficient for deconjugation; $k_{cle,H}$ - cleavage rate coefficient of X_H; $k_{cle,PAO}$ - cleavage rate coefficient of X_{PAO}; k_{ads} – adsorption rate coefficient; K_P – solid-liquid partitioning coefficient.

EE2 biodegradation was modeled as a pseudo first-order reaction as proposed by Ternes et al. (2004) for low concentration micropollutants. However, instead of relating biodegradation to the mixed liquor total suspended solids concentration which contains inert and biomass fractions, biodegradation was related to the heterotrophic biomass. As heterotrophic biomass in the ASM2d is separated into PAO biomass (X_{PAO}, g COD L^{-1}) and all other heterotrophic biomass (X_H, g COD L^{-1}), both X_{PAO} and X_H were included in the EE2 biodegradation equation with individual pseudo first-order biodegradation rate coefficients ($k_{bio,PAO}$ and $k_{bio,H}$, L g COD^{-1} d^{-1}) normalized to the respective biomass. EE2 biodegradation under aerobic, anoxic, and anaerobic conditions was modeled separately using switching functions based on the dissolved oxygen concentration (S_{O2}, mg O_2 L^{-1}), S_{NO3}, and S_{NO2}, as is done in the ASM2d. Reduction factors (η_{anox} and η_{anaer}) were added for biodegradation under reduced redox conditions.

Deconjugation was also modeled as a pseudo first-order reaction as a function of the conjugated EE2 concentration and the heterotrophic and PAO biomasses. Deconjugation associated with the different biomass fractions was characterized by individual cleavage rate coefficients ($k_{cle,H}$ and $k_{cle,PAO}$, L g COD^{-1} d^{-1}) normalized to the respective biomass. Microbial populations capable of EE2-3S deconjugation are unknown, but arylsulfatase activity associated with other conjugated compounds has been reported for multiple heterotrophic isolates (Beil et al., 1995; Cregut et al., 2013; Murooka et al., 1990; Yamada et al., 1978). A search of the genome of Candidatus Accumulibacter phosphatis clade IIA str. UW-1 from the GenBank database (accession number CP001715.1) revealed the presence of a gene homologous to arylsulfatase, indicating PAOs may also exhibit arylsulfatase activity. Autotrophic biomass was not included in the deconjugation equation as the added complexity to the model did not seem warranted based on its small fraction

36

of the total biomass and the lack of data supporting its importance. A separate equation was added for deconjugation of EE2-3S under reduced redox conditions, utilizing a switching function based on S_{O2} and a cleavage reduction factor (η_{cle}). Deconjugation of EE2-3S results in production of EE2 based on the ratio of the molecular weights of the free and conjugated EE2 (Table 3-1).

EE2 sorption was modeled assuming a linear sorption isotherm as has been observed for EE2 partitioning to AS at ng/L to µg/L concentrations (Andersen et al., 2005). EE2 sorption was modeled as a function of an adsorption rate coefficient (k_{ads}, L g VSS^{-1} d^{-1}), S_E, and the mixed liquor VSS concentration (X_{VSS}, g L^{-1}). EE2 desorption was modeled as a function of k_{ads}, the EE2 solid-liquid partitioning coefficient (K_P, L g VSS^{-1}), and X_E such that at equilibrium:

$$K_P = \frac{X_E}{X_{VSS} \cdot S_E} \tag{1}$$

GPS-X version 6.2.0 (Hydromantis, Canada) was used as a simulator environment for implementing the EE2 fate and transformation model integrated with the modified IWA ASM2d. This software was used to perform model calibrations, simulations, and sensitivity analyses. The model was calibrated and evaluated with bench-scale reactors treating municipal primary effluent amended with EE2 and conjugated EE2.

Bioreactors for model calibration and evaluation
Parallel 4-L sequencing batch reactors (SBRs) simulating aerobic-only, anoxic/aerobic, and anaerobic/aerobic processes for carbon, nitrogen, and phosphorus removal were operated at the King County West Point WWTP for model calibration and evaluation. The SBRs were fed

37

primary effluent amended with free estrogens or a mixture of free and conjugated estrogens. Supplemental carbon was added (~100 mg/L acetate) to promote biological nutrient removal as the primary effluent was weak. Four 6-hour cycles were used per day with approximately one-fourth of the reactor volume being decanted and replaced with primary effluent each cycle (hydraulic retention time of one day). Feeding occurred during the first 15 minutes of each cycle. Half of the solution containing acetate and estrogens was delivered at the beginning of the cycle along with the primary effluent; the other half was delivered 45 minutes into the cycle to ensure PAOs in the anaerobic/aerobic SBR had sufficient substrate following reduction of nitrate. All cycles ended with a 1-hour period for settling and decanting. Mixed liquor was wasted daily to maintain the target SRT based on previous measurements of the mixed liquor suspended solids (MLSS) and effluent total suspended solids (TSS) concentrations. The SBRs were operated in three phases as described below with a more detailed description provided in supplemental information at the end of the chapter.

Phase I SBR Operations. Phase I reactors provided data for calibrating the EE2 fate and transformation model and the IWA ASM2d. An aerobic-only, anoxic/aerobic and anaerobic/aerobic SBR were operated at an 8.5-day total SRT at $18 \pm 2°C$. The anoxic and anaerobic period of the respective SBR occurred during the first 1.5 hours of the cycle during which the mixed liquor was purged with nitrogen gas. The anoxic/aerobic SBR received supplemental nitrate in the feed at 11 mg N L^{-1}. All three SBRs had a 3.5 hour aerobic period resulting in a 5-day aerobic SRT. A 1.5 hour idle period completed the cycle for the aerobic-only SBR. The feed was supplemented with the free estrogens E1, E2, and EE2 at about 120 ng L^{-1}. These SBRs were operated for a time period equal to 12 aerobic SRTs.

38

Phase II SBR Operations. EE2 production from EE2-3S deconjugation was studied during Phase II with continued operation of the Phase I SBRs for an additional 3 aerobic SRTs. In addition to the free estrogens, the feed was supplemented with about 130 ng L^{-1} of estrone-3-sulfate (E1-3S), E2-3S, and EE2-3S. The temperature averaged $19 \pm 1°C$.

Phase III SBR Operations. Phase III examined the fate of EE2 in SBRs with different operational and feed conditions than previously used. Two aerobic-only SBRs were operated at a 6-day total SRT at $21 \pm 2°C$. Both SBRs had a 5 hour aerobic period resulting in a 5-day aerobic SRT. One SBR did not receive supplemental acetate. The feed was amended with E1, E2, and EE2 at 210, 60, and 120 ng L^{-1}, respectively, for the SBR receiving supplemental acetate, and 170, 10, and 80 ng L^{-1}, respectively, for the SBR without supplemental acetate. These reactors were operated for a time period equal to 5 aerobic SRTs.

Sampling and analyses

The primary effluent feed container was sampled five times weekly for TSS and VSS and three times weekly for total COD, soluble COD (sCOD), NH_3-N, and PO_4-P. The supplemental acetate and estrogen solution in a separate container was sampled at three different times during Phase II. For Phase III, composite feed samples consisting of the primary effluent and the supplemental solution were collected three times weekly. The MLSS, MLVSS, and effluent TSS and VSS concentrations of the SBRs were measured five times weekly. The effluent of the SBRs was collected and stored at 4°C. Effluent NH_3-N, NO_3-N, NO_2-N, PO_4-P, and sCOD were measured three times weekly. NO_3-N, NO_2-N, and PO_4-P at the end of the anoxic or anaerobic

39

cycle of the respective SBR were measured four times during each operational phase. Total and soluble EE2 concentrations of the SBR mixed liquor were measured at the end of the aeration cycle four times during Phase I to characterize EE2 partitioning to the AS. Total free estrogen concentrations (Phase I) or soluble free and conjugated estrogen concentrations (Phase II) were monitored throughout the course of the SBR cycle on two separate days. During Phase III, the total estrogen concentration of the mixed liquor at the end of the aeration cycle was collected three times weekly.

HACH kits and a HACH DR/4000 U Spectrophotometer (Loveland, CO) were used to measure COD (Method 8000) and NH_3-N (Method 10023). NO_3-N, NO_2-N, and PO_4-P were measured using a Dionex ICS-3000 Ion Chromatography System (Sunnyvale, California). Samples were filtered through a 0.45 μm Supor filter (Pall Sciences) prior to sCOD and NH_3-N analyses and a 0.2 μm Supor filter (Pall Sciences) prior to NO_3-N, NO_2-N, and PO_4-P analyses. TSS and VSS measurements were conducted according to Standard Methods (APHA, 2005) using 1.2 μm glass-fiber filters (Whatman Grade GF/C). Free estrogen measurements during Phases I and III and free and conjugated measurements during Phase II were conducted according to modified methods of Gaulke et al. (2008) and Kumar et al. (2009b), respectively. Details of the analytical methods used for determining free and conjugated estrogens are provided in the supplemental information.

Model calibration

The model was calibrated using the GPS-X module "Optimizer" by adjusting the following kinetic and stoichiometric parameters: b_H, i_{TSSBM}, $\eta_{NO3,H}$, $\eta_{NO2,H}$, Y_{PO4}, $k_{bio,H}$, $k_{cle,H}$, and $k_{cle,PAO}$

(parameter definitions provided in Tables 3-2 and 3-4). This tool employed the Nelder-Mead simplex method (Nelder and Mead, 1965) to iteratively adjust parameter values in order to minimize the sum of squares of residuals. The modified IWA ASM2d was calibrated to MLVSS (b_H), MLSS (i_{TSSBM}), NO$_3$-N and NO$_2$-N ($\eta_{NO3,H}$ and $\eta_{NO2,H}$), and PO$_4$-P (Y_{PO4}) data collected during Phase I. EE2 biodegradation kinetic coefficients were estimated by fitting the model to EE2 data collected over the course of the SBR cycle during Phase I. Similarly, EE2-3S deconjugation kinetic coefficients were estimated from the EE2-3S data collected during Phase II. Apparent K$_P$ values were calculated using Equation 1 based on X$_{VSS}$, S$_E$, and total EE2 (S$_E$ plus X$_E$) measurements taken at the end of the aeration cycle of all SBRs during Phase I.

Model evaluation

The calibrated EE2 fate and transformation model was applied to the Phase II and III SBRs to evaluate how well the model predicted EE2 concentrations following (1) addition of conjugated estrogens to the feed (Phase II), (2) reducing the total SRT from 8.5 to 6 days and increasing the aeration cycle time from 3.5 to 5 hours (Phase III), and (3) reducing the feed bCOD (Phase III SBR without supplemental acetate).

3.4 Results

Model calibration

The modified IWA ASM2d was calibrated for MLVSS, MLSS, and nutrient concentrations by adjusting model parameters (b_H, i_{TSSBM}, $\eta_{NO3,H}$, $\eta_{NO2,H}$, and Y_{PO4}) using the GPS-X Optimizer module and by adopting literature values (b_{PAO} and q_{PHA}) (Table 3-2). A summary of the mixed liquor solids and nutrient data used for calibrating the IWA ASM2d is shown in Table 3-3 (Phase

41

I SBRs). The estimated heterotrophic lysis rate constant (b_H) was 0.28 d^{-1} and 0.22 d^{-1} for the aerobic-only and anoxic/aerobic SBR, respectively. An average b_H value of 0.25 d^{-1} was selected for modeling and resulted in predicted aerobic-only and anoxic/aerobic MLVSS concentrations being within 4 percent of average measured values (Phase I, Table 3-3). The PAO biomass lysis rate constant (b_{PAO}) was reduced to 0.15 d^{-1} as has been reported by Lopez et al. (2006) and resulted in the simulated anaerobic/aerobic MLVSS being within 9 percent of the average measured value (Phase I, Table 3-3). Lysis rate constants (b_{PP} and b_{PHA}) for polyphosphate (PP) and polyhydroxy-alkanoates (PHA) were also reduced to 0.15 d^{-1} to ensure the PAO storage products decayed with the biomass. The estimated TSS to COD ratio for biomass (i_{TSSBM}) was 0.78 g TSS/g COD, resulting in predicted MLSS concentrations being within 3 percent of average observed values for all three SBRs (Phase I, Table 3-3). For the anoxic/aerobic SBR, estimated anoxic reduction factors for denitrification ($\eta_{NO3,H}$ and $\eta_{NO2,H}$, Table 3-2) were lower than those obtained by Kaelin et al. (2009) ranging from 0.15 to 0.25, indicating denitrification was partially inhibited in this SBR. For the anaerobic/aerobic SBR, a rate constant for storage of PHA (q_{PHA}) of 6 d^{-1} was adopted from Rieger et al. (2001). The estimated PP requirement per PHA stored (Y_{PO4}) was 0.6 g P g COD^{-1}. Smolders et al. (1994) showed Y_{PO4} linearly increased with pH in an acetate fed SBR, corresponding to Y_{PO4} values of 0.19 to 0.74 g P g COD^{-1} for pH values ranging from 5.5 to 8.5. For a pH of 7.7 as was observed during the anaerobic cycle of our SBR, the work by Smolders suggests a Y_{PO4} value of 0.59 g P g COD^{-1}, which is similar to our model calibrated value.

Table 3-2. Adjusted kinetic and stoichiometric coefficients of the modified IWA ASM2d at 20°C

Definition[a]	Symbol	Unit	Default Value	Adjusted Value	Calibration Data or Literature Source
		All SBRs			
Heterotrophic biomass lysis rate constant	b_H	d^{-1}	0.4	0.25	Phase I MLVSS data
TSS to COD ratio for biomass	i_{TSSBM}	g TSS g COD^{-1}	0.9	0.79	Phase I MLSS data
		Anoxic/Aerobic SBRs			
Anoxic reduction factor for NO$_3^-$ to NO$_2^-$	$\eta_{NO3,H}$	-	0.24[b]	0.12	Phase I NO$_3$-N and NO$_2$-N data
Anoxic reduction factor for NO$_2^-$ to N$_2$	$\eta_{NO2,H}$	-	0.36[b]	0.11	
		Anaerobic/Aerobic SBRs			
PAO biomass lysis rate constant	b_{PAO}	d^{-1}	0.2	0.15	Lopez et al. (2006)
PP lysis rate constant	b_{PP}	d^{-1}	0.2	0.15	Assumed to ensure PAO storage products
PHA lysis rate constant	b_{PHA}	d^{-1}	0.2	0.15	decay together with biomass
Rate constant for storage of PHA	q_{PHA}	d^{-1}	3	6	Rieger et al. (2001)
PP requirement per PHA stored	Y_{PO4}	g P g COD^{-1}	0.4	0.6	Phase I PO$_4$-P data

a. PHA – polyhydroxy-alkanoates; PP – polyphosphate

b. New model parameters, $\eta_{NO3,H}$ and $\eta_{NO2,H}$, and default values were added to the modified ASM2d for two-step denitrification

43

Table 3-3. Comparison of average (± one standard deviation) measured and modeled constituents of aerobic-only, anoxic/aerobic, and anaerobic/aerobic SBRs

| | MLSS (mg L^{-1}) | | MLVSS (mg L^{-1}) | | SRT (d) | | End of Anoxic or Anaerobic Cycle | | | | Effluent[c] | | | |
| | | | | | | | NO$_3$-N (mg L^{-1}) | | PO$_4$-P (mg L^{-1}) | | NO$_3$-N (mg L^{-1}) | | PO$_4$-P (mg L^{-1}) | |
SBR	*Data*	*Model*	*Data*	*Model*	*Data*	*Model*	*Data*	*Model*	*Data*	*Model*	*Data*	*Model*	*Data*	*Model*
							Phase I							
Aerobic	1090 (± 195)	1110	911 (± 119)	927	8.5	8.5					14.3 (± 3.8)	18.4	5.6 (± 0.3)	6.1
Anoxic/ Aerobic	1058 (± 95)	1030	878 (± 55)	847	8.6	8.6	1.1 (± 1.5)	0.6	5.6 (± 0.5)	5.8	12.0 (± 3.4)	12.8	5.3 (± 0.3)	5.9
Anaerobic/ Aerobic	1186 (± 160)	1180	960 (± 110)	880	8.4	8.4	< 0.2	< 0.2	14.5 (± 3.4)	14.2	5.9 (± 0.9)	7.4	1.3 (± 0.5)	1.6
							Phase II							
Aerobic	1048 (± 98)	1080	859 (± 86)	898	8.6	8.6					16.9 (± 3.8)	16.6	5.1 (± 1.1)	4.7
Anoxic/ Aerobic	983 (± 123)	956	754 (± 66)	784	8.1	8.1	2.8 (± 3.4)	0.2	4.6 (± 1.0)	4.4	15.6 (± 5.9)	11.0	4.6 (± 0.4)	4.5
Anaerobic/ Aerobic	1213 (± 119)	1130	899 (± 108)	842	8.4	8.4	< 0.2	< 0.2	12.3 (± 2.9)	13.5	5.4 (± 1.3)	6.7	0.7 (± 0.6)	0.5
							Phase III							
Aerobic	710 (± 68)	743	589 (± 59)	617	6.3	6.3					24.5 (± 1.8)	23.3	6.7 (± 0.9)	6.4
Aerobic[d]	531 (± 91)	560	434 (± 83)	460	6.5	6.5					29.5 (± 1.9)	30.4	6.9 (± 0.8)	6.9

a. SBR – sequencing batch reactor; MLSS – mixed liquor suspended solids; MLVSS – mixed liquor volatile suspended solids; SRT – solids retention time.
b. Average and standard deviation based on four or more measurements
c. Observed and modeled effluent NH$_3$-N concentrations were below 0.2 mg L^{-1} for all SBRs
d. SBR did not receive supplemental acetate

Kinetic parameter values of the calibrated EE2 fate and transformation model are shown in Table 3-4. Calibration of the EE2 fate and transformation model to Phase I total EE2 data using the GPS-X Optimizer module resulted in EE2 $k_{bio,H}$ values of 11.1, 10.3, and 10.9 L g COD^{-1} d^{-1} for the aerobic-only, anoxic/aerobic, and anaerobic/aerobic SBRs, respectively, assuming a $k_{bio,PAO}$ value of zero. An average EE2 $k_{bio,H}$ value of 10.8 L g COD^{-1} d^{-1} was used in model simulations (Figure 3-1). Reduction factors for EE2 biodegradation under anoxic and anaerobic conditions (η_{anox} and η_{anaer}) were set to zero based on insignificant EE2 biodegradation by AS under these conditions in our lab (reported in Chapters 4 and 5) and in this study. An EE2 adsorption rate (k_{ads}) coefficient of 50 L g VSS^{-1} d^{-1} was used in the estrogen fate and transformation model based on a value of 40 L g SS^{-1} d^{-1} proposed by Joss et al. (2004) and a VSS/TSS ratio of 0.8. This k_{ads} value results in rapid EE2 solid-liquid partitioning during the course of the SBR cycle. An average EE2 solid-liquid partitioning (K_P) coefficient of 0.55 ± 0.14 L g VSS^{-1} was calculated based on total and soluble EE2 concentrations collected at the end of the aeration cycle for all Phase I SBRs and was used in model simulations.

Table 3-4. Kinetic coefficients of the EE2 fate and transformation model at 20°C

Definition	Symbol	Unit	Value	Source
		Biodegradation		
Biodegradation rate coefficient of X_H	$k_{bio,H}$	L g COD^{-1} d^{-1}	10.8[a]	Calibrated to Phase I total EE2 data
Biodegradation rate coefficient of X_{PAO}	$k_{bio,PAO}$	L g COD^{-1} d^{-1}	0	Assumed
Anoxic reduction factor	η_{anox}	-	0	Visual observation
Anaerobic reduction factor	η_{anaer}	-	0	Visual observation
Oxygen half-saturation coefficient	$K_{O2,bio}$	mg O$_2$ L^{-1}	0.2	Henze et al. (1999)[b]
Nitrate/nitrite half-saturation coefficient	$K_{NOx,bio}$	mg N L^{-1}	0.5	Henze et al. (1999)[b]
		Deconjugation		
Cleavage rate coefficient of X_H	$k_{cle,H}$	L g COD^{-1} d^{-1}	3.7[a]	Calibrated to Phase II EE2-3S data
Cleavage rate coefficient of X_{PAO}	$k_{cle,PAO}$	L g COD^{-1} d^{-1}	3.7	Assumed the same value as $k_{cle,H}$
Anoxic/anaerobic reduction factor	η_{cle}	-	0	Visual observation
Oxygen half-saturation coefficient	$K_{O2,cle}$	mg O$_2$ L^{-1}	0.2	Henze et al. (1999)[b]
		Adsorption/ desorption		
Adsorption rate coefficient	k_{ads}	L g VSS^{-1} d^{-1}	50	Joss et al. (2004)[c]
Solid-liquid partitioning coefficient	K_P	L g VSS^{-1}	0.55[a]	Calculated from Phase I total and soluble EE2 data

a. Average of aerobic-only, anoxic/aerobic, and anaerobic/aerobic SBR values
b. Used same general half-saturation coefficient values as the IWA ASM2d
c. Based on proposed value of 40 L g TSS^{-1} d^{-1} and normalized to VSS using VSS/TSS ratio of 0.8
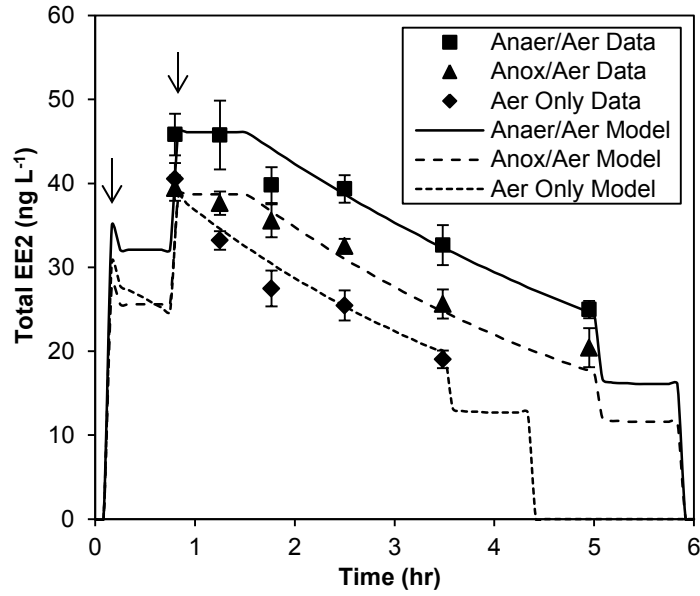
Figure 3-1. Comparison of observed (markers) and modeled (lines) total EE2 concentrations in Phase I anaerobic/aerobic, anoxic/aerobic, and aerobic-only SBRs using $k_{bio,H}$ of 10.8 L g COD^{-1} d^{-1}. Arrows ($\downarrow$) indicate the addition of supplemental feed containing estrogens. At the end of the SBR cycle, modeled lines show removal of sorbed EE2 during the settling period and the subsequent decant.

Calibration of the EE2 fate and transformation model to Phase II EE2-3S data collected over the course of the SBR cycle resulted in estimated $k_{cle,H}$ values of 3.6 and 3.4 L g COD^{-1} d^{-1} for the aerobic-only and anoxic/aerobic SBRs, respectively. Assuming the same cleavage rate by X_H and X_{PAO}, the estimated $k_{cle,H}$ and $k_{cle,PAO}$ value was 4.0 L g COD^{-1} d^{-1} for the anaerobic/aerobic SBR. A single value of 3.7 L g COD^{-1} d^{-1} was used in the model simulations for $k_{cle,H}$ and $k_{cle,PAO}$ (Figure 3-2) based on averaging the estimated values obtained with the three SBRs. The deconjugation rate coefficient was therefore less than the biodegradation rate coefficient, being one-third of its value. The reduction factor for EE2-3S deconjugation under anoxic and anaerobic conditions (η_{cle}) was set to zero based on insignificant removal of the conjugated estrogen under reducing conditions (Figure 3-2).

47

Model evaluation

Phase II SBRs. Application of the calibrated ASM2d to the Phase II SBRs resulted in predicted MLSS and MLVSS concentrations being within 7 percent of observed average values (Table 3-3); predicted effluent nutrient concentrations were within 35 percent of average values, but within one standard deviation. The EE2 fate and transformation model predicted the increase in soluble EE2 concentration in the Phase II SBRs following addition of EE2-3S to the feed (Table 3-5). Applying a $k_{bio,H}$ value of 10.8 L g COD^{-1} d^{-1}, the predicted soluble EE2 concentration at the end of the aeration cycle was within 8 percent of observed average values for the aerobic-only and anaerobic/aerobic SBRs (Table 3-5), and the modeled soluble EE2 concentrations throughout the SBR cycle generally agreed with actual measurements (Figures 3-2a and c). However, the model under predicted the soluble EE2 concentration for the anoxic/aerobic operation by about 23 percent (Figure 3-2b, Table 3-5). Decreasing $k_{bio,H}$ to 7.4 L g COD^{-1} d^{-1} (based on fitting the model to the Phase II soluble EE2 data using the GPS-X Optimizer module) resulted in improved model predictions (top line, Figure 3-2b), suggesting this value may have declined following the Phase I operations for some unknown reason.

Table 3-5. Average observed (± one standard deviation) and modeled soluble EE2 concentrations at the end of the aeration cycle for Phases I and II

SBR	Soluble EE2 (ng L^{-1})	
	Data	*Model*
Phase I		
Aerobic	12 ± 1	13
Anoxic/Aerobic	13 ± 2	12
Anaerobic/Aerobic	16 ± 3	16
Phase II		
Aerobic	27 ± 2	25
Anoxic/Aerobic	30 ± 2	23
Anaerobic/Aerobic	29 ± 2	31

a. Average and standard deviation based on four (Phase I) or six (Phase II) measurements
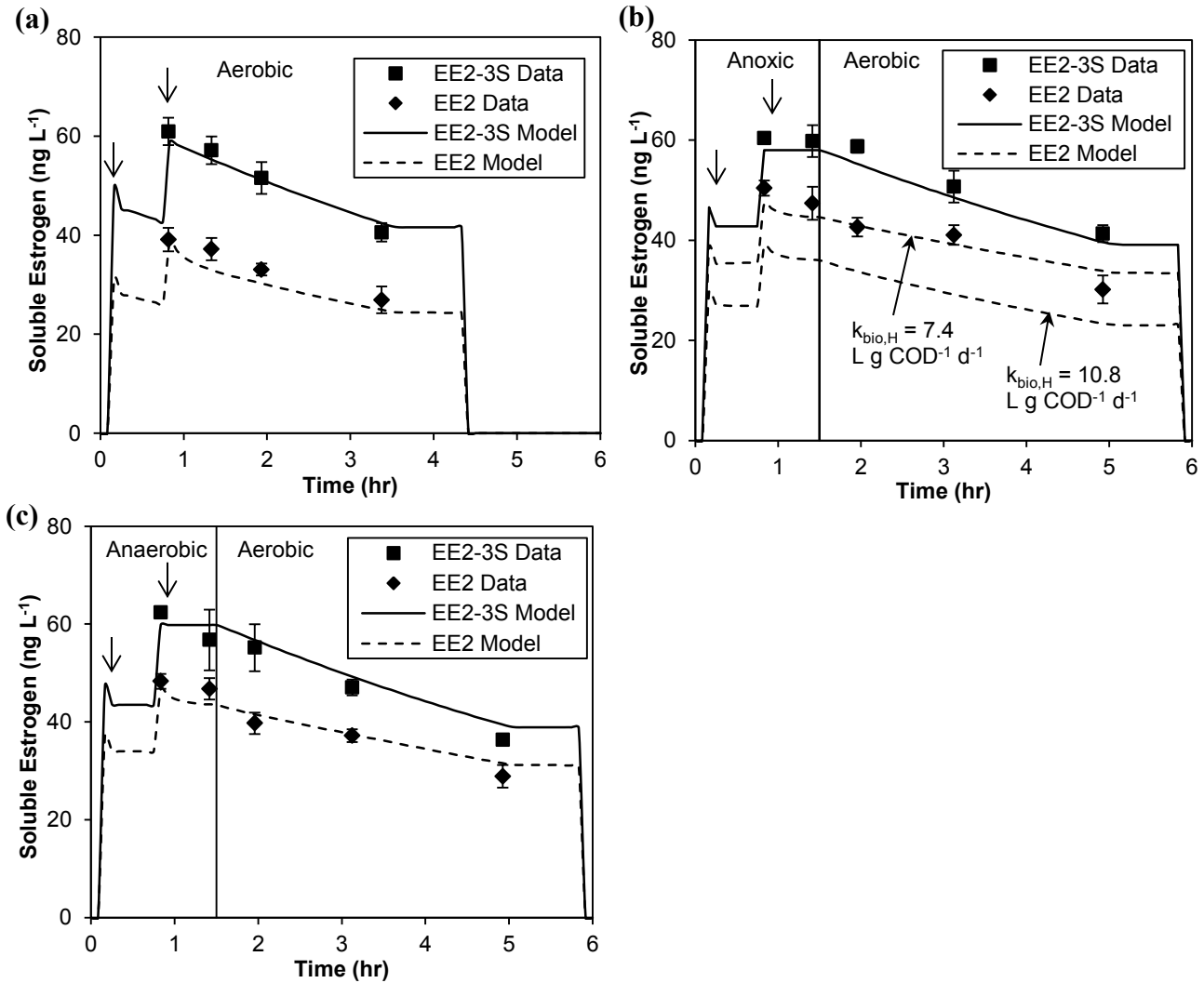
Figure 3-2. Comparison of observed (markers) and modeled (lines) soluble EE2 and EE2-3S concentrations in Phase II (a) aerobic-only, (b) anoxic/aerobic, and (c) anaerobic/aerobic SBRs using $k_{cle,H}$ and $k_{cle,PAO}$ of 3.7 L g COD^{-1} d^{-1} and $k_{bio,H}$ of 10.8 L g COD^{-1} d^{-1}. Arrows (↓) indicate the addition of supplemental feed containing estrogens.

Phase III SBRs. Application of the calibrated ASM2d to the Phase III SBRs resulted in predicted mixed liquor and effluent nutrient concentrations being within 6 percent of observed average values (Table 3-3). Total EE2 concentrations of the mixed liquor at the end of the aeration cycle ($n = 6$) averaged 17 ± 3 and 17 ± 2 ng L^{-1} for the aerobic-only SBR with and without supplemental acetate, respectively; the predicted value using the calibrated EE2 fate and

49

transformation model was 14 ng L^{-1} for both SBRs. This predicted value was within 18 percent of the observed average concentration. The SBR without supplemental acetate received 34 percent less EE2 in the feed than the SBR with supplemental acetate. The SBR with supplemental acetate removed 103 ng/L of the influent EE2 while the SBR without supplemental acetate removed 62 ng/L. The SBR fed less biodegradable COD (bCOD) therefore had poorer EE2 removal performance.

Sensitivity analysis

A sensitivity analysis was performed to evaluate how changes in kinetic parameters and operational conditions affect predicted effluent EE2 concentrations of AS systems with the same feed and operating conditions as the Phase II reactors. Simulations were performed to evaluate the change in the effluent EE2 concentration (Y) as a consequence of a change in one of the following input parameters (X_i): $k_{bio,H}$, $k_{cle,H}$, $k_{cle,PAO,}$ K_P, the feed bCOD/EE2 ratio, and the aerobic SRT. Normalized effluent EE2 concentrations (Y/Y_o) were plotted against normalized input parameter values ($X_i/X_{i,o}$) for the aerobic-only SBR (Figure 3-3) where Y_o and $X_{i,o}$ are the original effluent EE2 concentration and the original input parameter value, respectively. The effluent EE2 concentration was most sensitive to $k_{bio,H}$, almost doubling with a 50 percent decrease in $k_{bio,H}$ and being reduced by about half with a 200 percent increase in $k_{bio,H}$. The effluent EE2 concentration was also sensitive to the feed bCOD/EE2 ratio and the aerobic SRT and was relatively insensitive to $k_{cle,H}$ and K_P.

50
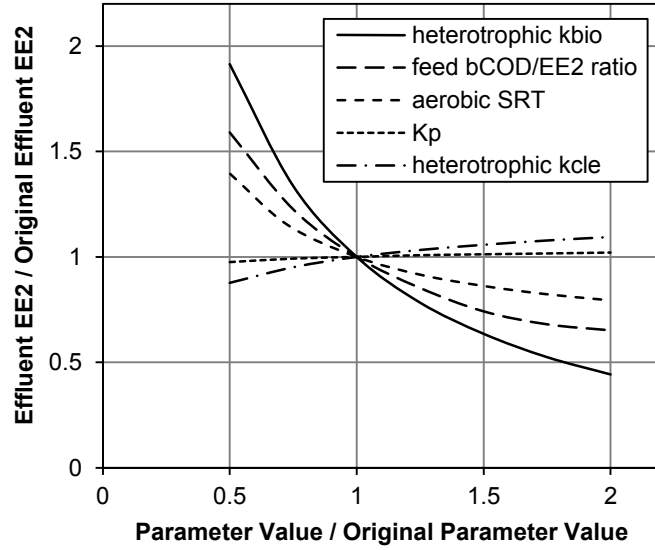
Figure 3-3. Sensitivity of effluent EE2 to changes in $k_{bio,H}$, feed bCOD/EE2 ratio, aerobic SRT, K_P, and $k_{cle,H}$ for Phase II aerobic-only SBR

Normalized sensitivity coefficients (S_i) were also calculated for the Phase II aerobic-only, anoxic/aerobic, and anaerobic/aerobic SBRs as follows:

$$S_i = \frac{(Y - Y_o)/Y_o}{(X_i - X_{i,o})/X_{i,o}} \tag{2}$$

where $(X_i - X_{i,o})/X_{i,o}$ was 0.1 (Makinia et al., 2005). In addition, S_i values were determined for a single continuous-flow completely stirred tank reactor (CSTR) and four CSTRs in series. The single and staged CSTRs were simulated as having the same operational conditions as the aerobic-only SBR including the same feed, aerobic SRT and heterotrophic biomass concentration of 862 mg COD L^{-1}. The sensitivity analysis (Table 3-6) showed $k_{bio,H}$, the feed bCOD/EE2 ratio, and the aerobic SRT have the greatest impact on predicted effluent EE2 concentrations regardless of reactor configuration with the four CSTR in series being the most sensitive to these parameters. The effluent EE2 concentration of the anaerobic/aerobic SBR was predicted to be

the least sensitive to the feed bCOD/EE2 ratio, which was a consequence of assuming a $k_{bio,PAO}$

value of zero.

Table 3-6. Sensitivity coefficients characterizing the change in effluent EE2 concentration to a
10 percent increase in kinetic or operational parameter

	$k_{bio,H}$	feed bCOD/EE2	aerobic SRT	K_P	$k_{cle,H}$	$k_{cle,PAO}$
Aerobic SBR	-0.98	-0.66	-0.37	0.04	0.16	-
Anoxic/Aerobic SBR	-0.86	-0.65	-0.34	0.03	0.15	-
Anaerobic/Aerobic SBR	-0.90	-0.13	-0.34	0.03	0.13	0.06
Aerobic CSTR	-0.78	-0.68	-0.46	0.01	0.12	-
Aerobic 4 CSTR in Series	-1.14	-0.95	-0.61	0.09	0.10	-

3.5 Discussion

The EE2 fate and transformation model integrated with the modified IWA ASM2d successfully

modeled EE2 production from deconjugation of EE2-3S, and the results showed a single

cleavage rate coefficient could be used to model EE2-3S deconjugation in aerobic and BNR AS

reactors. The measured deconjugation kinetics demonstrated that EE2-3S was not as recalcitrant

as suggested by a previous study where EE2-3S removals of less than 10 percent were observed

after 8 hours contact with AS (Gomes et al., 2009). As the AS in their study was fed synthetic

wastewater, the continual seed source to the SBRs in this study fed primary effluent may be

important for deconjugation kinetics. Therefore, EE2-3S in WWTP influents represents a

potential source of EE2 during AS treatment and should be considered when assessing EE2

removals across WWTPs. Studies are needed that measure influent EE2-3S concentrations to

determine if EE2-3S is present at high enough concentrations relative to EE2 such that its

deconjugation would have a significant impact on effluent EE2 concentrations.

The sensitivity analysis (Table 3-6) indicated predicted effluent EE2 concentrations have low sensitivity to the deconjugation rate coefficient and raises the question of how important characterizing this value and the factors impacting it may be in modeling the fate of EE2. Work by Fernandez et al. (2008) indicated effluent estrogen concentrations may be sensitive to changes in $k_{cle,H}/k_{bio,H}$ ratios as impacted by seasonal variations in temperature. They proposed the increased estrogenic potency of the effluent from a full-scale WWTP during warmer months was due to the production of the natural estrogen E1 from its conjugated form; a higher deconjugation rate (k of 1.6 L g TSS^{-1} d^{-1}) relative to the E1 biodegradation rate (k of 0.8 L g TSS^{-1} d^{-1}) was observed in the warmer months compared to little deconjugation during the cooler months. In order to assess the importance of $k_{cle,H}/k_{bio,H}$ ratios on predicted effluent EE2 concentrations, simulations were performed for $k_{cle,H}/k_{bio,H}$ ratios ranging from 0 to 2 for an AS system with a $k_{bio,H}$ of 3 or 10.8 L g COD^{-1} d^{-1} (Figure 3-4). These simulations were based on four CSTRs in series, the primary effluent characterized during Phase III, an influent EE2 concentration of 20 ng/L as measured in WWTP influents (Clara et al., 2005), and an influent EE2-3S concentration of 7 ng/L assuming 26 percent of the influent EE2 is conjugated (Adler et al., 2001) and in the sulfated form. The predicted effluent EE2 concentration was more sensitive to EE2-3S deconjugation at the lower $k_{bio,H}$, increasing from 9.2 to 11.4 ng L^{-1} for $k_{cle,H}/k_{bio,H}$ ratios of 0 to 2 (Figure 3-4). Modeling changes in EE2 deconjugation kinetics may be more important for WWTPs with lower $k_{bio,H}$ values, and there is a need to incorporate the effects of temperature on its kinetics.
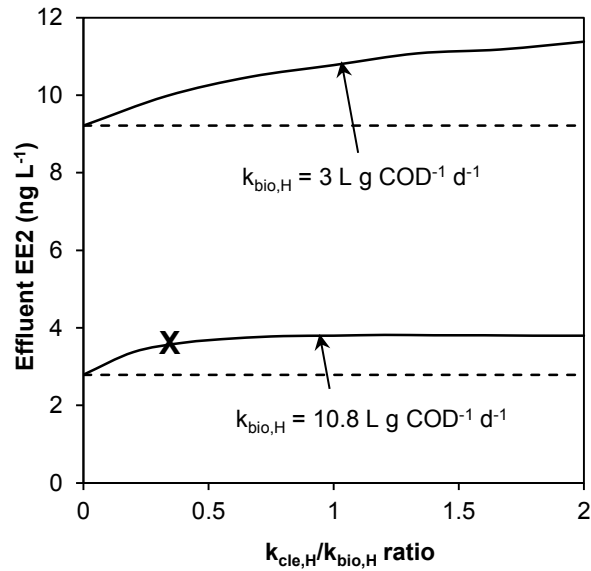
Figure 3-4. Impact of $k_{cle,H}/k_{bio,H}$ ratio on predicted effluent EE2 concentration for 4 CSTR in series with influent EE2 of 20 ng/L and EE2-3S of 7 ng/L. Dashed lines indicate predicted effluent EE2 concentration if EE2-3S is neglected. The symbol **X** indicates the $k_{cle,H}/k_{bio,H}$ ratio observed in this study.

The parameter $k_{bio,H}$ has the greatest impact on predicted effluent EE2 concentrations, highlighting the importance of understanding this value and the factors impacting it. A single $k_{bio,H}$ value of 10.8 L g COD^{-1} d^{-1} was used in this study for both aerobic and BNR AS processes. Reported EE2 biodegradation rate (k_b) coefficients normalized to MLVSS range from 2 to 19 L g VSS^{-1} d^{-1} (Estrada-Arriaga and Mijaylova, 2010; Gaulke et al., 2009; Joss et al., 2004; Ziels, 2013), suggesting this parameter value is variable. Operational factors affecting $k_{bio,H}$ are poorly understood, but substrate loading condition has been reported as impacting the biodegradation kinetics of AS fed municipal wastewater. Ziels (2013) observed higher k_b values in aerobic reactors having low substrate feeding concentrations favoring K-strategist microbial populations, with low half-velocity (K_S) constants, compared to parallel operations with high substrate feeding concentrations favoring r-strategist microbial populations, with high maximum specific growth rates (μ_{max}). The EE2 removal efficiency for varying k_{bio} values was simulated for the

54

Phase III aerobic SBR without supplemental acetate as well as for a single CSTR and four CSTR in series with the same primary effluent feed (Figure 3-5a). All simulations were based on a 5-day aerobic SRT, influent EE2 of 20 ng L^{-1}, influent EE2-3S of 7 ng L^{-1}, and a reactor heterotrophic biomass concentration of 388 mg COD L^{-1}. A lower range of $k_{bio,H}$ values was applied to the SBR compared to the CSTR to reflect the impact of substrate loading condition (Ziels, 2013). The EE2 fate and transformation model predicted there is the greatest potential for high EE2 removals with staged CSTR designs.

Predicted effluent EE2 concentrations were sensitive to $k_{bio,H}$, the influent bCOD/EE2 ratio, and the aerobic SRT, which likely has contributed to the varied EE2 removals reported in literature. Higher influent bCOD/EE2 ratios were predicted to improve EE2 removals by supporting more heterotrophic biomass participating in EE2 biodegradation. This prediction was confirmed during Phase II operations where the aerobic SBR without supplemental acetate had poorer removals compared to a parallel SBR with supplemental acetate. Simulations for four CSTR in series (described above for Figure 3-5a) showed longer aerobic SRTs promote higher EE2 removals by increasing the contact time between the biomass and EE2 (Figure 3-5b); however, increasing the SRT beyond about 15 days had limited improvement on EE2 removal. This impact of SRT on EE2 removal efficiency neglected the possible improvement of $k_{bio,H}$ at longer SRTs (Andersen et al., 2003). For aerobic SRTs ranging from 3 to 25 days, EE2 removals of 36 to 65 percent were predicted for a $k_{bio,H}$ of 3 L g COD^{-1} d^{-1} which increased to 74 to 92 percent for a $k_{bio,H}$ of 10.8 L g COD^{-1} d^{-1} (Figure 3-5b). By doubling the influent bCOD from 173 mg COD L^{-1} (bCOD/EE2 ratio of 8.7 mg/ng) to 346 mg COD L^{-1} (bCOD/EE2 ratio of 17.3 mg/ng), EE2 removals were predicted to increase to 55 to 80 percent for a $k_{bio,H}$ of 3 L g COD^{-1} d^{-1} at

55

SRTs of 3 to 25 days. Although longer SRTs and higher bCOD/EE2 ratios improved EE2 removals, removals greater than 90 percent required an AS with a higher $k_{bio,H}$ value. For example at a 15-day aerobic SRT, the model predicted $k_{bio,H}$ values of 10.4 and 6 L g COD^{-1} d^{-1} were needed to achieve 90 percent removals for influent bCOD/EE2 ratios of 8.7 and 17.3 mg/ng, respectively.
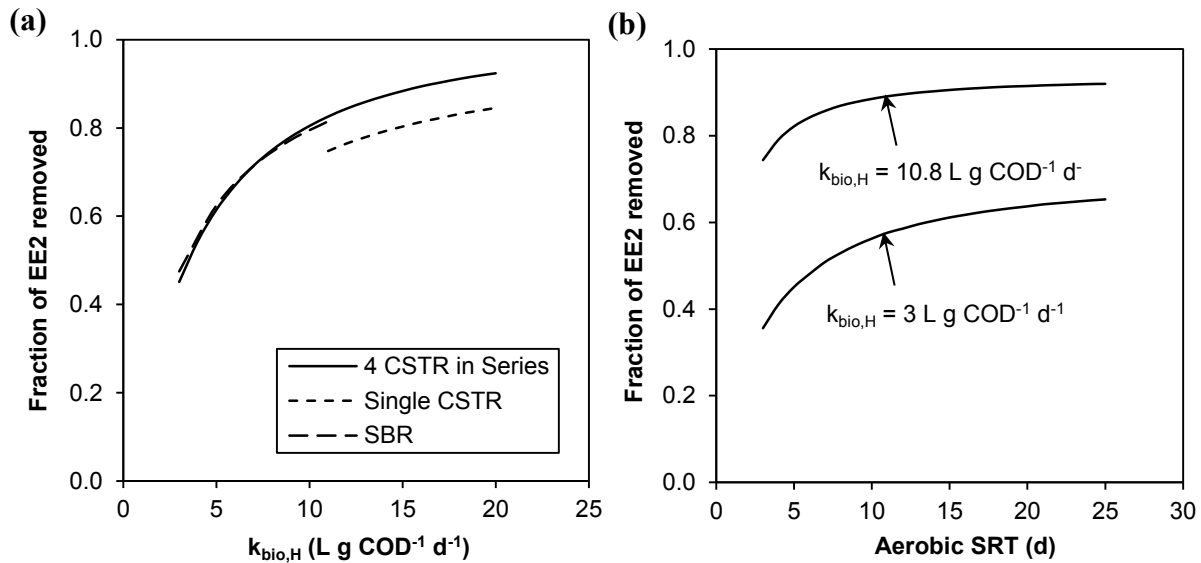
Figure 3-5. Fraction of EE2 removed versus (a) $k_{bio,H}$ for 5-day aerobic SRT and (b) aerobic SRT for $k_{bio,H}$ of 3 and 10.8 L g COD^{-1} d^{-1}

Knowledge of the microbial populations and enzyme(s) responsible for EE2 biodegradation in AS would improve the model. PAOs were assumed not to degrade EE2 during the model calibration in order to use the same $k_{bio,H}$ value for all SBRs. Whether this assumption is correct regarding the EE2-degrading ability of PAOs or was an artifact of this specific SBR set needs to be further evaluated as the relative contribution by PAOs and other heterotrophic biomass to EE2 biodegradation is currently unknown. Research elucidating the role of PAOs in EE2 biodegradation could simplify the model if they were found to be unimportant. EE2-degrading

56

bacteria have been proposed to be K-strategists promoted by longer SRTs (Koh et al., 2009) and/or low substrate feeding conditions (Ziels, 2013). A potential improvement to this model could be to model a K-strategist population characterized by K_S, μ_{max}, and $k_{bio,K-strategist}$ to better predict the impact of SRT and substrate feeding conditions on EE2 removals. Alternatively, identification of the enzyme(s) responsible for EE2 biodegradation could provide a useful probe for elucidating the fraction of heterotrophic EE2-degrading biomass and how process and operational conditions affect this fraction and enzyme expression.

3.6 Conclusions

An EE2 fate and transformation model integrated with the IWA ASM2d was successfully applied to model EE2 production and removal in aerobic and BNR AS reactors. Predicted effluent EE2 concentrations were most sensitive to parameters affecting biodegradation including the biodegradation rate coefficient ($k_{bio,H}$), the influent bCOD/EE2 ratio, and the aerobic SRT. EE2-3S deconjugation kinetics indicated that EE2 can be appreciably produced during AS treatment. While predicted effluent EE2 concentrations were relatively insensitive to the deconjugation rate coefficient ($k_{cle,H}$), the $k_{cle,H}/k_{bio,H}$ ratio may be an important consideration in evaluating effluent EE2 concentrations for AS systems with lower $k_{bio,H}$ values. Staged aerobic CSTR designs have the potential to achieve high EE2 removals.

Acknowledgements

57

3.7 Supplemental Information

This *Supplemental Information* includes: details of the lab-scale SBR operations, methods for estrogen analyses, and a description of the modifications made to the IWA ASM2d.

Lab-scale SBR Operations

Approximately one-fourth of the reactor volume was decanted and replaced with primary effluent each cycle. The primary effluent was drawn from a feed container that was replenished daily, and the feed volume per cycle ranged from 1050 mL when the feed container was full to 850 mL prior to the feed container being refilled. An average volume of 950 mL was used for the model simulations. The primary effluent constituents and fractions are summarized in Table 3-7. In addition, the SBRs received a supplemental solution containing acetate, estrogens, and PO_4-P. The volume of supplemental solution delivered per cycle averaged 9.4, 8.5, and 9.1 mL for the aerobic-only, anoxic/aerobic, and anaerobic/aerobic SBR. For model simulations of the Phase III SBRs, a volume of 9.4 and 9.1 mL was used for the aerobic-only SBR with and without supplemental acetate, respectively. Constituent concentrations of the supplemental solution and the resultant SBR feed concentration are shown in Table 3-8.

Table 3-7. Characterization of primary effluent fed reactors

Definition	Symbol	Unit	Phase I	Phase II	Phase III	Source
Average constituents						
Total chemical oxygen demand	COD_{inf}	mg COD L^{-1}	265	253	225	Measurements collected 3 times weekly
COD in filtered sample	$COD_{f,inf}$	mg COD L^{-1}	121	114	99	Measurements collected 3 times weekly
Total suspended solids	TSS_{inf}	mg L^{-1}	60	66	53	Measurements collected 5 times weekly
Volatile suspended solids	VSS_{inf}	mg L^{-1}	53	59	47	Measurements collected 5 times weekly
Ammonia in filtered sample	$NH_3\text{-}N_{inf}$	mg N L^{-1}	32	29	31	Measurements collected 3 times weekly
Total Kjeldahl nitrogen	TKN_{inf}	mg N L^{-1}	59	54	57	Calculated as: $NH_3\text{-}N_{inf}/0.54$[a]
Ortho-phosphate in filtered sample	$PO_4\text{-}P_{inf}$	mg P L^{-1}	2.7	1.3	3.1	Measurements collected 3 times weekly
Total phosphorus	TP_{inf}	mg P L^{-1}	5.0	3.5	5.0	Calculated as: $PO_4\text{-}P_{inf} + 0.01 \cdot (S_F + X_I + X_S)$[b]
Organic components						
5-day biochemical oxygen demand	$BOD_{5,inf}$	mg COD L^{-1}	152	145	129	Calculated as: $COD_{inf}/1.74$[c]
Total biochemical oxygen demand	$BOD_{ult,inf}$	mg COD L^{-1}	203	194	172	Calculated as: $BOD_{5,inf}/fbod$
Inert soluble COD	S_I	mg COD L^{-1}	20	21	22	Effluent soluble COD collected 3 times weekly
Biodegradable soluble COD	S_S	mg COD L^{-1}	101	93	77	Calculated as: $COD_{f,inf} - S_I$
Fermentation products (VFA[d])	S_A	mg COD L^{-1}	15	14	12	Calculated as: $0.15 \cdot S_S$[e]
Fermentable soluble COD	S_F	mg COD L^{-1}	86	79	65	Calculated as: $S_S - S_A$
Inert particulate COD	X_I	mg COD L^{-1}	42	38	31	Calculated as: $COD_{inf} - S_I - S_S - X_S$
Biodegradable particulate COD	X_S	mg COD L^{-1}	102	101	95	Calculated as: $BOD_{ult,inf} - S_S$
Fractions						
Particulate COD/VSS ratio	icv	g COD g VSS^{-1}	2.7	2.4	2.7	Calculated as: $(COD_{inf} - COD_{f,inf})/VSS_{inf}$
BOD$_5$/BOD$_{ult}$ ratio	$fbod$	-	0.75	0.75	0.75	Hydromantis default value for primary effluent
VSS/TSS ratio	ivt	g VSS g TSS^{-1}	0.88	0.89	0.89	Calculated as: VSS_{inf}/TSS_{inf}
Soluble fraction of total COD	$frscod$	-	0.46	0.45	0.44	Calculated as: $COD_{f,inf}/COD_{inf}$
Inert fraction of soluble COD	$frsi$	-	0.17	0.18	0.22	Calculated as: $S_I/(S_I + S_S)$
VFA fraction of soluble COD	$frslf$	-	0.13	0.12	0.12	Calculated as: $S_A/(S_I + S_S)$
Substrate fraction of particulate COD	$frxs$	-	0.71	0.73	0.76	Calculated as: $X_S/(X_I + X_S)$

a. Used average $NH_3\text{-}N_{inf}/TKN_{inf}$ ratio of 0.54 based on two sample measurements
b. Used IWA ASM2d value of 0.01 g P g COD^{-1} for P content of S_F, X_I, and X_S
c. Used average $COD_{inf}/BOD_{5,inf}$ ratio of 1.74 based on four sample measurements
d. VFA - volatile fatty acid
e. Used default value of EnviroSim Associates Ltd., BioWin 4.0 simulator of 0.15 for VFA fraction of S_S

59

Table 3-8. Constituent concentrations in supplemental feed stock solution and SBR influent

Phase	COD (mg L^{-1})	PO$_4$-P (mg L^{-1})	Estrogens (ng L^{-1}) E1	E2	EE2	E1-3S	E2-3S	EE2-3S
			Supplemental Feed Stock Solution					
I[a,b]	11,000	410	12,700	12,600	12,200	-	-	-
II[a]	11,000	410	12,700 - 18,100	12,600 - 3,300	12,200	12,000	13,500	14,100
III[c]	10,600	410	20,900	5,700	12,100	-	-	-
III[d]	-	390	17,300	1,200	8,200	-	-	-
			SBR Feed (primary effluent plus supplemental solution)					
I[e]	369	6.6	154	135	116	-	-	-
II[e]	357	5.2	154 - 205	135 - 47	116	127	128	134
III[c]	330	7.2	207	56	120	-	-	-
III[d]	225	6.8	166	11	79	-	-	-

a. Anoxic/aerobic SBR also received supplemental NO$_3$-N of 1,200 mg L^{-1}

b. Assumed same values as Phase II

c. Supplemental feed for SBR with supplemental acetate

d. Supplemental feed for SBR without supplemental acetate

e. Anoxic/aerobic SBR also received supplemental NO$_3$-N of 11 mg L^{-1}

Estrogen analyses

Free estrogens, estrone (E1), 17β-estradiol (E2) and 17α-ethynylestradiol (EE2), and conjugated estrogens, E1-3-sulfate sodium salt (E1-3S) and E2-3-sulfate sodium salt (E2-3S), were purchased from Sigma Aldrich (St. Louis, MO). EE2-3-sulfate sodium salt (EE2-3S) was obtained from Steraloids (Newport, RI). Deuterated labeled internal standards, E1-2,4,16,16-d_4 (d_4E1), E2-2,4,16,16-d_4 (d_4E2), EE2-2,4,16,16-d_4 (d_4EE2), and E2-3S-2,4,16,16-d_4 sodium salt (d_4E2-3S), were purchased from C/D/N Isotopes, Inc. (Pointe-Claire, QC, Canada). HPLC grade acetonitrile (ACN), methanol (MeOH), and water (H_2O) were supplied by EMD Chemicals (Billerica, MA). Individual stock solutions were prepared in MeOH and stored at -20ºC. Individual working solutions were prepared in Milli-Q water and stored at 4ºC.

Free estrogen measurements during Phase I and III. Free estrogen (E1, E2, and EE2) measurements were conducted according to a modified method from Gaulke et al. (2008). Briefly, 50 pg of each internal standard (d_4E1, d_4E2 and d_4EE2) was added to 500 µL of sample. For total estrogen measurements, the sample consisted of the mixed liquor containing both the aqueous and solid fractions. For soluble estrogen measurements, the sample consisted of the supernatant after centrifuging the mixed liquor at 3200 rpm for 10 minutes at 4°C. A liquid-liquid extraction was performed on the sample with 3 mL of ethyl acetate, and the organic fraction was transferred to a clean tube and evaporated to dryness with a gentle stream of nitrogen gas at 40°C. Samples were reconstituted with 100 µL of $NaHCO_3$ buffer (pH 10.5) and 100 µL of 1 mg/mL dansyl chloride in ACN and heated at 60°C for 30 minutes.

Estrogen analysis was performed using a Shimadzu LC-20AD high performance liquid chromatograph (Kyoto, Japan) and an Applied Biosystems 4000 QTrap tandem mass

spectrometer (Foster City, CA) (LC-MS/MS). Estrogen separation was achieved by injecting 20 µL of derivatized sample onto a Phenomenex Luna Phenyl-Hexyl column (50 x 3.0 mm id., 3 µm particle size) with a flow rate of 0.5 mL/min and mobile phases of 0.1% formic acid in H_2O (A) and ACN (B). Solvent B initially eluted at 50%, linearly increased to 95% within 3 minutes, remained isocratic to 5 minutes, returned to 50% within 5.1 minutes and re-equilibrated to 8 minutes. The MS/MS was equipped with an electrospray ionization (ESI) source and operated in positive ion mode with an ion spray voltage of 5000 volts. The transitions for E1, d_4E1, E2, d_4E2, EE2, and d_4EE2 were monitored at *m/z* 504.2 > 171.3, 508.2 > 171.3, 506.2 > 171.3, 510.2 > 171.3, 530.0 > 171.3, 534.0 > 171.3, respectively. The collision energy was 50 eV and the dwell time was 0.15 seconds for all compounds. Calibration standards contained 1, 5, 10, 25, 50, 100, 250, 500 and 1000 ng/L E1, E2 and EE2 and 100 ng/L of d_4E1, d_4E2 and d_4EE2. The limit of detection (LOD) for the method was 1 ng/L (signal-to-noise ratio of 3:1) and the method limit of quantification (LOQ) was 5 ng/L (signal-to-noise ratio of 10:1).

Free and conjugated estrogen measurements during Phase II. Soluble free estrogen (E1, E2, and, EE2) and conjugated estrogen (E1-3S, E2-3S, and EE2-3S) measurements were conducted according to a modified method from Kumar et al. (2009b). Samples (50 mL) were filtered through a 0.7 µm glass fiber filter (Whatman GF/F) and acidified with 50 µL of acetic acid. In addition, 10 ng of each internal standard (d_4E2, d_4EE2, and d_4E2-3S) was added to the sample. Samples were cleaned and concentrated using an AutoTrace Solid Phase Extraction (SPE) Workstation (Caliper Life Sciences, Hopkinton, MA) according to Kumar et al. (2009) with the following exceptions. Cartridges were washed with 6 mL of 60:40 Milli Q water:MeOH (rather than 5 mL of Milli Q water) and dried for 30 minutes (rather than 1 hour) before eluting the free

62

and conjugated estrogens in separate fractions. Final eluates were dried under a gentle stream of nitrogen gas at 40°C. Samples were reconstituted with 200 µL of 1:1 ACN:H$_2$O and analyzed using LC-MS/MS.

For the free estrogens, separation was achieved by injecting 20 µL of reconstituted sample onto a Phenomenex Luna Phenyl-Hexyl column (50 x 3.0 mm id., 3 µm particle size) with a flow rate of 0.5 mL/min and mobile phases of 0.1% formic acid in H$_2$O (A) and ACN (B). Solvent B initially eluted at 30%, linearly increased to 50% within 1 minute, linearly increased to 90% within 6 minutes, remained isocratic to 8 minutes, returned to 30% within 8.1 minutes and re-equilibrated to 12 minutes. The MS/MS was equipped with a positive atmospheric pressure chemical ionization (APCI) source and operated in positive ion mode with an ion spray voltage of 4500 volts. The transitions for E1, E2, d$_4$E2, EE2, and d$_4$EE2 were monitored at *m/z* 271.1 > 133.1, 255.1 > 159.1, 259.1 > 161.1, 279.1 > 133.1, and 283.1 > 135.1, respectively. The collision energy was 28 eV for E1 and 25 eV for all other compounds. The dwell time was 0.15 seconds. Free estrogen calibration standards contained 1, 5, 10, 25, 50, and 100 µg/L of E1, E2, and EE2 and 50 µg/L of d$_4$E2 and d$_4$EE2. The method detection limit (MDL) was 2 ng/L for E1 and E2 and 1 ng/L for EE2 according to standard methods (APHA, 2005). The method LOQ was 5 ng/L for E1 and E2 and 3 ng/L for EE2 (MDL:LOQ ratio of 4:10).

For the conjugated estrogens, separation was achieved by injecting 20 µL of reconstituted sample onto an Inertsil ODS-3 column (150 x 2.1 mm id., 5 µm particle size) with a flow rate of 0.5 mL/min and mobile phases of 20 mM ammonium acetate in H$_2$O (A) and ACN (B). Solvent B initially eluted at 20%, remained isocratic to 2 minutes, linearly increased to 50% within 4

minutes, linearly increased to 90% within 7 minutes, remained isocratic to 10 minutes, returned to 20% within 10.1 minutes and re-equilibrated to 12 minutes. The MS/MS was equipped with an ESI source and operated in negative ion mode with an ion spray voltage of -4500 volts. The transitions for E1-3S, E2-3S, d_4E2-3S, and EE2-3S were monitored at m/z 349.1 > 268.7, 351.1 > 270.8, 355.2 > 275.4, and 375.3 > 295.0, respectively. The collision energy was -50 eV for EE2-3S and -34 eV for all other compounds. The dwell time was 0.15 seconds. Conjugated estrogen calibration standards contained 1, 5, 10, 25, 50, and 100 µg/L of E1-3S, E2-3S, and EE2-3S and 50 µg/L of d_4E2-3S. The MDL was 1 ng/L for E1-3S and EE2-3S and 2 ng/L for E2-3S according to standard methods (APHA, 2005). The method LOQ was 3 ng/L for E1-3S and EE2-3S and 5 ng/L for E2-3S (MDL:LOQ ratio of 4:10).

Modifications to the IWA ASM2d

Four model component were introduced to the modified ASM2d: nitrate, (S_{NO3}, g N m^{-3}), nitrite (S_{NO2}, g N m^{-3}), ammonia oxidizing bacteria (X_{AOB}, g COD m^{-3}), and nitrite oxidizing bacteria (X_{NOB}, g COD m^{-3}). S_{NO3} and S_{NO2} replaced the ASM2d component of S_{NO3} (nitrate plus nitrite nitrogen). X_{AOB} and X_{NOB} replaced the ASM2d component of X_{AUT} (autotrophic, nitrifying biomass). Conversion factors (i_{ci}) to convert the units of component i to units of material c to be applied in the conservation equation (Equation 2 in Henze et al., 1999) are as follows: $i_{COD,NO2}$ of -48/14 g COD g N^{-1}, $i_{N,NO2}$ of 1 g N g N^{-1}, and $i_{Charge,NO2}$ of -1/14 moles+ g N^{-1}. Conversion factors for S_{NO3} are the same as for the original ASM2d S_{NO3}. Conversion factors for X_{AOB} and X_{NOB} are the same as for the original ASM2d X_{AUT}.

Modified and new process rate equations of the IWA ASM2d are shown in Table 3-9 where ρ_j refers to process rate equation j in Table 7 of Henze et al. (1999). New stoichiometric and kinetic parameters added to the ASM2d along with their default values are shown in Table 3-10. Nomenclature for original ASM2d variables presented below are provided in Table 3-11.

Nitrogen switching functions were modified using the new variables S_{NO3} and S_{NO2} and a new half saturation coefficient K_{NOX} resulting in modified hydrolysis and fermentation process equations (ρ_2, ρ_3, and ρ_8).

Denitrification was modeled as a two-step process using the same approach as Kaelin et al. (2009) applied for extension of the IWA ASM3. The original ASM2d models denitrification as a single-step process where a fraction of the heterotrophic and PAO biomass utilizes nitrate as an

65

electron acceptor with complete reduction to dinitrogen. The modified ASM2d includes nitrite as an intermediate product of denitrification, resulting in two rate equations for each denitrification process. The first equation bases anoxic respiration on nitrate serving as electron acceptor with reduction to nitrite. The second equation is based on nitrite serving as electron acceptor with reduction to dinitrogen. New anoxic reduction factors ($\eta_{NO3,H}$, $\eta_{NO2,H}$, $\eta_{NO3,PAO}$, and $\eta_{NO2,PAO}$) were introduced to reflect the fraction of heterotrophic and PAO biomass growth attributed to the specific electron acceptor. This ensures the summation of anoxic growth rates from respiration on both nitrate and nitrite does not exceed the maximum growth rate. Default values of the new anoxic reduction factors were calculated as a fraction of the original value based on the electron acceptor equivalence. Therefore, default values of $\eta_{NO3,H}$ and $\eta_{NO3,PAO}$ are 2/5 of the original value while default values of $\eta_{NO2,H}$ and $\eta_{NO2,PAO}$ are 3/5 of the original value (2 e^- for reduction of nitrate to nitrite and 3e^- for reduction of nitrite to dinitrogen). This model assumes the biomass yield on an electron basis is the same for nitrate and nitrite as electron acceptor (Koike and Hattori, 1975). Half-saturation coefficients for nitrate and nitrite (K_{NO3} and K_{NO2}) were also added to the ASM2d. The model expansion to a two-step denitrification process resulted in modified equations for anoxic growth (ρ_6, ρ_7, ρ_{14}, ρ_{22}, ρ_{23}, and $\rho_{25)}$ and polyphosphate storage (ρ_{12} and $\rho_{24)}$.

Nitrification was modeled as a two-step process where ammonia is first oxidized to nitrite which is further oxidized to nitrate. The original ASM2d models nitrification as a single-step with complete oxidization of ammonia to nitrate by nitrifying organisms. Nitritation (ammonia oxidation to nitrite) and nitratation (nitrite oxidation to nitrate) are carried out by different autotrophic populations in activated sludge treatment. The ASM2d was therefore modified to

66

have two distinct autotrophic biomasses, ammonia oxidizing bacteria (X_{AOB}) and nitrite oxidizing bacteria (X_{NOB}), with kinetic and stoichiometric parameters specific to each biomass. The modified ASM2d includes equations for aerobic growth of X_{AOB} and X_{NOB} (ρ_{18} and $\rho_{26)}$ on ammonia and nitrite, respectively, as well as lysis of X_{AOB} and X_{NOB} (ρ_{19} and ρ_{27}) based on specific lysis rate constants (b_{AOB} and b_{NOB}).

In addition, reduction factors for cell lysis as has been observed under anoxic and anaerobic conditions (Lopez et al., 2006; Munz et al., 2011; Salem et al., 2006; Siegrist et al., 1999) were introduced for all biomass types resulting in modified lysis equations (ρ_9, $\rho_{15,}$ $\rho_{19,}$ and ρ_{27}). Lysis rate equations for polyphosphate and polyhydroxy-alkanoates (ρ_{16} and ρ_{17}) were similarly modified so that the PAO storage products decay together with the PAO biomass.

Table 3-9. Modified and new process rate equations (highlighted in bold) of the ASM2d

j	Process	Process rate equation ρ_i
Hydrolysis of particulate substrate		
2	Anoxic hydrolysis	$K_h \cdot \eta_{NO3} \cdot \dfrac{K_{O2}}{K_{O2}+S_{O2}} \cdot \dfrac{S_{NO3}+S_{NO2}}{K_{NOX}+S_{NO3}+S_{NO2}} \cdot \dfrac{X_S/X_H}{K_X+X_S/X_H} \cdot X_H$
3	Anaerobic hydrolysis	$K_h \cdot \eta_{fe} \cdot \dfrac{K_{O2}}{K_{O2}+S_{O2}} \cdot \dfrac{K_{NOX}}{K_{NOX}+S_{NO3}+S_{NO2}} \cdot \dfrac{X_S/X_H}{K_X+X_S/X_H} \cdot X_H$
Heterotrophic biomass (X_H)		
6	Denitrification with S_F using S_{NO3}	$\mu_H \cdot \eta_{NO3,H} \cdot \dfrac{S_{NO3}}{K_{NO3}+S_{NO3}} \cdot \dfrac{K_{O2}}{K_{O2}+S_{O2}} \cdot \dfrac{S_F}{K_F+S_F} \cdot \dfrac{S_F}{S_F+S_A} \cdot \dfrac{S_{NH4}}{K_{NH4}+S_{NH4}} \cdot \dfrac{S_{PO4}}{K_P+S_{PO4}} \cdot \dfrac{S_{ALK}}{K_{ALK}+S_{ALK}} \cdot X_H$
22	**Denitrification with S_F using S_{NO2}**	$\mu_H \cdot \eta_{NO2,H} \cdot \dfrac{S_{NO2}}{K_{NO2}+S_{NO2}} \cdot \dfrac{K_{O2}}{K_{O2}+S_{O2}} \cdot \dfrac{S_F}{K_F+S_F} \cdot \dfrac{S_F}{S_F+S_A} \cdot \dfrac{S_{NH4}}{K_{NH4}+S_{NH4}} \cdot \dfrac{S_{PO4}}{K_P+S_{PO4}} \cdot \dfrac{S_{ALK}}{K_{ALK}+S_{ALK}} \cdot X_H$
7	Denitrification with S_A using S_{NO3}	$\mu_H \cdot \eta_{NO3,H} \cdot \dfrac{S_{NO3}}{K_{NO3}+S_{NO3}} \cdot \dfrac{K_{O2}}{K_{O2}+S_{O2}} \cdot \dfrac{S_A}{K_A+S_A} \cdot \dfrac{S_A}{S_F+S_A} \cdot \dfrac{S_{NH4}}{K_{NH4}+S_{NH4}} \cdot \dfrac{S_{PO4}}{K_P+S_{PO4}} \cdot \dfrac{S_{ALK}}{K_{ALK}+S_{ALK}} \cdot X_H$
23	**Denitrification with S_A using S_{NO2}**	$\mu_H \cdot \eta_{NO2,H} \cdot \dfrac{S_{NO2}}{K_{NO2}+S_{NO2}} \cdot \dfrac{K_{O2}}{K_{O2}+S_{O2}} \cdot \dfrac{S_A}{K_A+S_A} \cdot \dfrac{S_A}{S_F+S_A} \cdot \dfrac{S_{NH4}}{K_{NH4}+S_{NH4}} \cdot \dfrac{S_{PO4}}{K_P+S_{PO4}} \cdot \dfrac{S_{ALK}}{K_{ALK}+S_{ALK}} \cdot X_H$
8	Fermentation	$q_{fe} \cdot \dfrac{K_{O2}}{K_{O2}+S_{O2}} \cdot \dfrac{K_{NOX}}{K_{NOX}+S_{NO3}+S_{NO2}} \cdot \dfrac{S_F}{K_F+S_F} \cdot \dfrac{S_{ALK}}{K_{ALK}+S_{ALK}} \cdot X_H$
9	Lysis of X_H	$b_H \cdot \left[\dfrac{S_{O2}}{K_{O2}+S_{O2}} + \eta_{b,H} \cdot \dfrac{K_{O2}}{K_{O2}+S_{O2}} \right] \cdot X_H$
Polyphosphate accumulating biomass (X_{PAO})		
12	Anoxic storage of X_{PP} using S_{NO3}	$q_{PP} \cdot \eta_{NO3,PAO} \cdot \dfrac{S_{NO3}}{K_{NO3}+S_{NO3}} \cdot \dfrac{K_{O2}}{K_{O2}+S_{O2}} \cdot \dfrac{S_{PO4}}{K_{PS}+S_{PO4}} \cdot \dfrac{S_{ALK}}{K_{ALK}+S_{ALK}} \cdot \dfrac{\frac{X_{PHA}}{X_{PAO}}}{K_{PHA}+\frac{X_{PHA}}{X_{PAO}}} \cdot \dfrac{K_{MAX}-\frac{X_{PP}}{X_{PAO}}}{K_{PP}+K_{MAX}-\frac{X_{PP}}{X_{PAO}}} \cdot X_{PAO}$
24	**Anoxic storage of X_{PP} using S_{NO2}**	$q_{PP} \cdot \eta_{NO2,PAO} \cdot \dfrac{S_{NO2}}{K_{NO2}+S_{NO2}} \cdot \dfrac{K_{O2}}{K_{O2}+S_{O2}} \cdot \dfrac{S_{PO4}}{K_{PS}+S_{PO4}} \cdot \dfrac{S_{ALK}}{K_{ALK}+S_{ALK}} \cdot \dfrac{\frac{X_{PHA}}{X_{PAO}}}{K_{PHA}+\frac{X_{PHA}}{X_{PAO}}} \cdot \dfrac{K_{MAX}-\frac{X_{PP}}{X_{PAO}}}{K_{PP}+K_{MAX}-\frac{X_{PP}}{X_{PAO}}} \cdot X_{PAO}$
14	Anoxic growth on X_{PHA} using S_{NO3}	$\mu_{PAO} \cdot \eta_{NO3,PAO} \cdot \dfrac{S_{NO3}}{K_{NO3}+S_{NO3}} \cdot \dfrac{K_{O2}}{K_{O2}+S_{O2}} \cdot \dfrac{S_{NH4}}{K_{NH4}+S_{NH4}} \cdot \dfrac{S_{PO4}}{K_P+S_{PO4}} \cdot \dfrac{S_{ALK}}{K_{ALK}+S_{ALK}} \cdot \dfrac{X_{PHA}/X_{PAO}}{K_{PHA}+X_{PHA}/X_{PAO}} \cdot X_{PAO}$
25	**Anoxic growth on X_{PHA} using S_{NO2}**	$\mu_{PAO} \cdot \eta_{NO2,PAO} \cdot \dfrac{S_{NO2}}{K_{NO2}+S_{NO2}} \cdot \dfrac{K_{O2}}{K_{O2}+S_{O2}} \cdot \dfrac{S_{NH4}}{K_{NH4}+S_{NH4}} \cdot \dfrac{S_{PO4}}{K_P+S_{PO4}} \cdot \dfrac{S_{ALK}}{K_{ALK}+S_{ALK}} \cdot \dfrac{X_{PHA}/X_{PAO}}{K_{PHA}+X_{PHA}/X_{PAO}} \cdot X_{PAO}$
15	Lysis of X_{PAO}	$b_{PAO} \cdot \left[\dfrac{S_{O2}}{K_{O2}+S_{O2}} + \eta_{b,PAO} \cdot \dfrac{K_{O2}}{K_{O2}+S_{O2}} \right] \cdot \dfrac{S_{ALK}}{K_{ALK}+S_{ALK}} \cdot X_{PAO}$
16	Lysis of X_{PP}	$b_{PP} \cdot \left[\dfrac{S_{O2}}{K_{O2}+S_{O2}} + \eta_{b,PAO} \cdot \dfrac{K_{O2}}{K_{O2}+S_{O2}} \right] \cdot \dfrac{S_{ALK}}{K_{ALK}+S_{ALK}} \cdot X_{PP}$
17	Lysis of X_{PHA}	$b_{PHA} \cdot \left[\dfrac{S_{O2}}{K_{O2}+S_{O2}} + \eta_{b,PAO} \cdot \dfrac{K_{O2}}{K_{O2}+S_{O2}} \right] \cdot \dfrac{S_{ALK}}{K_{ALK}+S_{ALK}} \cdot X_{PHA}$
Ammonia oxidizing biomass (X_{AOB})		
18	Aerobic growth of X_{AOB}	$\mu_{AOB} \cdot \dfrac{S_{O2}}{K_{O2,AOB}+S_{O2}} \cdot \dfrac{S_{NH4}}{K_{NH4,AOB}+S_{NH4}} \cdot \dfrac{S_{PO4}}{K_{PO4}+S_{PO4}} \cdot \dfrac{S_{ALK}}{K_{ALK}+S_{ALK}} \cdot X_{AOB}$
19	Lysis of X_{AOB}	$b_{AOB} \cdot \left[\dfrac{S_{O2}}{K_{O2}+S_{O2}} + \eta_{b,AOB} \cdot \dfrac{K_{O2}}{K_{O2}+S_{O2}} \right] \cdot X_{AOB}$
Nitrite oxidizing biomass (X_{NOB})		
26	**Aerobic growth of X_{NOB}**	$\mu_{NOB} \cdot \dfrac{S_{O2}}{K_{O2,NOB}+S_{O2}} \cdot \dfrac{S_{NO2}}{K_{NO2,NOB}+S_{NO2}} \cdot \dfrac{S_{PO4}}{K_{PO4}+S_{PO4}} \cdot \dfrac{S_{ALK}}{K_{ALK}+S_{ALK}} \cdot X_{NOB}$
27	**Lysis of X_{NOB}**	$b_{NOB} \cdot \left[\dfrac{S_{O2}}{K_{O2}+S_{O2}} + \eta_{b,NOB} \cdot \dfrac{K_{O2}}{K_{O2}+S_{O2}} \right] \cdot X_{NOB}$

Table 3-10. Stoichiometric and kinetic parameters added to the modified IWA ASM2d

Symbol	Definition	Unit	Value (20°C)	Source[a]
Heterotrophic biomass (X_H)				
$Y_{H,NOX}$	Anoxic yield	g COD g COD^{-1}	0.54	(1)
$\eta_{NO3,H}$	Anoxic reduction factor for NO$_3^-$ to NO$_2^-$	-	0.32	See note[b]
$\eta_{NO2,H}$	Anoxic reduction factor for NO$_2^-$ to N$_2$	-	0.48	See note[b]
$\eta_{b,H}$	Reduction factor for lysis	-	0.5	(2)
Polyphosphate accumulating biomass (X_{PAO})				
$Y_{PAO,NOX}$	Anoxic yield	g COD g COD^{-1}	0.5	(3)
$\eta_{NO3,PAO}$	Anoxic reduction factor for NO$_3^-$ to NO$_2^-$	-	0.24	See note[b]
$\eta_{NO2,PAO}$	Anoxic reduction factor for NO$_2^-$ to N$_2$	-	0.36	See note[b]
$\eta_{b,PAO}$	Reduction factor for lysis	-	0.33	(3)
Ammonia oxidizing biomass (X_{AOB})				
Y_{AOB}	Yield of X$_{AOB}$	g COD g N^{-1}	0.22	(4)[c]
μ_{AOB}	Maximum growth rate	d^{-1}	0.9	(4)
b_{AOB}	Rate constant for lysis	d^{-1}	0.17	(4)
$\eta_{b,AOB}$	Reduction factor for lysis	-	0.5	(5)
$K_{O2,AOB}$	Saturation coefficient for oxygen	g O$_2$ m^{-3}	0.5	(4)
$K_{NH4,AOB}$	Saturation coefficient for ammonium	g N m^{-3}	0.5	(4)
Nitrite oxidizing biomass (X_{NOB})				
Y_{NOB}	Yield of X$_{NOB}$	g COD g N^{-1}	0.07	(4)[c]
μ_{NOB}	Maximum growth rate	d^{-1}	1.0	(4)
b_{NOB}	Rate constant for lysis	d^{-1}	0.17	(4)
$\eta_{b,NOB}$	Reduction factor for lysis	-	0.5	(5)
$K_{O2,NOB}$	Saturation coefficient for oxygen	g O$_2$ m^{-3}	0.9	(4)
$K_{NO2,NOB}$	Saturation coefficient for nitrite	g N m^{-3}	0.2	(4)
Half-saturation coefficients				
K_{NO3}	Saturation/inhibition coefficient for nitrate	g N m^{-3}	0.5	(6)
K_{NO2}	Saturation/inhibition coefficient for nitrite	g N m^{-3}	0.5	(6)
K_{NOX}	Saturation/inhibition coefficient for nitrate plus nitrite	g N m^{-3}	0.5	(6)

a. Source: (1) Gujer et al. (1999); (2) Koch et al. (2000); (3) Rieger et al. (2001); (4) Tchobanoglous et al. (2014); (5) Salem et al. (2006); (6) Henze et al. (1999)

b. Anoxic reduction factor of the original ASM2d (Henze et al., 1999) redefined as anoxic reduction factor for NO$_3^-$ to NO$_2^-$ calculated as 2/5 of original value and anoxic reduction factor for NO$_2^-$ to N$_2$ calculated as 3/5 of original value

c. Converted yield to g COD g N^{-1} from g VSS g N^{-1} using ASM2d conversion factor of 1.48 g COD g VSS^{-1}

69

Table 3-11. Nomenclature of select model components and parameters of the IWA ASM2d

Symbol	Definition	Unit
Model components		
S_{O2}	Dissolved oxygen	g O_2 m^{-3}
S_F	Readily biodegradable substrate	g COD m^{-3}
S_A	Fermentation products	g COD m^{-3}
S_{NH4}	Ammonium	g N m^{-3}
S_{PO4}	Phosphate	g P m^{-3}
S_{ALK}	Bicarbonate alkalinity	mole HCO_3^- m^{-3}
X_S	Slowly biodegradable substrate	g COD m^{-3}
X_{PP}	Stored polyphosphate of PAO	g P m^{-3}
X_{PHA}	Organic storage products of PAO	g COD m^{-3}
Hydrolysis of particulate substrate		
K_h	Hydrolysis rate constant	d^{-1}
η_{NO3}	Anoxic hydrolysis reduction factor	-
η_{fe}	Anaerobic hydrolysis reduction factor	-
Heterotrophic biomass (X_H)		
μ_H	Maximum growth rate	d^{-1}
q_{fe}	Maximum rate for fermentation	g S_F g X_H^{-1} d^{-1}
b_H	Rate constant for lysis	d^{-1}
Polyphosphate accumulating biomass (X_{PAO})		
μ_{PAO}	Maximum growth rate	d^{-1}
q_{PP}	Rate constant for storage of X_{PP}	g X_{PP} g X_{PAO}^{-1} d^{-1}
b_{PAO}	Rate constant for lysis	d^{-1}
K_{MAX}	Maximum ratio of X_{PP}/X_{PAO}	g X_{PP}^{-1} g X_{PAO}^{-1}
Y_{PHA}	PHA requirement for polyphosphate storage	g COD g P^{-1}
All biomass:		
f_{XI}	Fraction of inert COD generated in biomass lysis	g COD g COD^{-1}
Half-saturation coefficients		
K_{O2}	Saturation/inhibition coefficient for oxygen	g O_2 m^{-3}
K_X	Saturation coefficient for particulate COD	g X_S g X_H^{-1}
K_{NH4}	Saturation coefficient for ammonium	g N m^{-3}
K_{ALK}	Saturation coefficient for alkalinity	mole HCO_3^- m^{-3}
K_F	Saturation coefficient for S_F	g COD m^{-3}
K_A	Saturation coefficient for S_A	g COD m^{-3}
K_P	Saturation coefficient for phosphorus	g P m^{-3}
K_{PS}	Saturation coefficient for phosphorus in storage of X_{PP}	g P m^{-3}
K_{PP}	Saturation coefficient for polyphosphate	g X_{PP} g X_{PAO}^{-1}
K_{PHA}	Saturation coefficient for X_{PHA}	g X_{PHA} g X_{PAO}^{-1}

The stoichiometric matrix for the IWA ASM2d was modified as shown in Table 3-12. Stoichiometry for S_{O2}, S_{NH4}, S_{PO4}, S_{ALK} and X_{TSS} were computed from conservation.

Table 3-12. Stoichiometric matrix of the modified IWA ASM2d

Process	S_F	S_A	S_{NO3}	S_{NO2}	S_{N2}	X_I	X_S	X_H	X_{PAO}	X_{PP}	X_{PHA}	X_{AOB}	X_{NOB}
ρ6	$-\dfrac{1}{Y_{H,NOX}}$		$-\dfrac{(1-Y_{H,NOX})}{(1.14 \cdot Y_{H,NOX})}$	$\dfrac{(1-Y_{H,NOX})}{(1.14 \cdot Y_{H,NOX})}$				1					
ρ7		$-\dfrac{1}{Y_{H,NOX}}$	$-\dfrac{(1-Y_{H,NOX})}{(1.14 \cdot Y_{H,NOX})}$	$\dfrac{(1-Y_{H,NOX})}{(1.14 \cdot Y_{H,NOX})}$				1					
ρ12			$-\dfrac{Y_{PHA}}{1.14}$	$\dfrac{Y_{PHA}}{1.14}$						1	$-Y_{PHA}$		
ρ14			$-\dfrac{(1-Y_{PAO,NOX})}{(1.14 \cdot Y_{PAO,NOX})}$	$\dfrac{(1-Y_{PAO,NOX})}{(1.14 \cdot Y_{PAO,NOX})}$					1		$-\dfrac{1}{Y_{PAO,NOX}}$		
ρ18				$\dfrac{1}{Y_{AOB}}$								1	
ρ19						f_{XI}	$1-f_{XI}$					-1	
ρ22	$-\dfrac{1}{Y_{H,NOX}}$			$-\dfrac{(1-Y_{H,NOX})}{(1.72 \cdot Y_{H,NOX})}$	$\dfrac{(1-Y_{H,NOX})}{(1.72 \cdot Y_{H,NOX})}$			1					
ρ23		$-\dfrac{1}{Y_{H,NOX}}$		$-\dfrac{(1-Y_{H,NOX})}{(1.72 \cdot Y_{H,NOX})}$	$\dfrac{(1-Y_{H,NOX})}{(1.72 \cdot Y_{H,NOX})}$			1					
ρ24				$-\dfrac{Y_{PHA}}{1.72}$	$\dfrac{Y_{PHA}}{1.72}$					1	$-Y_{PHA}$		
ρ25				$-\dfrac{(1-Y_{PAO,NOX})}{(1.72 \cdot Y_{PAO,NOX})}$	$\dfrac{(1-Y_{PAO,NOX})}{(1.72 \cdot Y_{PAO,NOX})}$				1		$-\dfrac{1}{Y_{PAO,NOX}}$		
ρ26			$\dfrac{1}{Y_{NOB}}$	$-\dfrac{1}{Y_{NOB}}$									1
ρ27						f_{XI}	$1-f_{XI}$						-1

71

Chapter 4: Biodegradation Kinetics of 17α-Ethinylestradiol in Activated Sludge Treatment Processes

Prepared for submittal to Environmental Engineering Science

4.1 Abstract

Biodegradation is the primary removal mechanism of the potent endocrine-disrupting estrogen 17α-ethinylestradiol (EE2) during activated sludge (AS) wastewater treatment. Analysis of AS treatment process designs to optimize EE2 removal requires the use of EE2 biodegradation kinetics. However, EE2 biodegradation kinetics for different types of systems and under long-term studies is poorly understood. We investigated EE2 biodegradation kinetics using lab-scale sequencing batch reactors (SBRs) at 20°C fed synthetic wastewater and simulating aerobic, anaerobic/aerobic enhanced biological phosphorus removal, and anoxic/aerobic biological nitrogen removal processes. Three sets of reactor experiments were conducted using different municipal AS plant seed sources and with solids retention times (SRTs) ranging from 8 to 13 days. Pseudo first-order biodegradation rate coefficients (k_b) normalized to the reactor volatile suspended solids (VSS) were determined from batch degradation tests and from calibration of a reactor process model. Significant EE2 biodegradation occurred only under aerobic conditions. Observed EE2 k_b values for aerobic, anaerobic/aerobic, and anoxic/aerobic operations ranged from 4 to 22 L/g VSS-d, 4 to 19 L/g VSS-d, and 3 to 20 L/g VSS-d, respectively. The k_b values varied over time during long-term operating conditions. There was no correlation between the k_b values and the fraction of ammonia-oxidizing bacteria in the reactor VSS. Model simulations to evaluate the sensitivity of effluent EE2 concentrations to k_b values showed that a longer SRT, an increased number of aerobic reactor stages, and a higher influent biochemical oxygen demand

(BOD) to EE2 ratio can produce conditions that result in lower and more consistent effluent EE2 concentrations.

4.2 Introduction

Municipal wastewater treatment plant (WWTP) effluents are major sources of endocrine disrupting compounds in the environment. Feminized fish are more abundant in surface waters receiving WWTP effluents compared to reference sites with minimal anthropogenic inputs (Bjerregaard et al., 2006; Bjorkblom et al., 2013; Jobling et al., 2006; Tetreault et al., 2011; Vajda et al., 2008; Woodling et al., 2006; Xie et al., 2010), an effect that has been linked to exposure to estrogenic compounds in the effluents. The natural estrogens, estrone (E1) and 17β-estradiol (E2), and the synthetic estrogen, 17α-ethinylestradiol (EE2), are major contributors to feminization (Korner et al., 2001; Miege et al., 2009; Nakada et al., 2004; Snyder et al., 2001). Of the estrogens, EE2 is the most difficult to degrade (Joss et al., 2004) and the most potent (Van den Belt et al., 2004) with a predicted no-effect concentration of 0.1 ng/L in surface waters (Caldwell et al., 2012). The impact of EE2 at such low concentration indicates the need to identify processes and designs that can minimize WWTP effluent EE2 concentrations.

EE2 influent concentrations and removal efficiencies vary for municipal activated sludge (AS) WWTPs. Influent concentrations range from below detection to 330 ng/L, with a mean of 30 ng/L and median of 5 ng/L; removal efficiencies range from 34 to 98 percent, with a mean and median of 61 and 69 percent, respectively (Baronti et al., 2000; Cargouet et al., 2004; Cicek et al., 2007; Clara et al., 2005; Johnson et al., 2000; Joss et al., 2004; Koh et al., 2009; Ternes et al., 1999b; Zhou et al., 2012). Biodegradation is responsible for greater than 90 percent of estrogen removals during AS wastewater treatment with the remainder removed by sorption to wasted

solids (Andersen et al., 2003; Joss et al., 2004; Muller et al., 2008; Zhou et al., 2012). Heterotrophic bacteria are primarily responsible for EE2 biodegradation in AS systems (Bagnall et al., 2012; Gaulke et al., 2008; McAdam et al., 2010; Zhou and Oleszkiewicz, 2010).

Mechanistic models that predict the fate of estrogens during AS treatment (Joss et al., 2004; Lust et al., 2012) represent biodegradation as a pseudo first-order rate by normalizing biodegradation kinetics to the mixed liquor total suspended solids or heterotrophic biomass concentration. Integration of an estrogen fate model with the a comprehensive activated sludge model, as was done by Lust et al. (2012, paper shown in Appendix I), provides a basis for predicting estrogen removal as a function of influent wastewater characteristics, process design configuration, and operational conditions. Since it is unlikely that all heterotrophic bacteria in an AS system degrade estrogen, this formulation implies that a fraction of the total biomass degrades estrogen and that the fraction is constant. Recognizing these limitations, the ability to relate biodegradation kinetics to the amount of biomass provides a basis for evaluating a given AS process design. Knowledge of estrogen biodegradation kinetics and how conditions affect the kinetics is needed for such a model to serve as a useful tool for analyzing the effect of wastewater characteristics, process design, and reactor configuration on effluent estrogen concentrations.

The types of AS processes used for municipal wastewater treatment are influenced by treatment needs for nitrogen and/or phosphorus removal. Due to these treatment needs, a growing number of WWTPs incorporate anaerobic and/or anoxic zones prior to the aerobic basins in single-sludge AS systems to promote biological nutrient removal (BNR). In the anaerobic selector basin in

74

these systems (no oxygen, no nitrate/nitrite), influent soluble biodegradable chemical oxygen demand (sbCOD) is consumed to support the growth of polyphosphate accumulating organisms (PAOs), which results in enhanced biological phosphorus removal (EBPR) (Tchobanoglous et al., 2014). Alternatively, in an anoxic selector basin (no oxygen, nitrate/nitrite present), influent sbCOD is consumed to promote the growth of heterotrophic denitrifying bacteria that use nitrate/nitrite as the terminal electron acceptor. These systems select for different populations based on the different metabolic conditions during substrate uptake, and there has been little work showing how estrogen degradation kinetics may be affected by these different BNR processes compared to aerobic treatment only.

Previous studies measuring estrogen biodegradation kinetics of AS from BNR processes (Gaulke et al., 2009; Joss et al., 2004) have been confined to batch tests conducted with grab mixed liquor samples from full and pilot-scale municipal wastewater treatment facilities. No study, to our knowledge, has adequately compared estrogen degradation kinetics at ng/L concentrations in BNR AS systems under controlled long-term operating conditions. Dytczak et al. (2008) conducted experiments with consideration of aerobic and anoxic/aerobic operations; however, initial estrogen concentrations of 5 mg/L were substantially higher than those found at WWTPs and may misrepresent activities in AS (Xu et al., 2009). The objective of this research was to further evaluate estrogen biodegradation kinetics and observe how these kinetics may be affected by AS process designs by operating parallel lab-scale sequencing batch reactors (SBRs) amended with ng/L estrogen concentrations.

4.3 Methods

Sequencing batch reactor description and operating conditions

Three sets of lab-scale SBRs were operated with different seed sources obtained from municipal WWTPs as summarized in Table 4-1. The first set of SBRs compared aerobic-only and anoxic/aerobic processes over three phases. The reactors were seeded with return activated sludge (RAS) from the City of Puyallup, WA anoxic-aerobic BNR process operated at a 10-day SRT. During Phase I, two anoxic/aerobic SBRs were operated in parallel at an 8-day SRT to assess differences in estrogen biodegradation kinetics between systems operated under the same conditions. During Phase II, the mixed liquor of the anoxic/aerobic SBRs from Phase I were combined and used to seed an aerobic-only and an anoxic/aerobic SBR with operation at an 8-day SRT. During Phase III, the SRT of the aerobic-only and anoxic/aerobic SBRs was increased to 13-days. The second set of SBRs compared anaerobic/aerobic and anoxic/aerobic processes at a 10-day SRT. These reactors were seeded with mixed liquor from the Durham, OR anaerobic-anoxic-aerobic BNR process operated at an 11-day SRT. The third set of SBRs compared aerobic-only, anaerobic/aerobic, and anoxic/aerobic processes at a 13-day SRT. The reactors were seeded with mixed liquor from the King County, Renton, WA anaerobic-aerobic BNR process operated at a 4-day SRT. Prior to the 13-day SRT operation, these SBRs were operated 115 days at an 8-day SRT without any estrogen addition to assure that EPBR was well established.

Table 4-1. Summary of lab-scale aerobic-only, anaerobic/aerobic, and anoxic/aerobic SBR operation (20°C)

Seed Source		SBR[a]	Total SRT (d)	Aerobic SRT (d)	Aerobic Period (hr)	Cycles per day	MLVSS[e] (mg/L)	pH[e]
City of Puyallup, WA WWTP	Phase I	Anoxic/Aerobic	8	5	2.5	6	992 ± 52	7.7 ± 0.4
		Anoxic/Aerobic					991 ± 55	7.6 ± 0.3
	Phase II[b]	Aerobic-Only	8	7	3.5	6	781 ± 59	7.3 ± 0.2
		Anoxic/Aerobic		5	2.5		908 ± 50	7.7 ± 0.3
	Phase III[c]	Aerobic-Only	13	12	5.5	4	1183 ± 47	7.2 ± 0.1
		Anoxic/Aerobic		10	4.5		1014 ± 91	7.8 ± 0.2
Durham, OR Advanced WWTF		Anaerobic/Aerobic	10	7.5	4.5	4	1037 ± 84	7.4 ± 0.2
		Anoxic/Aerobic					762 ± 97	7.8 ± 0.2
Renton, WA South WWTP		Aerobic-Only[d]	13	10	4.5	4	987 ± 128	7.3 ± 0.1
		Anaerobic/Aerobic					1182 ± 70	7.3 ± 0.2
		Anoxic/Aerobic					1049 ± 45	7.8 ± 0.1

a. Anaerobic/Aerobic – first hour of cycle was anaerobic period; Anoxic/Aerobic – first hour of cycle was anoxic period

b. Combined SBR mixed liquor from Phase I to seed Phase II reactors

c. Continued operation from Phase II

d. First hour of cycle was idle period to maintain similar aerobic SRT

e. Average ± one standard deviation

The lab-scale SBRs consisted of 1-L Pyrex Erlenmeyer glass flasks with a working volume of 0.95 L and were maintained at 20°C in an environmental chamber in the dark. Mixing was achieved using magnetic stir bar s and air was supplied during the aerobic period by sparging through stone diffusers. The cycle times were 4 or 6 hours and the SRTs ranged from 8 to 13 days (Table 4-1). Either 1/4 of the reactor volume or 1/8 of the reactor volume (Puyallup seeded SBRs, Phase III only) was decanted and replaced with synthetic feed per cycle. Synthetic wastewater was delivered during the first 5 to 30 minutes of the cycle (1 to 8 % of the total cycle time) using peristaltic pumps. For the anaerobic/aerobic and anoxic/aerobic SBRs, the anaerobic or anoxic period lasted for the first hour of the cycle with purging of the 180-mL flask headspace with nitrogen gas at 600 mL/min. Aerobic periods ranged from 2.5 to 5.5 hours (Table 1). A 30-minute settling/decant period followed the aerobic period, and the supernatant was decanted during the last 5 minutes using a peristaltic pump. Reactor walls were scraped daily to minimize biofilm growth. Manual wasting of mixed liquor volume was done daily to maintain the target SRT, based on previous day effluent total suspended solids (TSS) and mixed liquor suspended solids (MLSS) concentration measurements.

The soluble synthetic wastewater fed to the SBRs had a chemical oxygen demand (COD) of 347 ± 39 mg/L. Organic constituents included 200 mg/L sodium acetate, 100 mg/L propionic acid, 55.2 mg/L peptone, and 20 mg/L casein. Phosphorus (28 ± 1 mg P/L) consisted of 100 mg/L K_2HPO_4 and 50 mg/L KH_2PO_4, and NH_4Cl was added at 10 ± 2 mg N/L. The feed of the anoxic/aerobic SBRs contained $NaNO_3$ at 51 ± 8 mg N/L. Macro-inorganic nutrients consisted of 346.6 mg/L $MgCl_2 \cdot 6H_2O$, 128.7 mg/L $CaCl_2 \cdot 2H_2O$, and 79.1 mg/L KCl. Two mL of trace element solution and one mL of vitamin solution were added to each liter of synthetic

wastewater. The trace element solution contained 515 mg/L $FeSO_4 \cdot 7H_2O$, 158 mg/L $ZnSO_4 \cdot 7H_2O$, 27.6 mg/L $CuSO_4 \cdot 5H_2O$, 28.1 mg/L $CoCl_2 \cdot 6H_2O$, 16.1 mg/L $Na_2MoO_4 \cdot 2H_2O$, 24.7 mg/L H_3BO_3, 24.9 mg/L KI, 11 mg/L $NiCl_2 \cdot 6H_2O$, 67.5 mg/L $Al_2(SO_4)_3 \cdot 18H_2O$, 142 mg/L $MnCl_2 \cdot 4H_2O$, and 3433 mg/L Na_2EDTA. The vitamin solution contained 140 mg/L each pantothenic acid, niacin, pyridoxine, p-aminobenzoic acid, cocarboxylate, inositol, thiamine, riboflavin, and choline chloride as well as 7 mg/L each biotin, cyancobalamin, and folic acid. Yeast extract (BD Bacto) (10 mg) was manually added to the SBRs every other day. Estrogens in the synthetic wastewater averaged 300 ± 45 ng/L E1, 313 ± 41 ng/L E2, and 298 ± 67 ng/L EE2. For the Durham and Puyallup seeded SBRs, alkalinity was added to the feed at 50 to 70 mg/L as $CaCO_3$ and carbon dioxide was added to the aeration line for pH control. No alkalinity was added to the feed of the Renton seeded SBRs.

During Phase III of the Puyallup-seeded SBRs, the synthetic wastewater strength was doubled with the exception of the phosphorus, macro-inorganic nutrients and yeast concentrations. The synthetic wastewater contained 706 ± 32 mg/L COD, 30 ± 1 mg PO_4-P /L, 19 ± 5 mg NH_3-N /L, and 94 ± 2 mg NO_3-N/L (anoxic/aerobic SBR only). Estrogen concentrations in the synthetic wastewater averaged 563 ± 115 ng/L E1, 435 ± 119 ng/L E2, and 420 ± 25 ng/L EE2.

Sampling and analyses

For each operational condition, the synthetic feed was sampled at least twice for COD and estrogens and at least once for nutrients (PO_4-P, NH_3-N, and NO_3-N). Mixed liquor and effluent solids and reactor pH were monitored daily. Reactor samples were collected three times a week at the end of the anaerobic or anoxic cycle and at the end of the aeration cycle for nutrient

analyses (PO$_4$-P, NH$_3$-N, NO$_3$-N, and NO$_2$-N). NO$_2$-N was not measured in the Renton-seeded SBRs. Soluble COD in the reactor samples was measured at least three times during each operational condition. For the Puyallup and Renton-seeded SBRs, total estrogen measurements of the mixed liquor were taken about twice weekly at the end of the aeration cycle during periods of reactor operation surrounding batch degradation tests; soluble estrogen concentrations were also measured for nine of these sampling events to characterize estrogen partitioning to the activated sludge. All estrogen measurements were conducted in duplicate.

Analytical methods

Estrogens, E1 (≥99%), E2 (≥98%), and EE2 (≥98%), were purchased from Sigma Aldrich. Deuterated labeled internal standards, estrone-2,4,16,16-d$_4$ (d$_4$E1), 17β-estradiol-2,4,16,16-d$_4$ (d$_4$E2) and 17α-ethynylestradiol-2,4,16,16-d$_4$ (d$_4$EE2), were purchased from C/D/N Isotopes, Inc. and were greater than 98 percent chemical purity. Reagents used in the estrogen analyses included dansyl chloride (≥99%) and formic acid obtained from Sigma Aldrich and HPLC grade acetonitrile (ACN) and methanol (MeOH) and analytical grade sodium bicarbonate (NaHCO$_3$) supplied by EMD Chemicals.

Estrogen and deuterated internal standard stock solutions were prepared in MeOH and stored at -20ºC. Calibration standards contained 1, 5, 10, 25, 50, 100, 250, 500 and 1000 ng/L E1, E2 and EE2 and 100 ng/L of d$_4$E1, d$_4$E2 and d$_4$EE2 in a 1:1 MeOH:H$_2$O solution. An internal standard working solution consisted of 1 µg/L d$_4$E1, d$_4$E2 and d$_4$EE2 in a 1:1 MeOH:H$_2$O solution. Individual E1, E2 and EE2 working solutions of 0.5 mg/L were prepared in Milli-Q water. Calibration standards and working solutions were stored at 4ºC. All glassware was washed with

detergent, soaked in a sulfuric acid solution containing NOCHROMIX oxidizer overnight, and rinsed three times with Milli-Q water, acetone, and methylene chloride prior to usage.

Estrogen measurements were conducted according to Gaulke et al. (2008) with slight modifications. Briefly, 50 pg of each internal standard (d_4E1, d_4E2 and d_4EE2) was added to 500 µL of sample. For total estrogen measurements, the sample consisted of the mixed liquor containing both the aqueous and solid fractions. For soluble estrogen measurements, the sample consisted of the supernatant after centrifuging 6 mL of mixed liquor at 3200 rpm for 10 minutes at 4°C. A liquid-liquid extraction was performed on the sample with 3 mL of ethyl acetate, and the organic fraction was transferred to a clean tube and evaporated to dryness with a gentle stream of nitrogen gas at 40°C. Samples were reconstituted with 100 µL of $NaHCO_3$ buffer (pH 10.5) and 100 µL of 1 mg/mL dansyl chloride in ACN and heated at 60°C for 30 minutes.

Estrogen analysis was performed using a Shimadzu LC-20AD high performance liquid chromatograph (Kyoto, Japan) and an Applied Biosystems 4000 QTrap tandem mass spectrometer (MS/MS) (Foster City, CA). Estrogen separation was achieved by injecting 20 µL of derivatized sample onto a Phenomenex Luna Phenyl-Hexyl column (50 x 3.0 mm id., 3 µm particle size) with a flow rate of 0.5 mL/min and mobile phases of 0.1% formic acid in water (A) and ACN (B). Solvent B initially eluted at 50%, linearly increased to 95% within 3 minutes, remained isocratic to 5 minutes, returned to 50% within 5.1 minutes and re-equilibrated to 8 minutes. The MS/MS was operated in electrospray positive mode with an ion spray voltage of 5000 volts and collision energy of 50 eV. The transitions for E1, d_4E1, E2, d_4E2, EE2, and d_4EE2 were monitored at m/z 504.2 > 171.3, 508.2 > 171.3, 506.2 > 171.3, 510.2 > 171.3, 530.0

> 171.3, 534.0 > 171.3, respectively. The limit of detection (LOD) for the method was 1 ng/L (signal-to-noise ratio of 3:1) and the method limit of quantification (LOQ) was 5 ng/L (signal-to-noise ratio of 10:1).

HACH kits and a HACH DR/4000 U Spectrophotometer (Loveland, CO) were used to analyze COD (HACH Method 8000) and nutrients, including PO_4-P (Method 8114), NH_3-N (Methods 10023 and 10031), NO_3-N (Methods 10049 and 10020) and NO_2-N (Method 10019). Samples were first filtered through a 0.45 μm Supor filter prior to nutrient analyses. TSS and volatile suspended solids (VSS) were measured according to standard methods (APHA, AWWA, WEF, 2005) using Whatman Grade GF/C (1.2 μm) glass fiber filters for filtration.

Estrogen biodegradation in situ batch kinetic tests
In situ estrogen biodegradation tests were conducted in the SBRs to determine the biodegradation kinetics for the particular SBR operating conditions. At the end of the feeding period, each SBR was amended with an additional 0 to 175 ng/L of E1, E2 and EE2 using aqueous stock solutions. Total estrogen concentrations were measured throughout one SBR cycle. To address any abiotic removals, autoclaved effluent (100 mL) from the aerobic-only and anoxic/aerobic SBRs were amended with an additional 200 ng/L of aqueous E1, E2 and EE2 and subjected to the same anoxic (nitrate of 23 mg N/L, headspace purged with nitrogen) and aerobic conditions (air sparged) as the corresponding SBRs. All estrogen measurements were conducted in duplicate.

Estrogen biodegradation kinetics and solids partitioning

Estrogen biodegradation was assumed to follow a pseudo first-order model as a function of the soluble estrogen and mixed liquor VSS (MLVSS) concentrations (Gaulke et al., 2009):

$$\frac{dE_T}{dt} = -k_b E_S X_{VSS} \qquad \textbf{(1)}$$

where E_T is the total estrogen concentration (ng/L), t is the time (d), k_b is the pseudo first-order estrogen biodegradation rate coefficient normalized to MLVSS (L/g VSS·d), and E_S is the soluble estrogen concentration (ng/L). X_{VSS} is the measured MLVSS concentration (g/L), which consists primarily of biomass as a result of feeding only soluble biodegradable substrate. Under equilibrium conditions, E_S is related to E_T by $E_S = E_T/(1+K_P X_{VSS})$, where K_P is the estrogen solids-liquid partitioning coefficient (L/g VSS). Assuming rapid solids-liquid equilibrium of the estrogen (Andersen et al., 2005) and insignificant change in MLVSS concentration during the test, the decline in total estrogen concentration during degradation tests was modeled as follows:

$$\ln\left(\frac{E_{T,t}}{E_{T,o}}\right) = \frac{-k_b X_{VSS} t}{(1+K_P X_{VSS})} \qquad \textbf{(2)}$$

Estrogen k_b values were calculated according to Gaulke et al. (2009) by performing a linear regression of $\ln(E_{T,t}/E_{T,o})$ versus time (Microsoft Office Excel 2007) and multiplying the slope of the linear trend line by $(1+K_P X_{VSS})/X_{VSS}$. Student's t-tests were used to compare k_b values (Microsoft Office Excel 2007).

Total and soluble estrogen concentrations were measured at the end of the SBR aerobic period to determine the apparent estrogen solids-liquid partitioning. Sorbed estrogen concentrations (E_{sorb}, ng/g) were calculated as follows:

$$E_{sorb} = \frac{E_T - E_S}{X_{VSS}} \tag{3}$$

and apparent K_P values were determined from total and soluble estrogen measurements at the end of the SBR aerobic period:

$$K_P = \frac{E_{sorb} \text{ (end of aerobic period)}}{E_S \text{ (end of aerobic period)}} \tag{4}$$

These K_P values were used in calculating estrogen k_b values as described above.

SBR model for total EE2 concentration versus reaction time

In addition to conducting estrogen degradation tests as previously described, EE2 k_b values were also determined by calibrating a SBR model for predicting total EE2 concentrations at the end of the aerobic period. After repetitive cycles with the same feed and SRT control, a steady state MLVSS concentration and final effluent nutrient concentrations occur for an SBR. Joss et al. (2006) developed a steady state SBR model for predicting effluent soluble pharmaceutical concentrations based on a mass balance that included rapid solid-liquid partitioning characterized by a solid-liquid partitioning coefficient (K_d, L/g TSS) and applying a pseudo first-order biodegradation rate model with a k_{biol} coefficient normalized to MLSS (L/g TSS-d). Equation 15 in Joss et al. (2006) was modified in this study to predict the total mixed liquor EE2 concentration at the end of the SBR aerobic period ($EE2_{T,\Theta aer}$, ng/L). Our model based EE2 biodegradation and sorption to solids on X_{VSS} (g VSS/L) rather than the mixed liquor total suspended solids (X_{SS}, g TSS/L), resulting in the replacement of k_{biol} (L/g TSS-d) and K_d (L/g TSS) in the Joss et al. model with k_b (L/g VSS-d) and K_P (L/g VSS), respectively. EE2 biodegradation was modeled as occurring only under aerobic conditions, and so the term $\Theta_h/(1+R)$ in the Joss et al. model defined as the SBR cycle time minus sedimentation and

decantation time was replaced in our model with the SBR aerobic cycle time (Θ_{aer}, d). Instead of representing the feed total concentration as a function of the soluble wastewater concentration (S_{WW}), the solid-liquid partitioning coefficient for primary sludge ($K_{d,prim}$), and the primary sludge concentration ($X_{SS,WW}$), the term $S_{WW}(1+K_{d,prim}X_{SS,WW})$ in the Joss et al. model was replaced in our model with one term for the feed total EE2 concentration ($EE2_f$, ng/L). The specific sludge production per volume of wastewater treated (SP) was represented in our model as $X_{VSS} \cdot V/(Q \cdot SRT)$ where V is the reactor volume (L) and Q is the flow (L/d). Finally, the Joss et al. model predicts the effluent soluble concentration, and so their equation was multiplied by $(1+K_P X_{VSS})$ in our model to obtain the predicted total EE2 concentration of the mixed liquor at the end of the aerobic period. These modifications resulted in the following equation for predicting $EE2_{T,\Theta aer}$:

$$EE2_{T,\theta aer} = \frac{EE2_f(1+K_P X_{VSS})}{\left[1 + K_P X_{VSS}\dfrac{V}{Q \cdot SRT} + (1+K_P X_{VSS})(1+R)(e^{k_b X_{VSS}\Theta_{aer}/(1+K_P X_{VSS})} - 1)\right]} \tag{5}$$

where R is the ratio of the SBR volume after decanting to the feed volume and all other variables have previously been defined. EE2 k_b values were calculated by fitting Equation 5 to measurements of $EE2_{T,\Theta aer}$, $EE2_f$, and X_{VSS} collected that day, average K_P values determined as described in the previous section, and operational values for all other parameters (V, Q, SRT, R, and Θ_{aer}).

SBR and continuous-flow CSTR models for EE2 removal efficiency
EE2 removals were modeled for a SBR and a single or series of continuous-flow completely stirred tank reactors (CSTRs) with secondary clarification to assess how biodegradation rate coefficients and operational conditions affect reactor performance. Biodegradation was related

to the active heterotrophic biomass concentration rather than the total MLVSS, as the fraction of biomass varies depending on SRT and influent wastewater characteristics. For the simple case where the influent substrate is completely biodegradable as in this study, the mixed liquor biomass concentration (X_{bio}, g/L) and MLVSS concentration (X_{VSS}, g/L) were modeled as follows:

$$X_{bio} = \frac{Y \cdot bCOD_f \cdot SRT}{(1+b \cdot SRT)HRT} \tag{6}$$

$$X_{VSS} = X_{bio}(1+f_d \cdot b \cdot SRT) \tag{7}$$

where Y is the heterotrophic biomass yield (g VSS/g COD), $bCOD_f$ is the feed biodegradable COD concentration (g/L), b is the heterotrophic decay coefficient (g VSS/g VSS-d), and f_d is the fraction of decayed biomass remaining as cell debris (g VSS/g VSS). X_{bio}/X_{VSS} ratios of the mixed liquor were estimated using the following equation:

$$\frac{X_{bio}}{X_{VSS}} = \frac{1}{1+f_d \cdot b \cdot SRT} \tag{8}$$

Pseudo first-order biodegradation rate coefficients normalized to biomass (k_{bio}, L/g biomass-d) were estimated by dividing measured k_b coefficients by these calculated X_{bio}/X_{VSS} ratios.

Assuming adequate clarification such that the sorbed effluent EE2 is negligible, EE2 removal was defined as $1 - EE2_S/EE2_f$ where $EE2_S$ is the soluble EE2 concentration leaving the reactor (ng/L) and $EE2_f$ is the total feed EE2 concentration (ng/L). For a SBR, the ratio $EE2_S/EE2_f$ was obtained from Equation 5 by replacing $E_{T,\Theta aer}/(1+K_P X_{VSS})$ with $EE2_S$ and $k_b X_{VSS}$ with $k_{bio} X_{bio}$. This ratio was used in combination with Equations 6 and 7 to model EE2 removals in a SBR. For an aerobic single or series of continuous-flow CSTRs, the ratio $EE2_S/EE2_f$ was modeled as

86

follows based on Equation 14 in Joss et al. (2006) which was modified as previously described for the SBR model.

$$\frac{EE2_S}{EE2_f} = \frac{1}{1 + K_P X_{VSS} \frac{HRT}{SRT} + (1+K_P X_{VSS})(1+R) \left[\left(1 + \frac{k_{bio} X_{bio}}{(1+R)(1+K_P X_{VSS})} \frac{HRT}{n} \right)^n - 1 \right]} \quad \textbf{(9)}$$

HRT is the hydraulic retention time (d), R is the ratio of the sludge recycle flow rate to the influent flow rate, n is the number of staged compartments, and all other variables have previously been defined.

4.4 Results and Discussion

SBR performance

The SBR BNR processes performed as designed, with a large portion of the influent soluble COD (sCOD) removal (average of 94 to 99 percent) occurring in the anaerobic or anoxic period and expected levels of EBPR and nitrate removal for the anaerobic/aerobic and anoxic/aerobic SBR systems, respectively. Removal of soluble phosphorus in the anaerobic/aerobic SBRs was greater than that in the parallel anoxic/aerobic and aerobic-only SBRs by 16 mg/L for the Durham-seeded reactors and 26 mg/L for the Renton-seeded reactors. The inorganic content of the anaerobic/aerobic SBRs mixed liquor was much higher than that for the other SBRs. The inorganic content of the mixed liquor is indicative of intercellular polyphosphate storage (Ekama and Wentzel, 2004). The VSS/TSS ratios of the anaerobic/aerobic SBRs were 0.70 ± 0.07 and 0.50 ± 0.02 for the Durham-seeded and Renton-seeded SBRs, respectively, compared to a VSS/TSS ratio of 0.88 ± 0.04 for all other SBRs. Denitrification in the anoxic/aerobic SBRs resulted in an average NO_3-N reduction of 48 ± 6 mg N/L with the exception of the Puyallup-seeded Phase III anoxic/aerobic SBR, which produced an average NO_3-N reduction of 80 ± 20 mg N/L.

87

Effluent NH_3-N concentrations were typically below 0.5 mg N/L except for the Durham-seeded anaerobic/aerobic SBR, which produced an average effluent of 10 ± 2 mg N/L. Based on effluent NO_3-N and NO_2-N measurements and accounting for NO_3-N and NO_2-N at the end of the anoxic period, the amount of ammonia oxidation for both the Durham-seeded anoxic/aerobic SBR and Puyallup-seeded Phases I and II SBRs averaged 7 ± 3 mg N/L. Ammonia oxidized averaged 2 ± 2 mg N/L for the Durham-seeded anaerobic/aerobic SBR and 15 ± 6 mg N/L for the Puyallup-seeded Phase III SBRs. Based on effluent and end of anoxic cycle NO_3-N concentrations (NO_2-N not measured during this experiment), the amount of ammonia oxidation in the Renton-seeded SBRs averaged 7 ± 3 mg N/L.

Estrogen biodegradation in SBR cycle

Biodegradation of EE2 only occurred during the aerobic period at a slower rate than the natural estrogens. A typical time course of EE2, E2, and E1 concentrations measured over time during an SBR cycle is shown in Figure 4-1. There was no estrogen removal from killed controls, confirming that the estrogen removal was from biological activity (Figure 4-1). EE2 was degraded much slower than the natural estrogens, E1 and E2. E1 concentrations declined below the LOQ of 5 ng/L within the first 3 hours of the aerobic period in 80 percent of the degradation tests *in situ*. E2 concentrations declined below the LOQ within 2 hours of the aerobic period in 90 percent of the tests. E1 and E2 k_b values were not determined due to the limited number of data points above the LOQ and the production of E1 from oxidation of E2 during the SBR cycle. EE2 was not removed during anaerobic or anoxic periods (e.g., Figure 4-1) as has been observed

in other studies (Dytczak et al., 2008; Zhang et al., 2011). The following results are based on

EE2 biodegradation kinetics that occurred during aerobic periods.
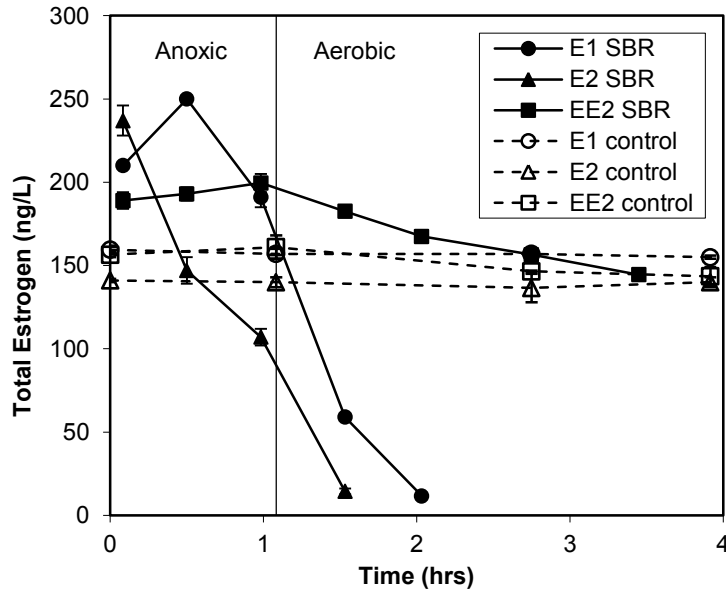
Figure 4-1. Estrogen degradation at 20°C during a typical SBR cycle in Puyallup-seeded anoxic/aerobic SBR (Phase I) and in autoclaved effluent (control).

EE2 biodegradation rate coefficients

The biodegradation rate coefficients (k_b) for EE2 are shown in Table 4-2 for the three reactor

sets. In addition, EE2 k_b values determined from in situ batch tests (Equation 2) and model

calibrations (Equation 5) are shown over time in Figure 4-2 for the Phase II and III Puyallup-

seeded SBRs. The aerobic-only SBR k_b values for the Puyallup-seeded reactors were

consistently higher than the anoxic/aerobic SBR values, and the model calibrated k_b values

closely matched the batch test values (Figure 4-2). After operation at a 7.5-day aerobic SRT for

five SRTs, average k_b values in the Durham-seeded SBRs determined from in situ batch

degradation tests were within the range of k_b values observed for the Puyallup-seeded SBRs

(Table 4-2). The Renton-seeded SBRs had the highest k_b values among the three sets of EE2

89

degradation experiments (Table 4-2). Following operation at a 10-day aerobic SRT for 3 SRTs,

average k_b values based on calibrated model results ($n = 3$) were 20.8 ± 0.9, 16.9 ± 1.0, and 16.4 ± 1.2 L/g VSS-d for the aerobic-only, anaerobic/aerobic, and anoxic/aerobic operations,

respectively. One in situ batch degradation test also showed relatively high k_b values in these

SBRs of 14.6, 19.0, and 20.4 L/g VSS-d for the aerobic-only, anaerobic/aerobic, and

anoxic/aerobic operations, respectively.

Table 4-2. Average ($\pm$ one standard deviation) pseudo first-order EE2 biodegradation rate (k_b) coefficients in aerobic-only, anaerobic/aerobic, and anoxic/aerobic SBRs at 20°C

Seed Source	SBR	Aerobic SRT (d)	EE2 k_b[a] (L/g VSS-d)	n
Puyallup, WA	Anoxic/Aerobic	5	4.6 ± 1.1	5
	Anoxic/Aerobic		3.3 ± 0.5	
	Aerobic-Only	7	9.1 ± 1.3^{b}	11
	Anoxic/Aerobic	5	5.9 ± 1.5^{c}	
	Aerobic-Only	12	6.3 ± 0.9^{b}	9
	Anoxic/Aerobic	10	4.2 ± 1.1^{c}	
Durham, OR	Anaerobic/Aerobic	7.5	5.7 ± 2.7	3
	Anoxic/Aerobic		4.3 ± 2.4	
Renton, WA	Aerobic-Only	10	19.2 ± 3.2	4
	Anaerobic/Aerobic		17.4 ± 1.3	
	Anoxic/Aerobic		17.4 ± 2.2	

a.   EE2 k_b values were determined from in situ batch degradation tests and modeled based on total feed and end of aerobic period EE2 concentrations

b,c. Different superscripts show statistically significant differences in EE2 k_b values between SBRs
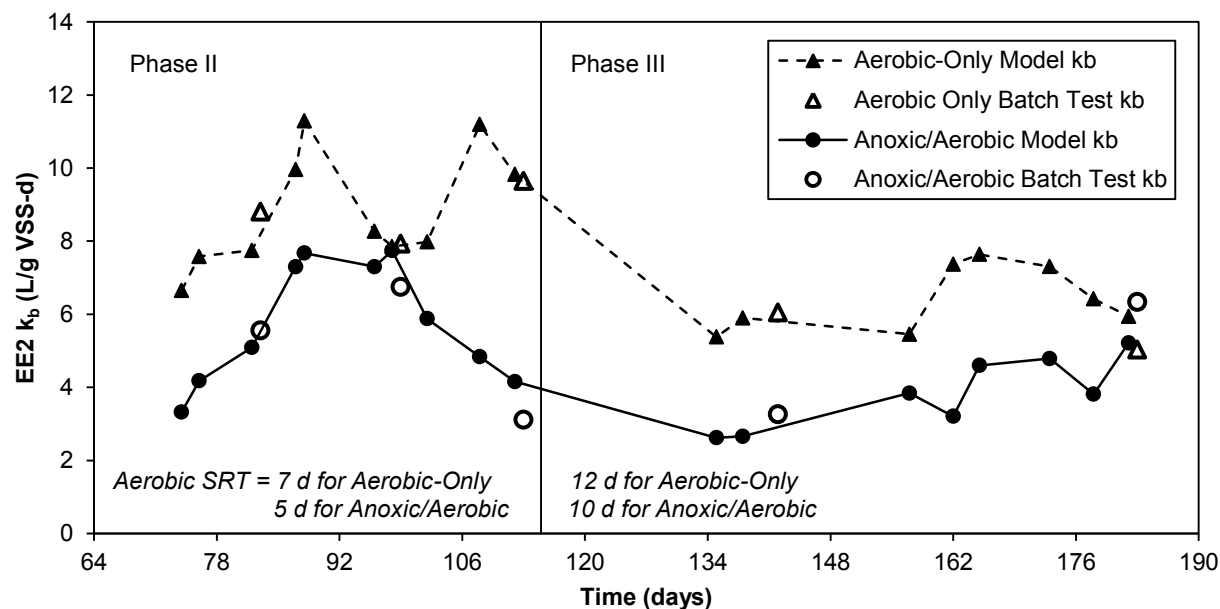
Figure 4-2. EE2 k_b values (20°C) in Puyallup-seeded aerobic-only and anoxic/aerobic SBRs (Phases II and III). EE2 k_b values were calculated from in situ batch degradation tests (open markers) or from model calibration (solid markers).

The variation in EE2 k_b values between SBRs and within a single SBR over time suggests there is a high degree of uncertainty in this value when predicting process performance. EE2 k_b values of 3 to 22 L/g VSS-d varied by a factor of 7 in this study and were similar to values reported in literature both in magnitude and variation. Reported EE2 k_b values vary by a factor of 6 (Table 4-3), ranging from 2 L/g VSS-d to 8 L/g TSS-d for WWTP AS and reaching 12 L/g VSS-d for lab-scale MBR AS fed synthetic wastewater. During Phase II of the Puyallup-seeded SBR operation (Figure 4-2), EE2 k_b values varied by a factor of 2.5 in the anoxic/aerobic SBR, ranging from 3 to 8 L/g VSS-d. In evaluating the potential performance of a system, it is therefore important to assess how variation in EE2 k_b values in combination with various operational conditions may impact EE2 removals.

91

Table 4-3. Pseudo first-order EE2 biodegradation rate (k_b) coefficients reported for aerobic batch degradation tests conducted at ng/L concentrations

Activated sludge source[a]	SRT (d)	Temp (°C)	EE2 k_b	Source
CAS WWTP, USA	3	20	1.6 L/g VSS-d	Gaulke et al. (2009)
A/O MBR WWTP, USA	30 - 40	20	1.7 L/g VSS-d	Gaulke et al. (2009)
CAS WWTP, United Kingdom	NA[b]	14.8	3.6 L/g SS-d[c]	Xu et al. (2009)
CAS WWTP, United Kingdom	NA[b]	20.5	4.3 L/g SS-d[c]	Xu et al. (2009)
A^2O pilot-scale MBR, Switzerland	30	16	6 L/g SS-d	Joss et al. (2004)
A/O CAS WWTP, Switzerland	12	16	8 L/g SS-d	Joss et al. (2004)
Lab-scale MBR, Mexico[d]	40	28	12.4 L/g VSS-d	Estrada-Arriaga and Mijaylova (2010)

a. CAS - conventional activated sludge; A/O - anoxic/aerobic; MBR - membrane bioreactor; A^2O – anaerobic/anoxic/aerobic

b. NA - not available

c. k_b values calculated from reported first-order degradation rate constant (k), mixed liquor suspended solids concentration (X) and estrogen solids-liquid partitioning coefficient (K_P) where $k_b = k(1+K_P X)/X$

d. Reactor was fed synthetic wastewater

Impact of activated sludge process type

Although results from the Puyallup-seeded SBRs suggest growth under aerobic-only conditions favors AS with a higher EE2 k_b than anoxic/aerobic conditions, the high k_b values in the Renton-seeded SBRs regardless of AS process type suggest other factors may have a greater impact on k_b. Statistically significant differences in k_b values were found only for the Puyallup-seeded SBRs (Table 4-2), where higher k_b values occurred with the aerobic-only process than the anoxic/aerobic process for both Phases II and III (two-tailed Student's t-test, $p = 0.00005$ and 0.0005 for Phases II and III, respectively). Also of consideration with these SBRs, however, is the operation at different aerobic SRTs. Although these SBRs were operated at the same total SRT, it is uncertain whether the longer aerobic SRT with the aerobic-only process promoted higher k_b values. Improved k_b values with aerobic-only versus anoxic/aerobic operations could not be confirmed with the Renton-seeded SBRs (Table 4-2).

The similar EE2 k_b values between the Renton-seeded SBRs as well as between the Durham-seeded SBRs raises the question of the growth substrate of EE2-degrading biomass. It is likely that heterotrophic EE2-degrading microbial populations in these experiments grew on substrates other than EE2, as the ng/L EE2 levels in the feed were too low to support observable biomass growth. Greater than 93 percent of the sCOD removal occurred in the anaerobic and anoxic phases of the respective SBR systems, supporting different microbial communities as indicated by the EBPR in the anaerobic/aerobic SBRs and the nitrate removal in the anoxic/aerobic SBRs. The similar EE2 k_b values between the Renton-seeded SBRs could be explained by one or a combination of the following possibilities: (1) the influent bCOD supported EE2-degraders which can be found in aerobic, PAO, and denitrifying communities, (2) the influent bCOD was

93

converted into storage products by EE2-degraders and later oxidized under aerobic conditions, (3) a small fraction of the influent bCOD supported EE2-degraders with growth under aerobic conditions, (4) EE2-degraders grew on cell lysis products, and /or (5) EE2-degraders were autotrophic bacteria.

Autotrophic bacteria in these SBRs were unlikely to be responsible for the observed EE2 degradation. Although previous studies have suggested ammonia-oxidizing bacteria (AOB) play a significant role in EE2 degradation (Khunjar et al., 2011), we calculate that the contribution of AOB to EE2 degradation in these experiments was insignificant based on the estimated concentration of AOB and their reported EE2 degradation kinetics. Based on the amount of nitrate production, a synthesis yield of 0.15 g VSS_{AOB}/g N oxidized, and an endogenous decay rate of 0.17 g VSS/g VSS-d (Tchobanoglous et al., 2014), the estimated AOB concentration in the SBR mixed liquor in this study ranged from 0 to 9 mg/L, representing a maximum of one percent of the MLVSS concentration. Khunjar et al. (2011) reported an EE2 biotransformation rate by AOB of 13.6 L/g COD_{AOB}-d at 200 μg/L EE2 and 15 mg/L NH_3-N, while Gaulke et al. (2008) observed no EE2 removals by AOB at a more environmentally relevant EE2 concentration of 500 ng/L and 10 mg/L NH_3-N. Even if AOB transformed EE2 at 13.6 L/g COD_{AOB}·d (19.3 L/g VSS_{AOB}-d), the contribution to the observed mixed liquor k_b values in this study of 3 to 20 L/g VSS-d would be less than 0.2 L/g VSS-d. In addition, the observed k_b values did not correlate with the estimated AOB fraction of the biomass (data not shown). Therefore, heterotrophic bacteria were primarily responsible for the estrogen biodegradation observed in this study. Further studies are needed to address the identity and growth substrate of heterotrophic estrogen-degrading populations.

EE2 solids-liquid partitioning

EE2 K_P values of 440, 360, and 290 L/kg VSS were used to determine EE2 k_b values for aerobic-only, anaerobic/aerobic, and anoxic/aerobic SBR mixed liquors, respectively, but k_b coefficients were relatively insensitive to K_P. These K_P values were based on average apparent values of 436 $\pm$ 211 ($n = 9$), 358 $\pm$ 34 ($n = 4$), and 289 $\pm$ 100 ($n = 13$) L/kg VSS for aerobic-only, anaerobic/aerobic, and anoxic/aerobic SBR mixed liquors, respectively. Using these K_p values to calculate k_b coefficients from in situ estrogen degradation tests (Equation 2), 17 to 35 percent of the total EE2 concentration in the system was sorbed for MLVSS concentrations ranging from 706 to 1233 mg/L. Sensitivity of k_b coefficients to K_p values was such that a 20 percent difference in K_p values resulted in approximately 3 to 7 percent difference in calculated k_b coefficients. Average apparent K_p values normalized to TSS were 391, 240, and 254 L/kg TSS for the aerobic-only, anaerobic/aerobic, and anoxic/aerobic mixed liquors, respectively, and were within the range of values reported in literature of 210 to 690 L/kg TSS (Andersen et al., 2005; Clara et al., 2004; Estrada-Arriaga and Mijaylova, 2010; Gomes et al., 2011; Xu et al., 2008).

Modeled EE2 removals in SBR and Continuous-flow CSTRs

EE2 removals were modeled for aerobic-only SBR and continuous-flow CSTR systems to assess how variability in biodegradation rate coefficients and operational conditions affect reactor performance (Figure 4-3). Biodegradation kinetics were based on the active biomass concentration instead of MLVSS to account for changes in the fraction of active biomass with SRT. The values for b and f_d used to calculate X_{bio} and X_{VSS} concentrations (Equations 6 and 7) were 0.12 g VSS/g VSS-d and 0.15 g VSS/g VSS, respectively (Tchobanoglous et al., 2014).

95

The biomass yields (Y) obtained by fitting the model to average X_{VSS} concentrations observed for the aerobic-only, anaerobic/aerobic, and anoxic/aerobic SBRs were 0.43 ± 0.11, 0.52 ± 0.02, and 0.42 ± 0.04 g VSS/g COD, respectively. A Y of 0.43 g VSS/g COD was therefore used for the model simulations. The EE2 biodegradation k_b values were adjusted to provide the pseudo first-order biodegradation rate coefficients normalized to biomass (k_{bio}) instead of VSS. Estimated X_{bio}/X_{VSS} ratios of the SBR mixed liquors (Equation 8) were from 0.81 to 0.87 for SRTs from 8 to 13 days. Applying these X_{bio}/X_{VSS} ratios to observed k_b values resulted in k_{bio} values of 3 to 27 L/g biomass-d.

EE2 removals were modeled for an aerobic SBR, a single CSTR, and four CSTR in series at 20°C. Assumed operating conditions for the SBR system were a V/Q of 1 day, R of 3, and Θ_{aer} of 5 hours (see Equation 5). Model simulations were done for a wastewater $bCOD_f$ of 400 and 200 mg/L, resulting in $bCOD_f/EE2_f$ ratios of 20 mg/ng and 10 mg/ng, respectively, for a possible influent EE2 ($EE2_f$) concentration of 20 ng/L (Clara et al., 2005). Predicted biomass concentrations in the SBR were 432 to 1101 mg/L for aerobic SRTs of 3 to 23 days and a $bCOD_f$ of 400 mg/L; half that for $bCOD_f$ of 200 mg/L. Model simulations for a single CSTR (n = 1 in Equation 9) and four CSTR in series (n = 4) were based on a HRT of 0.92 days and R of 0.8, resulting in predicted biomass concentrations within five percent of the SBR for any given aerobic SRT. All predicted EE2 removals were based on a K_P of 0.44 L/g VSS as measured in this study.
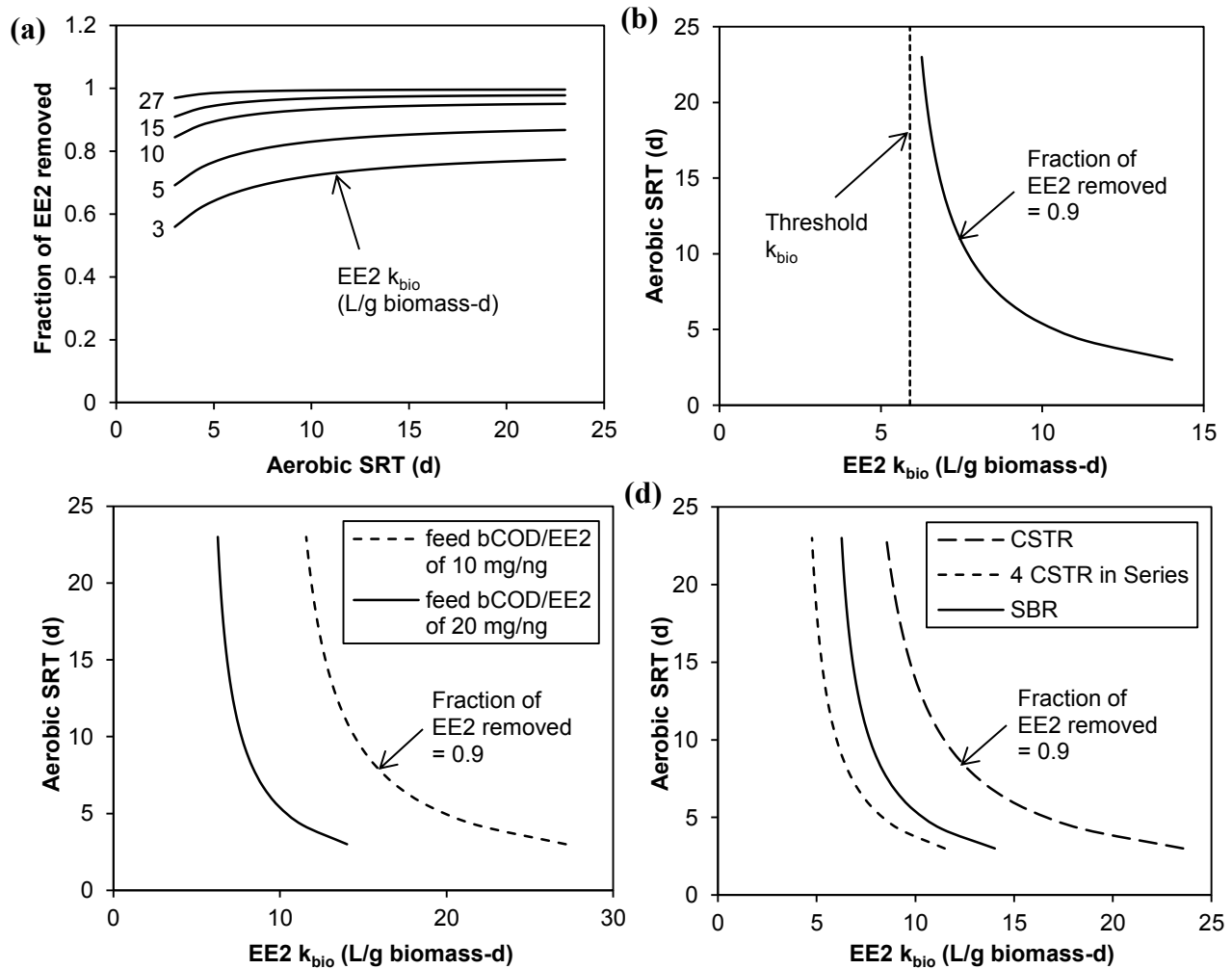
Figure 4-3. Model simulation results for (a) fraction of EE2 removed as a function of aerobic SRT and k_{bio} for SBR, (b) aerobic SRT for 90 percent EE2 removal in SBR, (c) effect of feed bCOD/EE2 ratio for SBR, and (d) effect of reactor configurations.

The model simulation results with a $bCOD_f/EE2_f$ ratio of 20 mg/ng in Figures 4-3a shows how k_{bio} and aerobic SRT values affect the EE2 removal efficiency. Below an aerobic SRT of about 10 days, the predicted EE2 removal efficiency was more sensitive to k_{bio} values than for aerobic SRTs above 10 days, especially for variations in k_{bio} between 3 and 10 L/g biomass-d as was observed with long-term operation of the Puyallup-seeded SBRs (Figure 4-2). Variations in k_{bio} values between 15 and 27 L/g biomass-d, as was observed with the Renton-seeded SBR

97

operations, were predicted to have less of an impact on EE2 removal efficiency, with the system maintaining relatively high removals greater than 90 percent.

As shown in model simulation results in Figure 4-3b, longer aerobic SRTs enable a system to achieve a given EE2 removal efficiency with lower k_{bio} values. A SBR with a $bCOD_f/EE2_f$ ratio of 20 mg/ng was predicted to achieve 90 percent EE2 removal with a k_{bio} value of 11.8 L/g biomass-d at a 4-day aerobic SRT as well as with a k_{bio} of 6.4 L/g biomass-d by increasing the aerobic SRT to 20 days. However, as the aerobic SRT was increased further, a threshold k_{bio} value of 5.9 L/g biomass-d was reached below which 90 percent removals could no longer be obtained. Longer aerobic SRTs provide greater contact time between the biomass and estrogen, however, longer SRTs also reduce the observed biomass yield. Therefore, longer SRTs could not completely compensate for the lowest k_b values observed in this study to obtain 90 percent EE2 removals, indicating a minimum k_b value is needed for a system to achieve a given removal efficiency.

The influent $bCOD_f/EE2_f$ ratio and reactor configuration impacted the predicted threshold k_{bio} and ability of a system to achieve a given EE2 removal efficiency (Figures 4-3c and 4-3d). At higher feed bCOD/EE2 ratios, more biomass is available relative to the amount of EE2 so that a lower k_b is possible to achieve a given removal efficiency. The model predicted a threshold k_{bio} of 10.6 L/g biomass-d was needed to obtain 90 percent EE2 removal in a SBR with a $bCOD_f/EE2_f$ ratio of 10 mg/ng; this predicted threshold k_{bio} was reduced to 5.9 L/g biomass-d for a $bCOD_f/EE2_f$ ratio of 20 mg/ng (Figure 4-3c). For the higher $bCOD_f/EE2_f$ ratio of 20 mg/ng, EE2 removals of 90 percent or greater could be achieved for 65 percent of the estimated k_{bio}

98

values in this study while similar removals could only be achieved for 22 percent of the k_{bio} values with the lower $bCOD_f/EE2_f$ ratio. For systems with a $bCOD_f/EE2_f$ ratio of 20 mg/ng, the predicted threshold k_{bio} needed to obtain 90 percent EE2 removal was 7.1 L/g biomass-d for the single CSTR and 4.4 L/g biomass-d for the four CSTR in series (Figure 4-3d). Compared to the SBR that could achieve 90 percent or greater EE2 removals for 65 percent of the k_{bio} values, the single and four-staged CSTR were predicted to achieve the same level of removal for 52 and 79 percent of the k_{bio} values, respectively. Therefore, staged CSTR designs with high $bCOD_f/EE2_f$ ratios and long aerobic SRTs were predicted to result in greater and more stable EE2 removal performance for the k_{bio} values estimated in this study.

The four CSTR in series was predicted to provide better EE2 removal performance than the SBR even though the SBR promotes batch kinetics. The difference in EE2 removals between these configurations was due to the sludge recycle ratio, R, selected for each configuration (R = 0.8 for staged CSTR and R = 3 for SBR) to be representative of values used in practice.

The model results shown in Figure 4-3 indicate EE2 removals are highly sensitive to biodegradation rate coefficients and highlight the importance of understanding the factors governing these values. Research is needed addressing how operational factors, such as wastewater characteristics, SRT, and substrate loading conditions, affect k_b values and the mechanisms behind their impact, either by promoting growth of EE2-degrading biomass and/or altering their biodegradation kinetics.

99

4.5 Conclusions

A pseudo first-order model was successfully applied to measure EE2 biodegradation kinetics in lab-scale SBRs operating under aerobic only, anaerobic/aerobic, and anoxic/aerobic conditions. Biodegradation occurred only under aerobic conditions. Observed pseudo first-order EE2 biodegradation rate (k_b) coefficients normalized to MLVSS ranged from 3 to 22 L/g VSS-d at 20°C. Aerobic-only AS processes may promote higher k_b values than anoxic/aerobic AS processes, but high k_b values can be obtained with all BNR process types. Model simulations indicate more reliable and higher EE2 removals can be achieved with these k_b values with longer aerobic SRTs, staging of aerobic reactors, and higher feed bCOD/EE2 ratios.

Chapter 5: Estrogen Biodegradation by Enriched Denitrifying Communities

5.1 Introduction

High estrogen removals are reported for WWTPs with biological nitrogen removal (Joss et al., 2004), but the contribution of denitrifying populations to estrogen degradation in these activated sludge (AS) systems is unknown. Estrogen degradation is primarily due to heterotrophic bacteria (Bagnall et al., 2012; Gaulke et al., 2008; McAdam et al., 2010) that grow on substrates other than estrogens as influent ng/L estrogen concentrations are too low to support significant biomass growth. Incorporation of anoxic zones prior to aeration basins promotes the growth of heterotrophic denitrifying bacteria that consume biodegradable chemical oxygen demand (bCOD) using nitrate as the terminal electron acceptor. As the influent substrate in AS systems with biological nitrogen removal can largely be consumed by denitrifiers, this raises the question of the role of denitrifying bacteria in estrogen removal.

Studies have shown enriched denitrifying communities degrade 17α-ethinylestradiol (EE2) under anoxic conditions, but weakly. However, no research to our knowledge has examined EE2 degradation by enriched denitrifying communities under aerobic conditions. Suarez et al. (2010) reported EE2 removals of 20 ± 13 percent in an anoxic AS laboratory reactor, and Zeng et al. (2009) observed greater than 97 percent EE2 removal after 72 hours with an enriched denitrifying culture under anoxic conditions. These removals correspond to low pseudo first order EE2 biodegradation rate coefficients (k_b) of 0.4 L/g TSS-d (Suarez et al., 2010) and 0.6 L/g TSS-d (Zeng et al., 2009). Given the retention time of anoxic basins at full-scale WWTPs, EE2 degradation at these low rates would not be expected to significantly contribute to overall EE2

removals during AS treatment. Insignificant removal of EE2 in anoxic basins has been reported for full-scale WWTPs (Andersen et al., 2003; Zhang et al., 2011). As many denitrifiers are facultative aerobes, research is needed examining whether they contribute to EE2 degradation in aeration basins.

The objective of this research was to examine anoxic and aerobic degradation of estrone (E1), 17β-estradiol (E2), and EE2 by enriched denitrifying communities grown under anoxic conditions in comparison to a denitrifying community grown under anoxic/aerobic conditions. In the first experiment, an anoxic/aerobic and anoxic-only sequencing batch reactor (SBR) were operated in parallel and EE2 concentrations were monitored over the course of the SBR cycle. In addition, mixed liquor was removed from the anoxic-only SBR for estrogen batch degradation tests under aerobic conditions. A second experiment was performed to test the estrogen-degrading ability of an enriched denitrifying community after exposure to aerobic conditions for one day to allow time for adaption to aerobic conditions and expression of enzymes before monitoring estrogen degradation. An anoxic/aerobic SBR was converted to anoxic-only operation to enrich for denitrifiers and was subsequently converted to aerobic-only operation.

5.2 Methods

Sequencing Batch Reactor (SBR) Set Up and Operation

A lab-scale anoxic/aerobic and anoxic-only SBR were operated in parallel at an 8-day SRT for 49 days (Phase I) and at a 13-day SRT for 68 days (Phase II). The reactors were seeded with mixed liquor from two laboratory anoxic/aerobic SBRs operated at an 8-day SRT, which were seeded with return activated sludge (RAS) from the City of Puyallup, WA anoxic-aerobic BNR process operated at a 10-day SRT. A separate SBR was seeded with mixed liquor from the

Durham, OR anaerobic-anoxic-aerobic BNR process operated at an 11-day SRT. This SBR was operated at a 10-day SRT under anoxic/aerobic operation for 55 days, converted to anoxic-only operation for 37 days, and converted to aerobic-only operation for one day at the end of the experiment.

The lab-scale SBRs consisted of 1-L Pyrex Erlenmeyer glass flasks with a working volume of 0.95 L and were maintained at 20°C in an environmental chamber in the dark. Mixing was achieved using magnetic stir bars. The cycle time was 4 hours for the Puyallup-seeded Phase I SBRs and 6 hours for the Puyallup-seeded Phase II SBRs and Durham-seeded SBR. Either 1/4 of the reactor volume (Puyallup-seeded Phase I SBRs and Durham-seeded SBR) or 1/8 of the reactor volume (Puyallup seeded Phase II SBRs) was decanted and replaced with synthetic feed per cycle. Synthetic wastewater was delivered during the first 30 to 45 minutes of the cycle (8 to 13 percent of the total cycle time) using peristaltic pumps. Anoxic conditions were achieved by purging the 180-mL flask headspace with nitrogen gas at 600 mL/min. For the anoxic/aerobic SBRs, the anoxic period lasted for the first hour of the cycle; aerobic periods were either 2.5 hours (Puyallup-seeded Phase I SBR) or 4.5 hours (Puyallup-seeded Phase II SBR and Durham-seeded SBR) where air was supplied by sparging through stone diffusers. A 30-minute settling/decant period occurred at the end of the cycle, and the supernatant was decanted during the last 5 minutes using a peristaltic pump. Reactor walls were scraped daily to minimize biofilm growth. Manual wasting of mixed liquor volume was done daily to maintain the target SRT, based on previous day effluent total suspended solids (TSS) and mixed liquor suspended solids (MLSS) concentration measurements.

The soluble synthetic wastewater fed to the SBRs had a chemical oxygen demand (COD) of 346 $\pm$ 37 mg/L. Organic constituents included 200 mg/L sodium acetate, 100 mg/L propionic acid, 55.2 mg/L peptone, and 20 mg/L casein. Phosphorus (29 ± 1 mg P/L) consisted of 100 mg/L K_2HPO_4 and 50 mg/L KH_2PO_4, and NH_4Cl was added at 9 ± 2 mg N/L. The feed of the anoxic/aerobic and anoxic-only SBRs contained $NaNO_3$ at 45 ± 7 and 88 ± 11 mg N/L, respectively. Macro-inorganic nutrients consisted of 346.6 mg/L $MgCl_2 \cdot 6H_2O$, 128.7 mg/L $CaCl_2 \cdot 2H_2O$, and 79.1 mg/L KCl. Two mL of trace element solution and one mL of vitamin solution were added to each liter of synthetic wastewater. The trace element and vitamin solutions are described in Chapter 4, "Biodegradation Kinetics of 17α-Ethinylestradiol in Activated Sludge Treatment Processes." Yeast extract (BD Bacto) (10 mg) was manually added to the SBRs every other day. Carbon dioxide was added to the aeration line for pH control, and alkalinity was added to the feed at 50 to 70 mg/L as $CaCO_3$. The pH of the anoxic-only SBR was controlled by adding hydrochloric acid (HCl) to the synthetic wastewater at 5 to 10 mM. Estrogens in the synthetic wastewater averaged 281 ± 39 ng/L E1, 302 ± 51 ng/L E2, and 279 ± 46 ng/L EE2.

During Phase II of the Puyallup-seeded SBRs, the synthetic wastewater strength was doubled with the exception of the phosphorus, macro-inorganic nutrients and yeast concentrations. The synthetic wastewater contained 712 ± 28 mg/L COD, 30 ± 1 mg PO_4-P /L, 17 ± 4 mg NH_3-N /L, 94 ± 2 mg NO_3-N/L (anoxic/aerobic SBR), and 190 ± 3 mg NO_3-N/L (anoxic-only SBR). Estrogen concentrations in the synthetic wastewater averaged 570 ± 105 ng/L E1, 457 ± 106 ng/L E2, and 433 ± 23 ng/L EE2. HCl in the anoxic-only SBR feed was 16 mM to control the pH.

Analytical Methods

Analytical methods for measuring volatile suspended solids (VSS), chemical oxygen demand (COD), nutrients (PO_4-P, NO_3-N, NO_2-N, and NH_3-N), and estrogens (E1, E2, and EE2) are described in Chapter 4.

Estrogen Degradation Tests

Estrogen degradation tests were conducted as in situ tests. At the end of the feeding period, each SBR was spiked with an additional E1, E2 and EE2 concentration ranging from 0 to 175 ng/L and the total estrogen concentrations were measured throughout one SBR cycle. In addition to measuring estrogen concentrations in the anoxic-only Puyallup-seeded SBR, 40 mL of the anoxic-only mixed liquor was transferred to a 100 mL flask and aerated with a stone diffuser to examine estrogen removals under aerobic conditions. All estrogen measurements were conducted in duplicate.

Terminal restriction fragment length polymorphism (TRFLP)

Microbial communities from the Puyallup-seeded SBRs were profiled using TRFLP. Mixed liquor samples (2 mL) were collected during the estrogen degradation tests, pelleted, and stored at -80°C until processing. DNA was extracted using the UltraClean Soil DNA Isolation kit (MO BIO Laboratories, Carlsbad, CA) according to the manufacturer's instruction except bead-beating took place in a FastPrep bead-beater (MP Biomedicals, Solon, OH) for 20 seconds at 4.5 m/s. Extracted DNA was stored at -80°C.

A region of the 16s rRNA gene targeting the Bacterial domain was amplified using the polymerase chain reaction (PCR) with primers 8F and 1492R (Delong, 1992). The 8F primer was modified by adding a fluorophore (6-carboxyfluorescein (6-FAM), Operon, Huntsville, AL). The PCR mixture consisted of 0.3 µL of each primer (10 µM working stock), 0.2 µL bovine serum albumin (10 mg/ml), 8.2 µL PCR-grade water, 10 µl of 2X PCR Master Mix (Fermentas K0171, Glen Burnie, MD) and 1 µL of template DNA for a total volume of 20 µL per reaction. The reaction took place in a 96-well thermocycler (Eppendorf Mastercycler ep realplex[4], Hauppauge, NY) programmed for 3 minutes at 94°C followed by 32 cycles of 94°C for 30 seconds, 52°C for 45 seconds and 72°C for 1 minute. The program finished with 4 minutes at 72°C and was held at 4°C until sample removal. PCR products were digested using the restriction enzyme RsaI (Promega, Madison, WI). The digestion mixture consisted of 0.1 µL bovine serum albumin (10 mg/ml), 3.4 µL of PCR-grade water, 1 µL of 10X Buffer C (Promega), 0.5 µL of enzyme (10U/µL) and 5 µL of PCR product for a total volume of 10 µL per reaction. Samples were incubated for 8 hours at 37°C. The restriction fragments were precipitated with ethanol.

Fragment analysis of digested samples was carried out with an ABI 3130xl Genetic Analyzer equipped with an 80 cm capillary array with POP-7 polymer (Applied Biosystems, Foster City, CA). Each sample was resuspended in a mixture consisting of 24.1 µL Hi-Di formamide (Applied Biosystems) and 0.9 µL MapMarker 1000 with X-Rhodamine label (BioVentures, Murfreesboro, TN) and denatured at 90°C for 2 minutes prior to being loaded on the instrument. Collected profiles were analyzed using the DAx software package (Van Mierlo Software Consultancy, Eindhoven, The Netherlands) with automated peak calling from 50 to 1000 bp and

106

a size limit of 1% of the total peak area. Principal component analysis of the TRFLP profiles was performed using JMP 6.0 (SAS, Cary, NC) statistical software.

5.3 Results and Discussion

SBR performance

High levels of nitrate removal occurred in the anoxic/aerobic and anoxic-only SBRs. For the anoxic/aerobic SBRs, denitrification resulted in an average NO_3-N reduction of 47 ± 6 mg/L for the Puyallup-seeded Phase I and Durham-seeded SBRs and 80 ± 20 mg/L for the Puyallup-seeded Phase II SBR. For the anoxic-only SBRs, denitrification resulted in an average NO_3-N reduction of 86 ± 9 mg/L for the Puyallup-seeded Phase I and Durham-seeded SBRs and 175 ± 8 mg/L for the Puyallup-seeded Phase II SBR. Ninety-seven to 99 percent of the total influent soluble COD (sCOD) removal occurred in the anoxic period.

Nitrification occurred in all of the anoxic/aerobic SBRs with effluent NH_3-N concentrations typically below 0.5 mg N/L. Based on effluent NO_3-N and NO_2-N measurements and accounting for NO_3-N and NO_2-N at the end of the anoxic period, the amount of ammonia oxidized averaged 8 ± 4 mg N/L for the Puyallup-seeded Phase I and Durham-seeded SBRs and 10 ± 3 mg N/L for the Puyallup-seeded Phase II SBR. Average effluent NH_3-N concentrations of the anoxic-only SBRs were 7 ± 1 mg N/L for the Puyallup-seeded Phase I and Durham-seeded SBRs and 15 ± 1 mg N/L for the Puyallup-seeded Phase II SBR.

The anoxic-only SBRs consistently had a higher mixed liquor VSS (MLVSS) concentration than the corresponding anoxic/aerobic SBRs. The MLVSS concentration (mg/L) averaged 908 ± 50 (anoxic/aerobic) and 944 ± 130 (anoxic-only) for the Puyallup Phase I SBRs; 1014 ± 91

107

(anoxic/aerobic) and 1136 ± 175 (anoxic-only) for the Puyallup Phase II SBRs; and 762 ± 97 (anoxic/aerobic) and 894 ± 114 (anoxic-only) for the Durham-seeded SBRs. The higher MLVSS concentrations in the anoxic-only SBRs was likely due to reduced endogenous decay under anoxic conditions versus aerobic conditions (Siegrist et al., 1999). The pH averaged 7.8 ± 0.2 in the anoxic/aerobic SBRs and 7.9 ± 0.4 in the anoxic-only SBRs.

Microbial community analysis

Divergence of SBR microbial communities occurred following operation under anoxic/aerobic and anoxic-only conditions as illustrated by TRFLP profiles for the Puyallup-seeded SBRs (Figure 5-1). Based on principal component analysis (Aguado and Rosen, 2008) of the bacterial TRFLP profiles, the operating redox conditions and aerobic SRT explained the greatest variation between the different SBR communities (Figure 5-2). Principal components 1 and 2 grouped microbial communities based on the anoxic/aerobic operation at a 5-day aerobic SRT, the anoxic/aerobic operation at a 10-day aerobic SRT, and the anoxic-only operation, explaining 51 percent of the variation between TRFLP profiles.
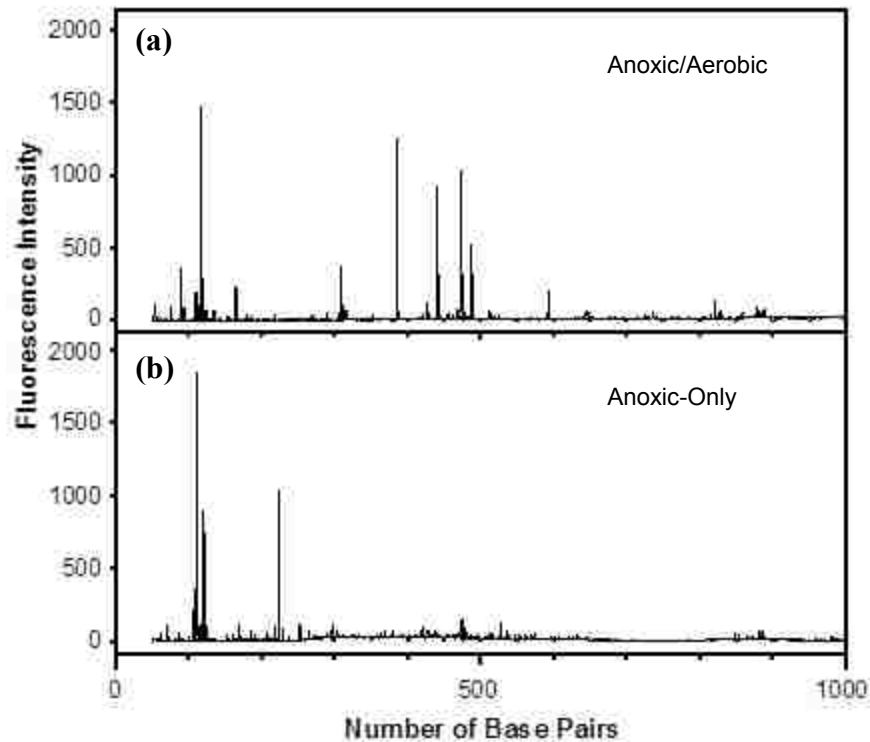
Figure 5-1. TRFLP electropherograms showing difference between (a) anoxic/aerobic and (b) anoxic-only SBR communities in Phase II Puyallup-seeded SBRs
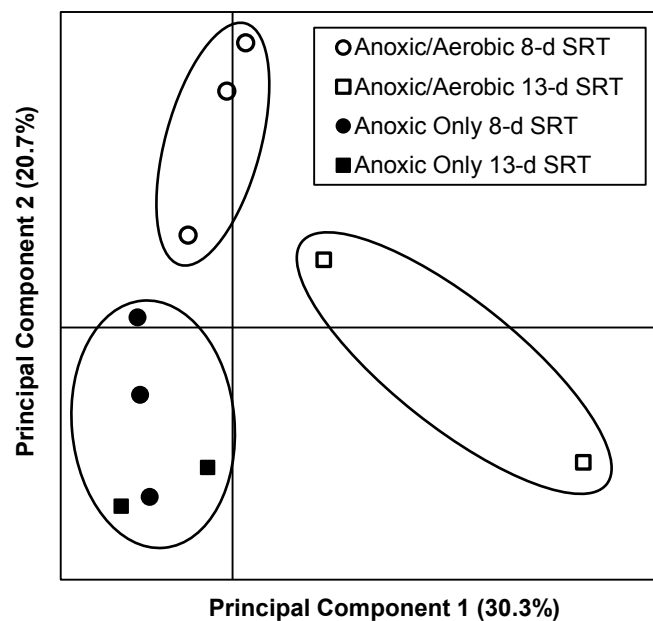

Figure 5-2. Principal component analysis of bacterial TRFLP profiles for Puyallup-seeded anoxic/aerobic and anoxic-only SBR communities

109

EE2 biodegradation

The Puyallup-seeded anoxic-only biomass did not degrade EE2 during anoxic operation. A plot of the total mixed liquor EE2 concentration at the end of the react period (prior to settling) normalized to the feed concentration showed EE2 was consistently not removed in the anoxic-only SBR whereas EE2 was degraded in the anoxic/aerobic SBR (Figure 5-3). Both Suarez et al. (2010) and Zeng et al. (2009) reported enriched denitrifying communities grown in anoxic laboratory reactors degraded EE2 under anoxic conditions, but the anoxic degradation rates were extremely slow with pseudo first order EE2 biodegradation rate coefficients (k_b) normalized to reactor TSS of 0.4 L/g TSS-d and 0.6 L/g TSS-d (Zeng et al., 2009), respectively. Although in situ batch tests in this study showed no EE2 removals occurred during the 3.5-hour or 5.5-hour long anoxic period of the anoxic-only SBR (Phases I and II), Zeng et al. (2009) monitored EE2 removals with an enriched denitrifying community for 72 hours to capture their degradation kinetics. To address whether the anoxic-only biomass degraded EE2 at a slow rate, EE2 k_b values were calculated as described in Chapter 4 by fitting an SBR model to the total mixed liquor EE2 concentration at the end the anoxic period ($EE2_{T,\Theta anox}$, ng/L). Equation 5 presented in Chapter 4 was slightly modified by replacing $EE2_{T,\Theta aer}$ with $EE2_{T,\Theta anox}$ and the aerobic cycle time (Θ_{aer}) with the anoxic cycle time (Θ_{anox}), resulting in the following equation:

$$EE2_{T,\theta anox} = \frac{EE2_f(1+K_PX_{VSS})}{\left[1 + K_PX_{VSS}\frac{V}{Q \cdot SRT} + (1+K_PX_{VSS})(1+R)(e^{k_bX_{VSS}\Theta_{anox}/(1+K_PX_{VSS})} - 1)\right]} \quad (1)$$

$EE2_f$ is the feed total EE2 concentration (ng/L), K_P is the EE2 solid-liquid partitioning coefficient (L/g VSS), X_{VSS} is the mixed liquor VSS (g/L), V is the reactor volume (L), Q is the flow (L/d), and R is the ratio of the SBR volume after decanting to the feed volume. An average apparent K_P of 0.27 ± 0.10 L/g VSS (*n* = 5) was determined as described in Chapter 4. EE2 k_b

values calculated by fitting Equation 1 to measurements of $EE2_{T,\Theta anox}$, $EE2_f$, and X_{VSS} collected that day resulted in averages of 0.1 ± 0.08 and 0.07 ± 0.04 L/g VSS-d for Phases I and II, respectively. This enriched denitrifying community therefore did not degrade EE2 in the anoxic-only SBR.

Figure 5-3. Comparision of the total mixed liqour EE2 concentration at the end of the react period normalized to the feed concentration in the Puyallup-seeded anoxic-only and anoxic/aerobic SBRs

The Puyallup-seeded anoxic-only biomass also did not degrade EE2 under aerobic conditions or the degradation was at such a low rate that it was unobservable. While an average of 32 percent of the EE2 was removed during the 2.5-hour aerobic period of the Phase I anoxic/aerobic SBR (based on three in situ batch tests), insignificant EE2 degradation occurred with the anoxic-only biomass in aerobic batch tests (Figure 5-4). Similarly, the Phase II anoxic-only biomass did not degrade EE2 in aerobic batch tests, but an average of 51 percent of the EE2 was removed during the 4.5-hour aerobic period of the corresponding anoxic/aerobic SBR (based on two in situ batch tests). The lack of EE2 degradation by the anoxic-only biomass indicates some denitrifying

111

bacteria may not degrade EE2. Alternatively, these bacteria may have been capable of aerobically degrading EE2 but did not have adequate time for expression of EE2-degrading genes, as their EE2-degrading ability was examined immediately after exposure to aerobic conditions.
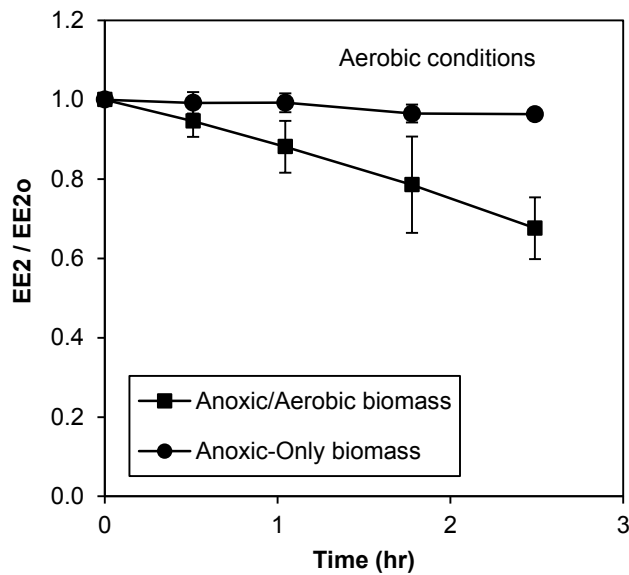
Figure 5-4. Comparison of EE2 degradation by the Phase I anoxic-only and anoxic/aerobic biomasses under aerobic conditions

In a second experiment, EE2 degradation by the Durham-seeded anoxic-only biomass was similarly not detected under anoxic conditions or following conversion to aerobic conditions for one day. Upon switching the anoxic-only SBR to aerobic-only operation, 81 mg of sCOD, representing 98 percent of the initial sCOD after feeding, was utilized within an hour while only 2.6 mg of NO_3-N was partially denitrified to NO_2-N (oxygen equivalent of 3 mg), suggesting that oxygen was the primary terminal electron acceptor. Results from single in situ batch tests conducted at the end of the anoxic and aerobic operations are shown in Figure 5-5. No EE2 was removed during the 5.5-hour aerobic period. EE2 increased by about 20 percent during the
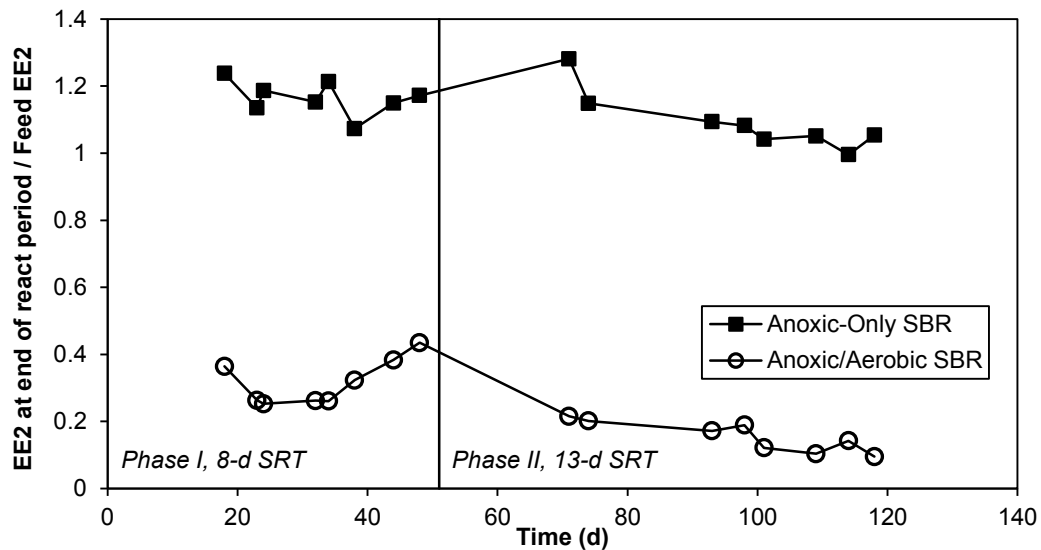
5.5-hour anoxic period, which was likely due to analytical error. A plot of the total mixed liquor EE2 concentration at the end of the react period normalized to the feed concentration (Figure 5-6) also indicated EE2 was not removed during the anoxic or aerobic operations. EE2 feed concentrations were not collected for all of these days, and six of the data points in Figure 5-6a (including the two data points below one) were based on feed concentrations measured on previous days. The results from this second experiment support previous observations of the first experiment that some denitrifying bacteria do not degrade EE2.
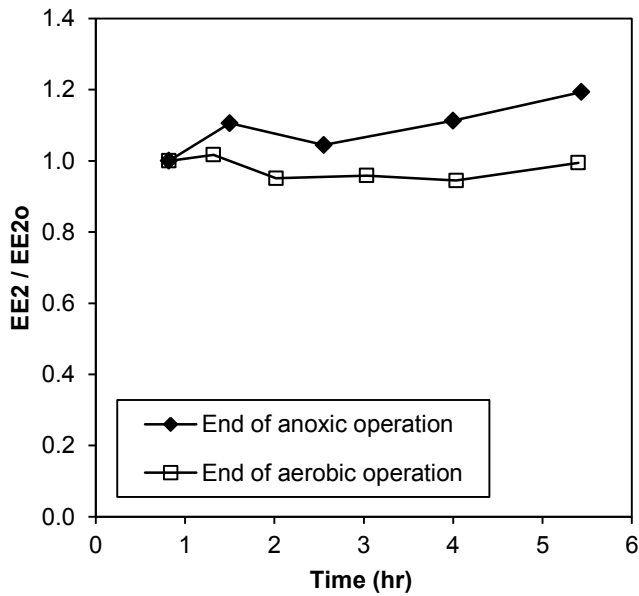
Figure 5-5. Results from in situ EE2 degradation tests for the Durham-seeded SBR at the end of anoxic and aerobic operations
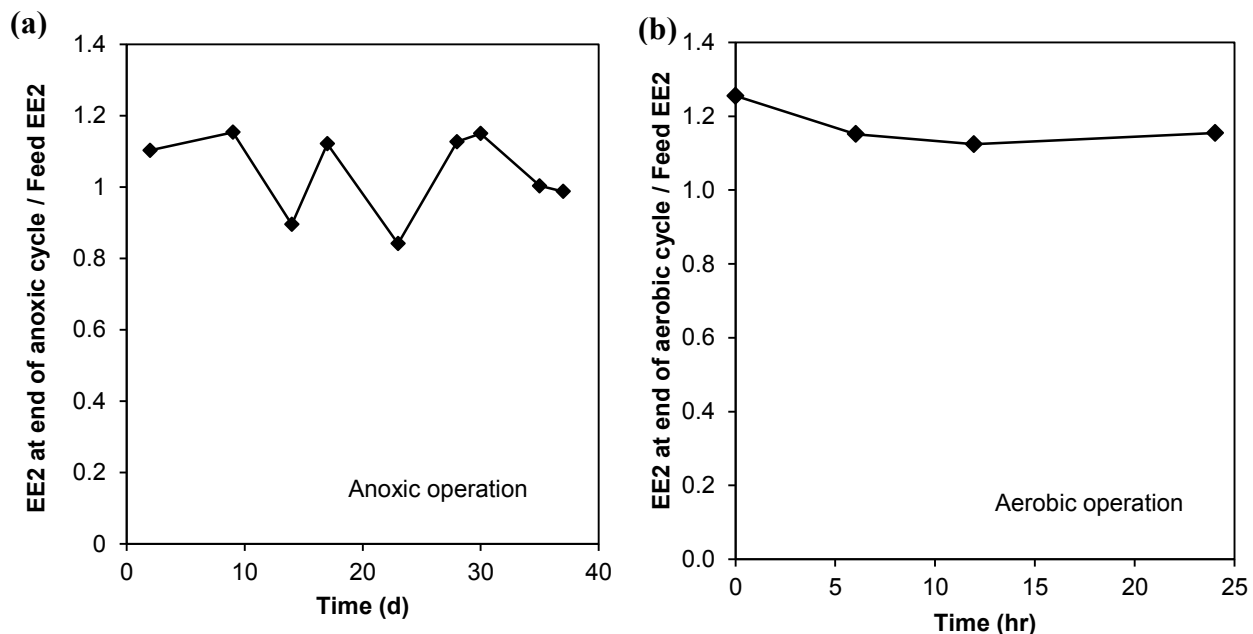
Figure 5-6. Total mixed liquor EE2 concentration at the end of the react period normalized to the feed concentration in the Durham-seeded SBR for (a) anoxic-only operation and (b) after conversion to aerobic-only operation

EE2 was degraded in corresponding anoxic/aerobic SBRs where the majority of influent substrate supported denitrifying biomass. Average EE2 k_b values of the anoxic/aerobic biomass determined in Chapter 4 were 5.9, 4.2, and 4.3 L/g VSS-d for the Puyallup-seeded Phase I anoxic/aerobic SBR (corresponds to Phase II in Chapter 4), Puyallup-seeded Phase II anoxic/aerobic SBR (corresponds to Phase III in Chapter 4), and Durham-seeded anoxic/aerobic SBR, respectively. Based on NO_3-N and NO_2-N measurements at the end of the anoxic period and accounting for effluent NO_3-N and NO_2-N, the amount of COD oxidized for nitrate reduction accounted for 47 and 41 percent of the total COD removed during the anoxic period for the Puyallup-seeded and Durham-seeded anoxic/aerobic SBRs, respectively. Assuming no storage, the resulting biomass yields are 0.53 and 0.59 g COD/g COD for the respective SBRs, which are similar to the reported anoxic yield of heterotrophic biomass of 0.54 g COD/g COD (Gujer et al., 1999). The COD removed during the anoxic period was therefore unlikely due to

114

storage but rather to support the growth of denitrifying bacteria respiring nitrate. As 97 to 99 percent of the total influent sCOD removal occurred in the anoxic period, the majority of the feed substrate supported denitrifying biomass in these anoxic/aerobic SBRs.

As the majority of influent substrate supported denitrifying biomass in the anoxic/aerobic SBRs but enrichment for denitrifying biomass resulted in loss of EE2-degrading ability, at least some of the influent substrate in the anoxic/aerobic SBRs did not support EE2-degrading biomass. Although EE2 degradation in the anoxic/aerobic SBRs could have been due to denitrifying biomass that did not thrive under the anoxic-only operation, another possibility deserving further research is the growth of EE2-degrading populations on cell lysis products during the aeration cycle. Cometabolism of EE2 by ammonia oxidizing bacteria (AOBs) growing on inorganic carbon was likely not an important contribution to EE2 degradation as discussed in Chapter 4 for these anoxic/aerobic SBRs.

E1 and E2 biodegradation

E1 and E2 were degraded to below the limit of quantification of 5 ng/L in the Puyallup-seeded anoxic-only SBR during both phases. Removal of E1 and E2 under anoxic conditions has also been observed in an lab-scale anoxic-only reactor (Suarez et al., 2010), in the anoxic compartment of a lab-scale anaerobic/anoxic/aerobic reactor (Li et al., 2011), and in the anoxic basin at a full-scale WWTP (Andersen et al., 2003). Bacteria able to grow on E1 and E2 as the sole carbon source while respiring nitrate have also been isolated (Fahrbach et al., 2008, 2006). Anoxic degradation of E1 and E2 by denitrifying bacteria is therefore an important removal mechanism in BNR AS systems due to the upstream location of anoxic basins.

The Puyallup-seeded anoxic-only biomass also degraded E1 and E2 in aerobic batch tests, albeit at lower rates than under anoxic conditions. E1 production from oxidation of E2 made calculating E1 removals ambiguous. Therefore, (E1 + E2) removals were calculated as a means of quantifying overall degradation of the natural estrogens. The average (E1 + E2) removal was about 30 percent during both 2.5-hour (Phase I) and 4.5-hour (Phase II) aerobic batch tests. Denitrifying bacteria may therefore contribute to degradation of natural estrogens under aerobic conditions as well.

The Durham-seeded anoxic-only biomass reduced E1 to E2 during anoxic operations but had limited subsequent degradation of the natural estrogens (Figure 5-6a). Following conversion of the SBR to aerobic operation, E2 was oxidized to E1 within one SBR cycle with minor overall removals of the natural estrogens (Figure 5-7b). The oxidation of E2 indicated aerobic steroid transformations were able to occur within one day of switching to aerobic conditions. These results suggest some denitrifying bacteria are capable of interconverting E1 and E2 but are unable to further degrade the natural estrogens.
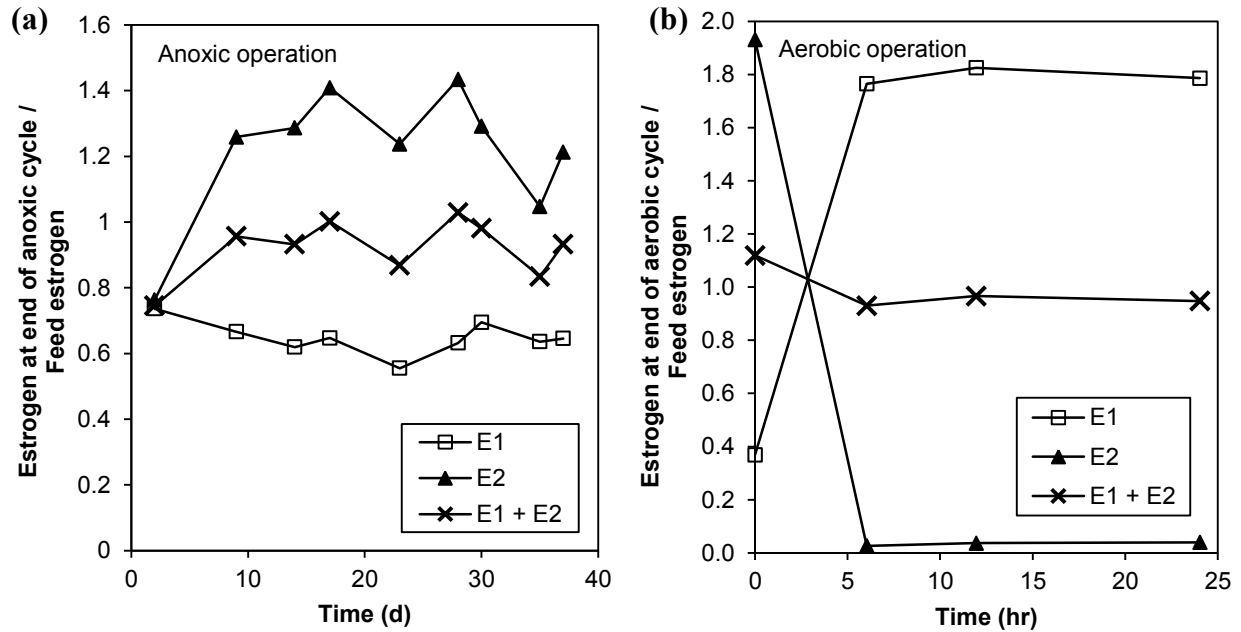
Figure 5-7. Total mixed liquor E1, E2, and E1 + E2 concentrations at the end of the react period normalized to the feed concentration in the Durham-seeded SBR for (a) anoxic-only operation and (b) after conversion to aerobic-only operation

5.4 Conclusions

Enriched denitrifying communities did not degrade EE2 under anoxic or aerobic conditions, suggesting at least some of the influent substrate in anoxic/aerobic operations does not support EE2-degrading biomass. Denitrifying communities can degrade E1 and E2 under both anoxic and aerobic conditions, but there are some denitrifying communities that can only interconvert E1 and E2 without further degradation.

117

Chapter 6: Degradation, Inhibition, and Transposome Mutagenesis Experiments with the EE2-degrading bacterium *Rhodococcus equi*

6.1 Introduction

A central focus of this research was to improve the ability to model EE2 biodegradation in activated sludge (AS) systems. Estrogen biodegradation in the model presented in Chapter 3, "Extension of ASM2d to Model the Fate of 17α-Ethinylestradiol in Activated Sludge Systems," is currently based on the heterotrophic biomass concentration. The fraction of EE2-degraders in the AS heterotrophic population may vary based on wastewater composition, process configuration, and operational conditions. As a consequence, predicting the fate and transformation of EE2 would be improved by directly relating biodegradation to a known concentration of EE2-degrading biomass. The concentration of bacteria associated with a specific metabolic activity has been quantified in other work based on key functional genes such as ammonia monooxygenase, toluene dioxygenase, naphthalene dioxygenase, nitrite reductase, and sulfate reductase (Ben-Dov et al., 2007; Busi da Silva and Corseuil, 2012; Geets et al., 2007). However, the lack of knowledge on EE2 biodegradation pathways and functional genes prevents the ability to quantify EE2-degrading biomass for different activated sludge processes.

Though heterotrophic bacteria responsible for EE2 degradation in AS systems are currently unknown, bacteria have been isolated that can grow solely on EE2 or degrade EE2 with growth on another substrate (Table 6-1).

Table 6-1. Source and co-substrate needs of EE2-degrading isolates

Isolate	Source	Co-substrate	Reference
Degrades EE2 as sole carbon source			
Sphingobacterium sp. JCR5	Oral contraceptive factory AS	-	Haiyan et al. (2007)
Rhodococcus zopfii Y50158	Municipal AS	-	Yoshimoto et al. (2004)
Rhodococcus equi Y50155	Municipal AS	-	Yoshimoto et al. (2004)
Rhodococcus equi Y50156	Municipal AS	-	Yoshimoto et al. (2004)
Rhodococcus equi Y50157	Municipal AS	-	Yoshimoto et al. (2004)
Degrades EE2 with growth on co-substrate			
Acinetobacter sp. BP8	Compost	E1 and E2	Pauwels et al. (2008)
Acinetobacter sp. BP10	Compost	E1 and E2	Pauwels et al. (2008)
Ralstonia pickettii BP2	Compost	E1 and E2	Pauwels et al. (2008)
Phyllobacterium myrsinacearum BP1	Compost	E1 and E2	Pauwels et al. (2008)
Pseudomonas aeruginosa BP3	Compost	E1 and E2	Pauwels et al. (2008)
Pseudomonas sp. BP7	Compost	E1 and E2	Pauwels et al. (2008)
Pseudomonas aeruginosa ATCC 15692	ATCC[a]	Ethanol	Larcher and Yargeau (2013)
Pseudomonas putida ATCC 12633	ATCC	Ethanol	Larcher and Yargeau (2013)
Bacillus subtilis ATCC 6051	ATCC	Ethanol	Larcher and Yargeau (2013)
Rhodococcus rhodochrous ATCC 13808	ATCC	Ethanol	Larcher and Yargeau (2013)
Rhodococcus zopfii ATCC 51349	ATCC	Ethanol	Larcher and Yargeau (2013)
Rhodococcus erythropolis ATCC 4277	ATCC	ethanol, adipic acid	Larcher and Yargeau (2013), O'Grady et al. (2009)
Rhodococcus equi ATCC 13557	ATCC	ethanol, glucose	Larcher and Yargeau (2013), O'Grady et al. (2009)

a. ATCC – American Type Culture Collection

Of the identified EE2-degrading strains, only Rhodococci have been isolated from municipal AS. Three of these four isolates were *R. equi* species. *R. equi* may be an EE2-degrader in AS and was selected to be used in this study.

This chapter presents experiments with a *R. equi* strain to examine its biodegradation kinetics, effect of inhibition, and the application of a transposon mutagenesis technique to identify genes involved in EE2 degradation. The first experiment examined EE2 biodegradation kinetics of *R. equi* at ng/L concentrations and assessed the impact of growth condition on the biodegradation rate. The second experiment explored inhibition of EE2 degradation by azole compounds. Azole compounds are competitive inhibitors of cytochrome P450 mono-oxygenases (CYPs), a family of enzymes with primarily hydrophobic substrates (McLean et al., 2002). CYPs are involved in mammalian metabolism of steroids and xenobiotics (Omura, 2010) and have been identified in bacterial transformations of steroids and xenobiotics as well (Lewis and Wiseman, 2005). Agematu et al. (2006) screened 213 bacterial CYPs and found 24 that hydroxylated testosterone, including CYPs from *Streptomyces, Rhodococcus, Nocardia,* and *Bacillus.* CYPs are commonly found in actinomycetes, including *Mycobacterium, Streptomyces, Nocardia,* and *Rhodococcus*, as well as other genera including *Bacillus* and *Pseudomonas* (Kelly and Kelly, 2013; Lewis and Wiseman, 2005). Interest in CYPs for this second experiment was based on their involvement in steroid transformations and their presence in *Rhodococci* and other EE2-degrading species.

The last experiment involved isolation of a *R. equi* mutant with hindered EE2-degrading ability using transposome mutagenesis and the yeast estrogen screen (YES) assay. The

120

transposome is a protein-DNA complex consisting of a hyperactive Tn5 transposase and a DNA fragment containing a kanamycin resistance gene. Upon introduction of the transposome into cells by electroporation, the transposase becomes active in the presence of magnesium and facilitates transposition of the DNA fragment into the host DNA. Screening of mutants for loss of EE2-degrading ability was done with the YES assay (Routledge and Sumpter, 1996) which provides colorimetric identification of estrogenic potency. The YES assay employs a genetically modified yeast that expresses a human estrogen receptor. Binding of estrogenic compounds to the receptor results in production of the enzyme β-galactosidase, which metabolizes a yellow substrate (chlorophenol red-β-D-galactopyranoside) into a red product. Research identifying the cause of the mutant's loss of EE2-degrading ability was expected to reveal useful information about the EE2 degradation pathway and possibly the genes involved.

6.2 Methods

Bacterial strain and growth conditions

R. equi ATCC 13557 was from the American Type Culture Collection (Manassas, VA, USA). *R. equi* was grown in autoclaved Luria Bertani (LB) broth (Lennox, EMD Millipore) or in filter sterilized (0.2 μm supor membrane) glucose minimal media. The glucose minimal media consisted of Modified Mineral Salt Media supplemented with 0.1 g/L yeast extract (BD Bacto) and either 0.5 g/L glucose (biodegradation kinetics experiment) or 2 g/L glucose (azole inhibition and mutation experiments). The Modified Mineral Salt Media was prepared according to O'Grady et al. (2009) and contained 4 g/L NH_4NO_3, 4 g/L KH_2PO_4, 6 g/L Na_2HPO_4, 0.2 g/L $MgSO_4·7H_2O$, 0.01 g/L $CaCl_2·2H_2O$, 0.01 g/L $FeSO_4·7H_2O$, and 0.014 g/L Na_2EDTA. Growth

on solid media was on LB agar (Miller, Fisher BioReagents) plates. When appropriate during the mutagenesis experiment, the growth media was supplemented with 200 µg/mL kanamycin.

Growth and chemical oxygen demand measurements

R. equi growth was monitored by measuring the optical density at 500 nm (OD_{500}) using a HACH DR/4000 U Spectrophotometer (Loveland, CO). Volatile suspended solids (VSS) and soluble chemical oxygen demand (sCOD) concentrations were measured as described in Chapter 3.

EE2 batch degradation tests

A 1-L Erlenmeyer flask with foam plug containing 350 mL of glucose minimal media without EE2 was inoculated with 5 mL of *R. equi* in LB and placed in a shaking incubator at 27°C. *R. equi* growth was monitored by OD_{500}. At Day 1 and Day 7.7, 40 mL of the *R. equi* culture was transferred to a sterilized 250-mL flask to conduct EE2 batch degradation tests at exponential and stationary growth phases, respectively. Batch tests consisted of amending the *R. equi* culture with approximately 120 ng/L of EE2 using an aqueous stock solution and shaking the culture in the dark. Total EE2 and OD_{500} measurements were collected over a 72-hour period for the exponential phase batch test and a 36-hour period for the stationary phase batch test. The experiment was conducted in duplicate. For determining the EE2 k_b value, the OD_{500} measurements were converted to a VSS basis using a linear relationship obtained by removing mixed liquor samples for VSS measurements in parallel to OD_{500} measurements at various stages of the growth curve. The specific growth rate (µ) was determined in the presence of EE2 using the exponential phase EE2 batch degradation test data (culture in 250-mL flask) as well as in the

absence of EE2 using the corresponding data for the culture in the 1-L flask. Between Day 4 and 4.9 of the experiment, the temperature was reduced to 20°C and shaking ceased due to an incubator failure. Normal operating conditions were resumed from Day 4.9 to 9.2. EE2 batch degradation tests in the 250-mL flasks were conducted prior to and after the incubator failure period.

EE2 batch degradation tests with azole compounds

An *R. equi* culture grown in glucose minimal media at 27°C was amended with 0.85 mg/L EE2 using an aqueous stock solution, and 50 mL aliquots were transferred to sterilized 250-mL flasks with foam plugs. Individual flasks were amended with 0.5 mM clotrimazole, 0.5 mM ketoconazole, or no azole compound as a control. All flasks contained 2 percent v/v dimethyl sulfoxide (DMSO) which was used as a cosolvent. The flasks were shaken in the dark at 27°C, and total EE2 concentrations were measured over a 48-hour period. VSS concentrations of the culture were measured at the beginning and at the end of the experiment. The degradation tests were conducted in duplicate.

Transposome mutagenesis

Random insertion mutagenesis was performed using the EZ-Tn5 <R6Kγ*ori*/KAN-2>Tnp Transposome kit (Epicentre, Madison, WI) as described by Mangan and Meijer (2001). Briefly, electrocompetent *R. equi* were electroporated with the transposome, and a kanamycin-resistant mutant library was obtained by plating the electroporated mixture on LB plates containing 200 µg/ml kanamycin.

Screening mutants using YES Assay

Kanamycin-resistant colonies obtained from transposome mutagenesis were picked into individual wells of 96-well microtiter plates containing 150 µL of LB broth and 200 µg/ml kanamycin. The microtiter plates were sealed with masking tape and mutants were grown overnight at 30°C. Ten µl of each mutant in LB was subsequently transferred to individual wells of microtiter plates containing 140 µL of glucose minimal media, 200 µg/mL kanamycin, and 1 µg/L EE2. The microtiter plates were sealed with masking tape and shaken (175 rpm) for 3 days at 30°C in the dark to allow for EE2 degradation. Ten-µL samples from each well were then transferred to microtiter plates and analyzed using the YES assay according to Routledge and Sumpter (1996). Mutants corresponding to "pink" wells were identified as potential non-EE2-degraders; mutants corresponding to "yellow" wells were assumed to be EE2-degraders. In a second transposome mutagenesis experiment, mutants were screened as just described except the glucose minimal media contained 2 µg/L EE2 and degradation was allowed to take place for 4 days prior to conducting the YES assay.

Estrogen degradation tests with mutants

Sterilized 250-mL Erlenmyer flasks with foam plugs containing 45 mL of glucose minimal media were amended with 200 µg/mL kanamycin and 70 µg/L of E1, E2, and EE2. Batch tests conducted during the second transposome mutagenesis experiment did not contain E2. Mutant cultures grown overnight in LB were diluted with LB such that all cultures had the same starting OD_{500}. The flasks were inoculated with the mutant in LB and shaken at 30°C in the dark. Total estrogen and OD_{500} concentrations were measured over the course of four to seven days. Streak

plates were performed at the end of each experiment to confirm there was no contamination. All degradation tests were conducted in triplicate.

Identification of transposon insertion site

Rescue cloning was performed in order to identify the location of the transposon insertion site in *R. equi* mutants. DNA manipulations were carried out according to the manufacturer's instructions unless noted otherwise. Genomic DNA was isolated using the PowerLyzer PowerSoil DNA Isolation kit (MO BIO Laboratories, Inc., Carlsbad, CA) where *R. equi* cells were incubated at 70°C for 10 minutes prior to the bead-beating step and bead-beating took place in a FastPrep bead-beater (MP Biomedicals, Solon, OH) for 30 seconds at 5 m/s (repeated twice). Genomic DNA was digested using the restriction enzyme KpnI (Promega, Madison, WI) and the DNA fragments were subsequently self-ligated using T4 DNA ligase (Promega, Madison, WI). The transposon contains a R6Kγ origin of replication which requires the Π initiation protein for vector replication. Electrocompetent *E. coli* expressing the Π protein (TransforMax EC100D *pir*-116 Electrocompetent *E. coli* from Epicentre, Madison, WI) were electroporated with the ligation mixture using a Bio-Rad Gene Pulser II (25 µF, 200 Ω, 12.5 kV/cm) in a 2 mm gapped cuvette (Bio-Rad, Hercules, CA). The electroporation mixture was plated on LB agar plates containing 50 µg/mL kanamycin and incubated at 37°C. Plasmid DNA was isolated from kanamycin-resistant *E. coli* harboring the EZ-Tn5 <R6Kγ*ori*/KAN-2> transposon vector using the PureLink Quick Plasmid Miniprep kit (Invitrogen, Grand Island, NY). The DNA flanking the transposon insertion site was sequenced using SimpleSeq DNA sequencing (Eurofins MWG Operon, Huntsville, AL) and the primers provided with the transposome kit.

Estrogen analyses

EE2 measurements at ng/L concentrations were according to a modified method of Gaulke et al. (2008) as described in Chapter 3. E1, E2, and EE2 measurements at µg/L concentrations were obtained by vortexing 500 µl of sample with 500 µl of internal standard solution (100 µg/L of E2-d_4 and EE2-d_4 in ACN) in a microcentrifuge tube. The sample was centrifuged for 10 minutes at 10,000 rpm at 4°C, and the supernate was analyzed for non-derivatized free estrogens as described in Chapter 3.

EE2 biodegradation kinetics and solid-liquid partitioning

EE2 biodegradation was modeled as a pseudo first-order rate as a function of the soluble estrogen concentration and biomass VSS as described in Chapter 4, "Biodegradation Kinetics of 17α-ethinylestradiol in Activated Sludge Treatment Processes." For estrogen degradation during exponential growth, the biomass VSS concentration (X, g VSS/L) can be modeled as follows:

$$X = X_o e^{\mu t} \tag{1}$$

where X_o is the initial biomass concentration (g VSS/L), μ is the specific growth rate coefficient accounting for growth and endogenous decay (g VSS/g VSS-d), and t is the time (d). Estrogen biodegradation during exponential growth was described by the following differential equation:

$$\frac{dE_T}{dt} = \frac{-k_b E_T X_o e^{\mu t}}{1 + K_P X_o e^{\mu t}} \tag{2}$$

where E_T is the total EE2 concentration (ng/L), k_b is the pseudo first-order biodegradation rate coefficient (L/g biomass VSS-d), and K_P is the EE2 solid-liquid partitioning coefficient (L/g VSS). Solving for E_T (integration shown in Appendix II) results in the following model for estrogen biodegradation during exponential growth:

126

$$E_{T,t} = E_{T,o} \left(\frac{1+K_P X_o e^{\mu t}}{1+K_P X_o} \right)^{-\frac{k_b}{K_P \mu}}$$ (3)

The value for μ was obtained by fitting Equation 1 to biomass VSS concentrations using the nonlinear least squares (nls) function in R (version 2.15.2). Similarly, the EE2 k_b value was determined by fitting Equation 3 to total EE2 concentrations collected during the batch degradation test. Confidence intervals for μ were calculated using the confidence intervals for model parameters (confint) function in R.

Total and soluble EE2 (E_S, ng/L) concentrations of the *R. equi* culture were measured to determine an apparent EE2 K_P. Three measurements were collected over the course of 20 hours during the stationary phase of the growth curve when EE2 was not being degraded. K_P values were determined using the following equation:

$$K_P = \frac{E_T - E_S}{X \cdot E_S}$$ (4)

These K_P values were used in calculating EE2 k_b values as described above.

6.3 Results and Discussion

The following are the results from experiments with *R. equi* examining EE2 biodegradation kinetics, inhibition of EE2 degradation by azole compounds, and isolation of mutants with hindered EE2-degrading ability.

EE2 biodegradation kinetics

Based on the VSS versus OD_{500} results (Figure 6-1) and the OD_{500} versus time results (Figure 6-2a), a μ of 0.69 g/g-d (95 percent confidence interval of 0.67 to 0.71 g/g-d) was observed during exponential growth. The presence of EE2 at ng/L concentrations did not affect the growth rate of *R. equi* as a similar μ of 0.71 g/g-d (95 percent confidence interval of 0.69 to 0.73 g/g-d) was observed with the *R. equi* culture with EE2 present (Figure 6-2b). *R. equi* degraded EE2 at ng/L concentrations during exponential growth with a fitted k_b value of 3.4 L/g VSS-d (Figure 6-2b), but did not degrade EE2 during the stationary phase (Figure 6-2c).
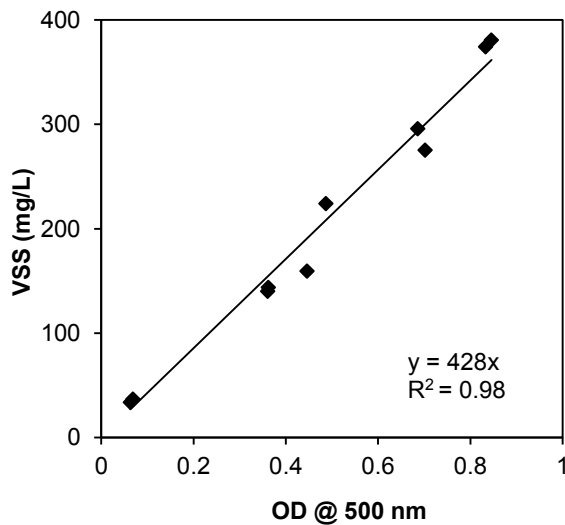
Figure 6-1. VSS versus OD_{500} of *R. equi* culture grown on glucose
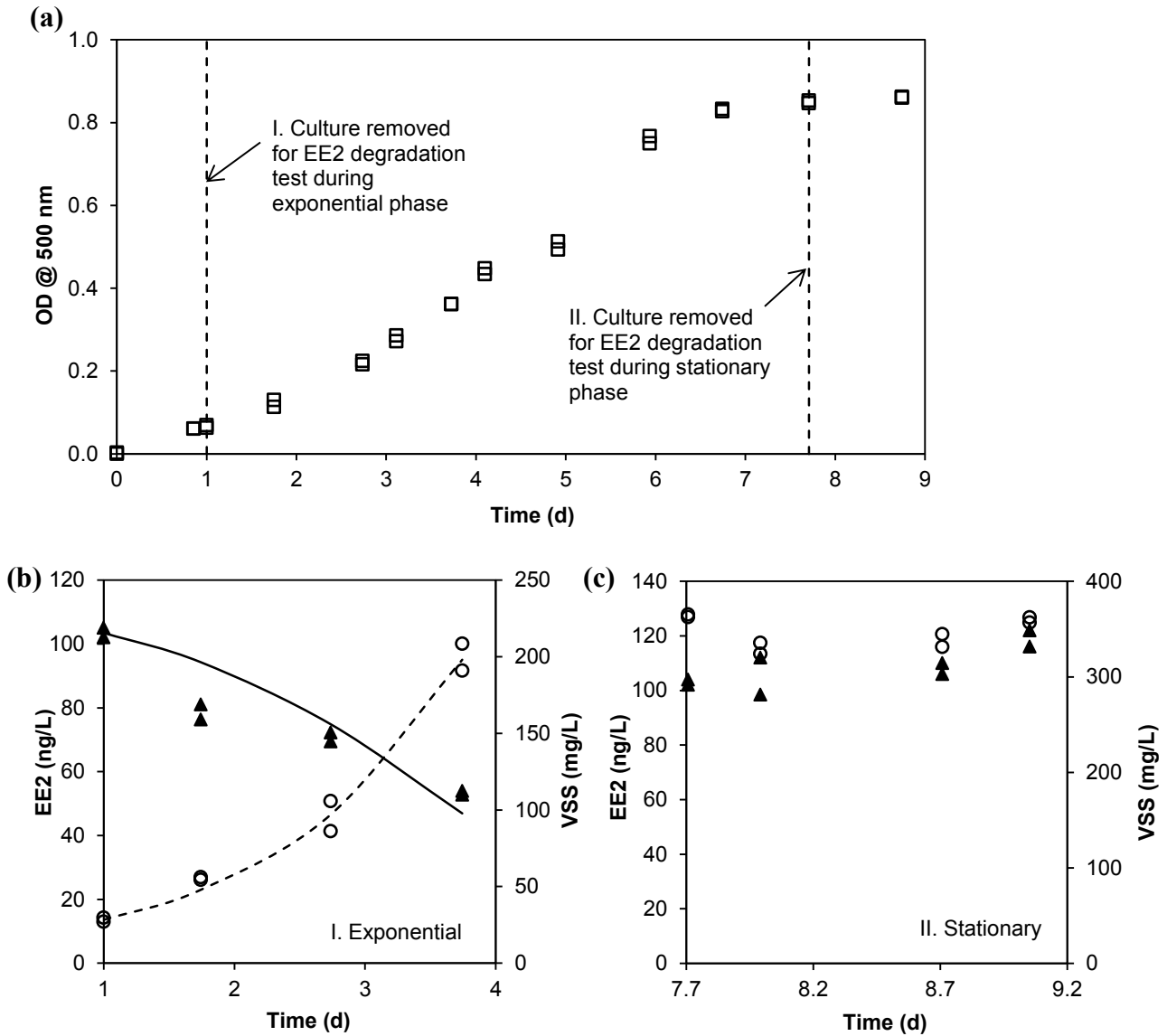
Figure 6-2. (a) Growth curve of *R. equi* at 27°C and results of EE2 batch degradation tests conducted with *R. equi* culture at (b) exponential and (c) stationary phases. Data is indicated by markers ($\square$ – OD_{500}, $\blacktriangle$ – EE2, $\circ$ - VSS). Modeled VSS and EE2 concentrations based on fitted μ and k_b values are shown by dashed and solid lines, respectively.

An average EE2 K_P value of 0.25 ± 0.04 L/g VSS was measured during the *R. equi* stationary phase and used in Equation 3 to determine EE2 k_b values. Based on a K_P value of 0.25 L/g VSS, 8 percent of the total EE2 was sorbed to the *R. equi* biomass which was similar to the results of O'Grady et al. (2009) where up to about 5 percent of the total EE2 was sorbed to the biomass.

129

The calculated k_b values were insensitive to K_P where a 50 percent change in K_P value resulted in less than a 3 percent change in k_b value.

The EE2 k_b value of 3.4 L/g VSS-d for this *R. equi* strain was low compared to those measured for AS fed synthetic wastewater presented in Chapter 4. EE2 k_b values of AS were 3 to 22 L/g VSS-d, and these values were obtained under low substrate concentrations as the majority of influent COD was removed during selector periods. The EE2 degradation rate of *R. equi* under these conditions would be expected to be lower as the substrate concentrations would be similar to those during stationary growth when no EE2 removal was observed. Larcher and Yargeau (2013) and O'Grady (2007) also showed that this *R. equi* strain degraded EE2 while growing on ethanol and glucose, respectively. Larcher and Yargeau (2013) reported EE2 removals of approximately 46 percent during the first 120 hours of the batch test during *R. equi* growth on ethanol and an additional 15 percent during the last 180 hours during the stationary growth phase. Their work suggests *R. equi* may degrade EE2 at low substrate concentrations during stationary growth, although at a much lower rate. Thus, this strain is not a likely contributor to EE2-degradation observed in activated sludge.

R. equi growth and EE2 degradation may have been impacted by using glucose as the growth substrate. Baryshnikova et al. (1985) noted Rhodococci generally grow slower on glucose than on preferred aliphatic substrates such as fatty acids, alcohols, and alkanes. Koronelli and Nesterova (1990) observed a similar μ of 0.62 g/g-d for *R. maris* with growth on glucose at 28°C which increased to 1.7 g/g-d with hexadecane. Growth substrate also affects the cell wall characteristics of bacteria belonging to the mycolata taxon. As members of this taxon,

Rhodococci have cell walls containing mycolic acids which facilitate the uptake of hydrophobic compounds (Martinkova et al., 2009). Wick et al. (2002) showed Mycobacteria produced more hydrophobic mycolic acids when growing on alkanes and polycyclic aromatic hydrocarbons (PAHs) compared to growth on glucose. Growth on hydrophobic substrates may also increase the cell wall permeability to hydrophobic compounds, where *R. erythropolis* became more sensitive to rifampin, a relatively hydrophobic antibiotic, and less sensitive to tetracycline, a water soluble antibiotic, following growth on longer-chain hydrocarbons (Sokolovska et al., 2003). The impact of substrate type on growth, EE2 partitioning to biomass, and EE2 biodegradation kinetics of EE2-degrading isolates would need to be addressed with future research.

Inhibition of EE2 degradation by azole compounds

The presence of 0.5 mM clotrimazole but not 0.5 mM ketoconazole inhibited EE2 degradation by *R. equi* as shown in Figure 6-3 by comparing the decrease in EE2 for the control to that with the azoles added. *R. equi* growth could not be monitored by OD_{500} due to the development of turbidity following the addition of the clotrimazole. The average VSS concentration of the *R. equi* culture was 268 mg/L (replicates of 261 and 274) at the beginning of the experiment. Final VSS concentrations averaged 407 (replicates of 407 and 407), 400 (replicates of 393 and 407), and 563 (replicates of 547 and 580) mg/L at the end of the experiment for batch tests conducted with clotrimazole, ketoconazole, and the control, respectively. The sCOD concentration of the *R. equi* culture prior to adding the DMSO was 952 mg/L. For the control where the VSS concentration increased by 295 mg/L, the estimated sCOD consumed during the batch test is 870 mg/L assuming a yield (Y) of 0.47 g VSS/g COD (Ng, 1969) and a temperature corrected decay

131

(b) coefficient of 0.16 g VSS/g VSS-d (Tchobanoglous et al., 2014). The *R. equi* culture was likely exposed to high substrate concentrations for the majority of the batch test.
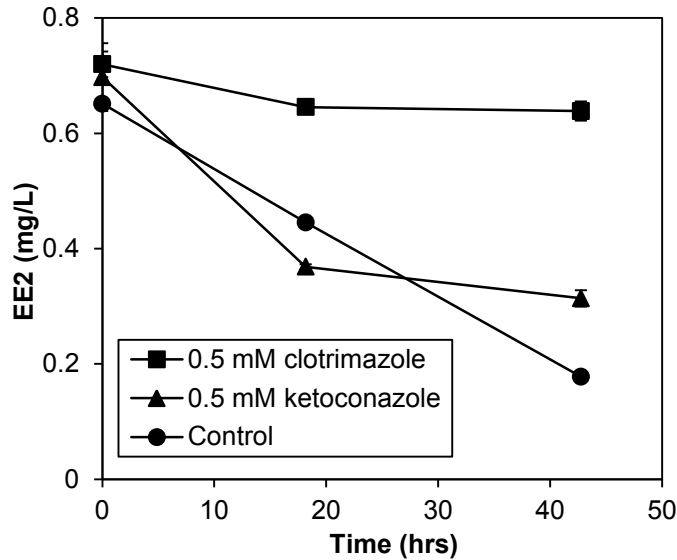
Figure 6-3. EE2 degradation by *R. equi* in presence of 0.5 mM clotrimazole, 0.5 mM ketoconazole, and without any azole compound present (control). All batch tests conducted at 27°C with 2 percent DMSO used as a cosolvent.

Inhibition of EE2 degradation by clotrimazole suggested a cytochrome P450 mono-oxygenase (CYP) may be involved in its degradation. One possible explanation for the inhibition of EE2 degradation by clotrimazole and not ketoconazole is the presence of a CYP with a higher binding affinity for clotrimazole. For example, Driscoll et al. (2011) reported a CYP purified from *Mycobacterium tuberculosis* binds more tightly to clotrimazole than ketoconazole, with the dissociation constant for ketoconazole being 360 times greater than that for clotrimazole. The presence of these azole compounds also hindered *R. equi* growth as reflected by the lower VSS concentrations at the end of the experiment, suggesting one or multiple CYPs of *R. equi* may be involved in growth. Inhibition of *R. equi* growth has previously been shown with these and other azole compounds (Dabbs et al., 2003).

132

Isolation of mutant with hindered EE2-degrading ability

The first transposome mutagenesis experiment resulted in the selection of 1548 mutants, and only one of these mutants (Mutant I) was identified as having lost its ability to degrade EE2. The results from batch degradation tests with Mutant I and two mutants having EE2-degrading ability (postive Controls I and II) are shown in Figure 6-4. One of the triplicate flasks of Control I was contaminated as revealed by streak plates conducted at the end of the experiment, and so the results of the contaminated flask are not included in the presented results. Mutant I had the same biomass growth rate as Controls I and II (Figure 6-4a) but severely hindered EE2-degrading ability (Figure 6-4b). Mutant I's mutation also hindered its ability to degrade E1, but did not impair its ability to oxidize E2 to E1. Mutant I rapidly transformed E2 to E1 within an hour similar to the controls (Figures 6-4c and d), indicating the mutation did not impact expression of 17β-hydroxysteroid dehydrogenase involved in E2 conversion to E1 (Donova et al., 2005). Conversely, Mutant I had hindered E1-degrading ability such that 6.5 days was required to achieve greater than 85 percent E1 removal compared to 1.5 days for the positive controls (Figure 6-4d). The impairment of both EE2 and E1 degradation could be due to a mutation having global impacts on the synthesis of many enzymes. However, Mutant I's unhindered ability to transform E2 suggests the impact of its mutation was specific to a subset of enzymes involving E1 and EE2 degradation pathways.

Figure 6-4. Comparison of (a) growth curves, (b) EE2 degradation, (c) E2 transformation, and (d) E1 degradation by Mutant I, positive controls, and growth media at 30°C.

A second transposome mutagenesis experiment resulted in the creation of 9298 *R. equi* mutants. No mutants were identified as having lost their ability to degrade EE2, although three mutants (Mutants II – IV) had partially hindered EE2-degrading ability (Figure 6-5b). After 4 days, the EE2 removal was 71 percent for Control I compared to 50, 59, and 62 percent for Mutants II, III, and IV, respectively. Prior to inoculating the glucose minimal media for these batch tests, the mutant cultures gown overnight in LB were diluted with LB such that all cultures had the same OD_{500}. Therefore, initial biomass concentrations were expected to be the same in all batch tests. The similar growth rates of Mutants II and IV to Control I (Figure 6-5a) indicate similar VSS concentrations were present in these tests; Mutant III, however, had an increased growth rate relative to the control. E1 degradation in Mutants II through IV was also partially hindered as shown in Figure 6-5c.
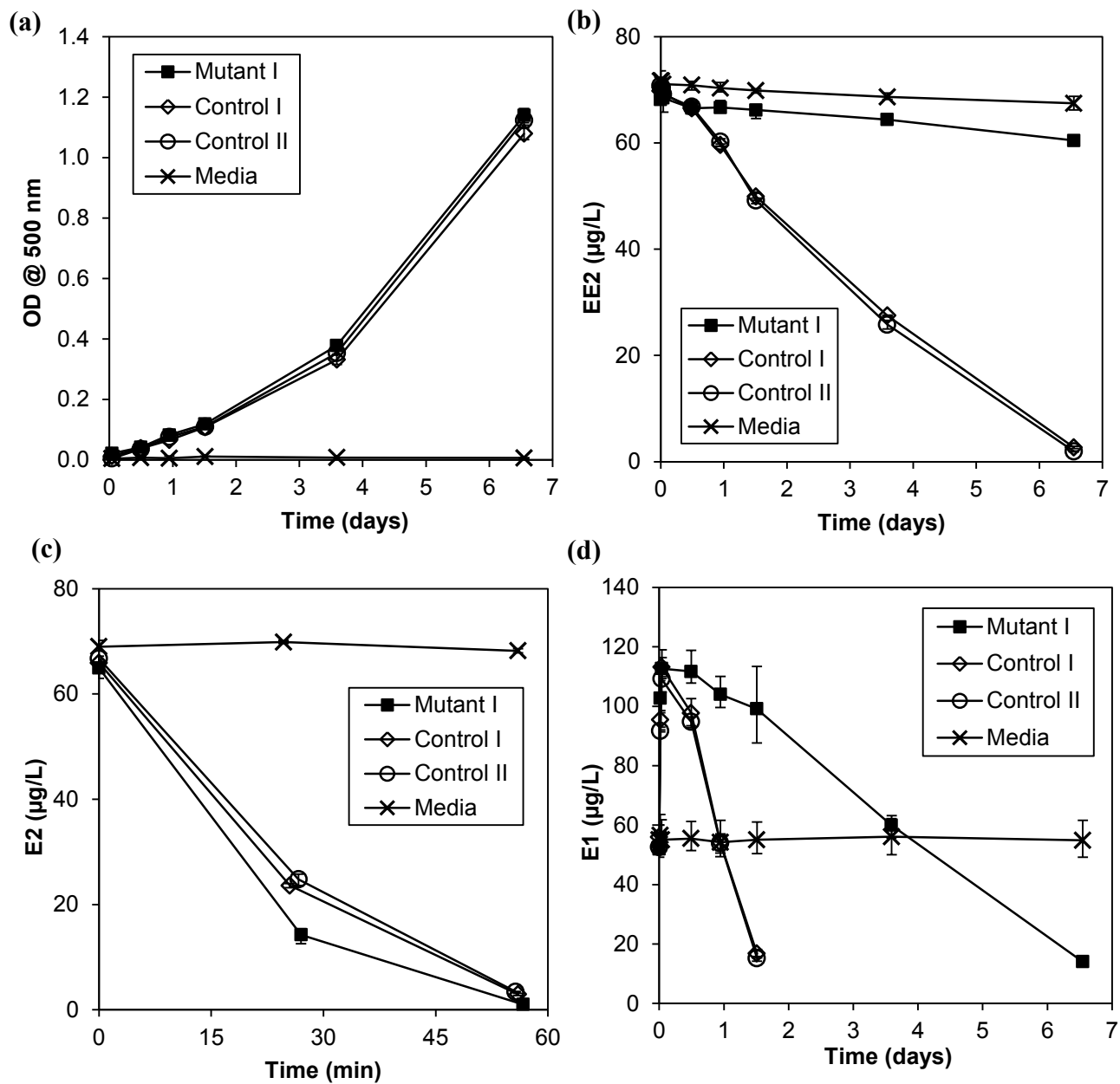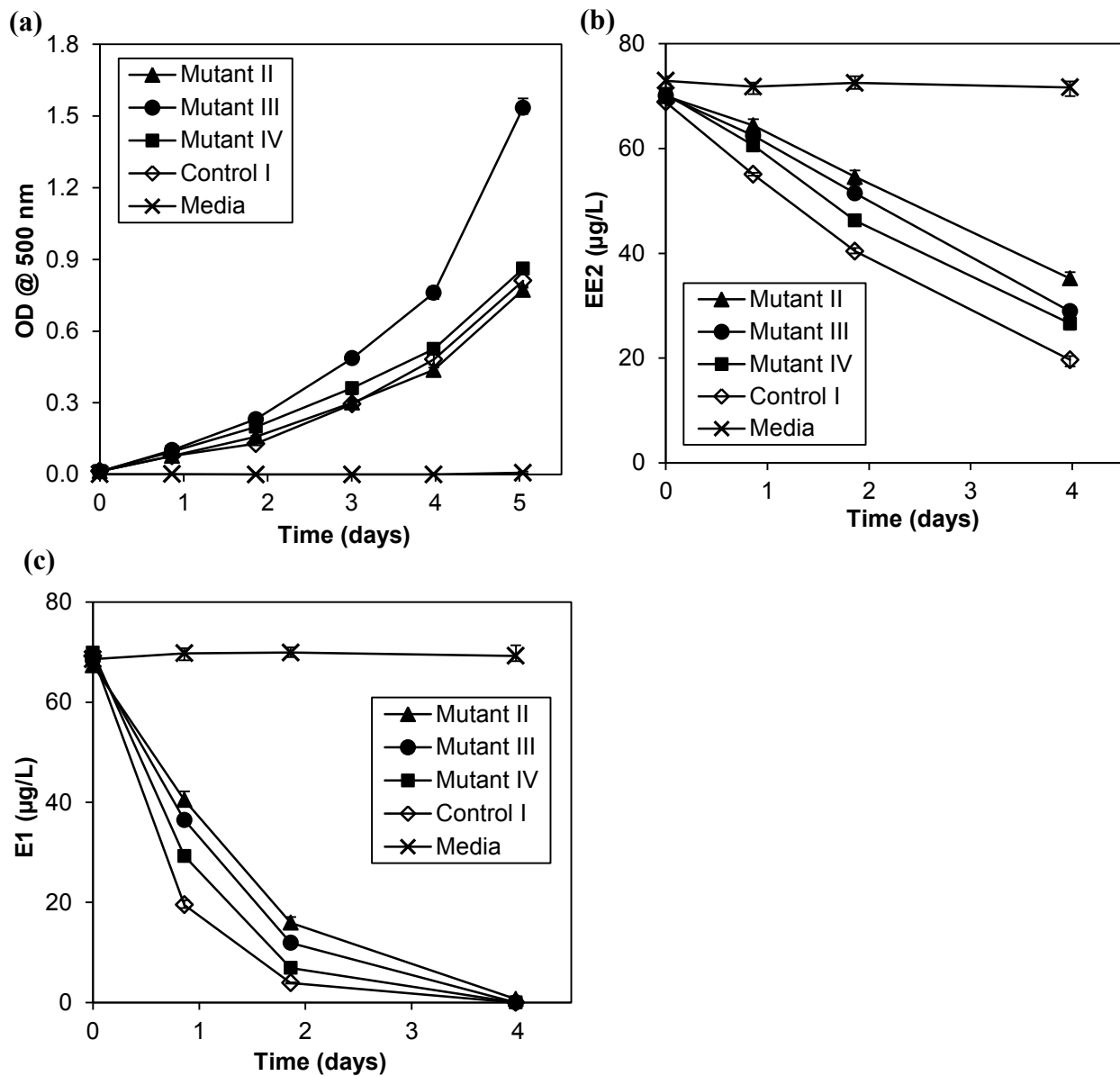
Figure 6-5. Comparison of (a) growth curves, (b) EE2 degradation, and (c) E1 degradation by Mutants II - IV, positive control, and growth media at 30°C.

Rescue cloning was performed to identify the location of the insertion site of the EZ-Tn5 transposon in the genomic DNA of Mutants I – IV. DNA sequencing results showed the transposon was flanked by a 9 base pair repeat, confirming the mutations were due to a Tn5 transposition event. BLAST (National Center for Biotechnology Information) search results revealed the Tn5 transposon was inserted in a 23S-5S ribosomal RNA interspatial region in

136

Mutant I, a translation initiation factor 3 in Mutant II, and a 23S ribosomal RNA gene in Mutants III and IV. Ribosomal RNA and the translation initiation factor 3 are involved in protein synthesis, and these mutations are likely unspecific to EE2 degradation. It is unknown why the insertion of a transposon in the 23S-5S ribosomal RNA interspatial region would result in loss of EE2-degrading ability. One possible explanation is another event occurred during the mutation experiment that impacted EE2 degradation, such as loss of a plasmid containing the EE2-degrading genes. Comparison of the genomes and transcriptomes of Mutant I and the wild type may provide an explanation for Mutant I's loss of EE2-degrading ability.

6.4 Conclusions

R. equi ATCC 13557 degraded EE2 at ng/L concentrations; however, the low EE2 degradation rate coupled with high substrate conditions during degradation suggests this isolate would not be a primary EE2-degrader in activated sludge treatment. A cytochrome p450 mono-oxygenase may be involved in EE2 degradation as inhibition was observed in the presence of clotrimazole. Transposome mutagenesis coupled with a YES screening method was successfully applied to isolate an *R. equi* mutant with hindered EE2-degrading ability. The enzyme involved in the oxidation of E2 to E1 is not involved in the initial transformation of EE2.

137

Chapter 7: Summary and Conclusions

The main objective of this research was to expand our ability to model the fate of EE2 across AS systems.

In Chapter 3, an EE2 fate and transformation model was developed based on the following mechanisms: (1) EE2 production from deconjugation of EE2-3S, (2) EE2 biodegradation by heterotrophic biomass growing on other substrates, and (3) EE2 sorption/desorption with AS. These mechanisms were incorporated into the IWA ASM2d to model biomass and solids production based on site specific wastewater characteristics and operating conditions. EE2 biodegradation and EE2-3S deconjugation were modeled as pseudo first-order rates as a function of the soluble estrogen concentration and the heterotrophic biomass. No biodegradation or deconjugation was modeled as occurring under anoxic or anaerobic conditions. The model was successfully calibrated and evaluated using lab-scale aerobic and BNR AS reactors fed primary effluent and operated at SRTs of 6 and 8.5 days. Conclusions from this research are:

- Predicted effluent EE2 concentrations are most sensitive to parameters and conditions affecting biodegradation: the pseudo first-order biodegradation rate coefficient ($k_{bio,H}$), the influent bCOD/EE2 ratio, and the aerobic SRT.

- EE2 can be appreciably produced from deconjugation of EE2-3S during AS treatment.

- Predicted effluent EE2 concentrations are relatively insensitive to the pseudo first-order deconjugation rate coefficient ($k_{cle,H}$) and the solid-liquid partitioning coefficient.

- Predicted effluent EE2 concentrations are more sensitive to the $k_{cle,H}/k_{bio,H}$ ratio for AS systems with low biodegradation kinetics.

138

- Staged aerobic CSTR designs have the potential to achieve high EE2 removals.

The research in Chapter 4 applied a pseudo first-order model to measure EE2 biodegradation kinetics in lab-scale SBRs simulating aerobic, anaerobic/aerobic enhanced biological phosphorus removal, and anoxic/aerobic biological nitrogen removal processes. Three sets of reactor experiments were conducted using different municipal AS plant seed sources and with SRTs ranging from 8 to 13 days. Pseudo first-order biodegradation rate coefficients (k_b) normalized to the reactor VSS were determined from in situ batch degradation tests and from calibration of a reactor process model. Conclusions from this research include:

- Significant EE2 biodegradation occurs only under aerobic conditions.

- EE2 k_b values for aerobic, anaerobic/aerobic, and anoxic/aerobic operations can range from 4 to 22 L/g VSS-d, 4 to 19 L/g VSS-d, and 3 to 20 L/g VSS-d, respectively.

- EE2 k_b values can vary over time during long-term operation.

- Aerobic AS processes may promote higher EE2 k_b values than anoxic/aerobic AS processes.

- High EE2 k_b values can be obtained with all BNR AS process types.

- Model simulations indicate longer SRTs, an increased number of aerobic reactor stages, and a higher influent bCOD/EE2 ratio can produce conditions that result in lower and more consistent effluent EE2 concentrations for these observed k_b values.

The research in Chapter 5 examined anoxic and aerobic degradation of EE2, E1, and E2 by enriched denitrifying communities grown under anoxic conditions in comparison to a denitrifying community grown under anoxic/aerobic conditions. Two sets of reactor experiments

139

were conducted using different municipal AS plant seed sources and with SRTs ranging from 8 to 13 days. Conclusions from this research are:

- EE2 is not degraded by some denitrifying populations under anoxic or aerobic conditions.

- At least some of the influent substrate in anoxic/aerobic operations does not support EE2-degrading biomass.

- Some denitrifying populations can degrade E1 and E2 under both anoxic and aerobic conditions.

- Some denitrifying populations can only interconvert E1 and E2 without further degradation.

Chapter 6 described experiments conducted with an EE2-degrading isolate, *Rhodococcus equi*, to examine its biodegradation kinetics, inhibition of EE2 degradation by azole compounds, and application of a transposon mutagenesis technique to identify genes involved in EE2 degradation. Conclusions from this research are:

- *R. equi* ATCC 13557 degrades EE2 at ng/L concentrations during exponential growth on glucose with a k_b of 3.4 L/g VSS-d at 27°C.

- *R. equi* ATCC 13557 does not appreciably degrade EE2 during stationary growth.

- A cytochrome p450 mono-oxygenase may be involved in EE2 degradation.

- Transposome mutagenesis coupled with a YES screening method can be used to isolate *R. equi* mutants with hindered EE2-degrading ability.

- The enzyme involved in the oxidation of E2 to E1 is not involved in the initial transformation of EE2.

Questions requiring future research that would improve the EE2 fate and transformation model are:

- What fraction of the heterotrophic AS biomass is EE2-degrading biomass?

- What are the EE2 biodegradation kinetics of EE2-degrading populations in AS and how variable are these kinetics between populations?

- How do wastewater characteristics, operating conditions, and process configuration affect the fraction of EE2-degrading biomass in AS and their EE2 biodegradation kinetics?

- What microbial populations are responsible for EE2 biodegradation and EE2-3S deconjugation in AS?

- What substrates are microbial populations responsible for EE2 biodegradation and EE2-3S deconjugation growing on?

- How does temperature affect EE2 biodegradation and EE2-3S deconjugation kinetics?

- What concentrations of EE2, EE2-3S, and EE2-3G are arriving at WWTPs?

Research identifying microbial genes involved in EE2-degradation could provide useful probes for monitoring the growth of EE2-degrading biomass and their expression of EE2-degrading genes, which could aid in answering most of these questions.

Bibliography

Adler, P., Steger-Hartmann, T., Kalbfus, W., 2001. Distribution of natural and synthetic estrogenic steroid hormones in water samples from Southern and Middle Germany. Acta Hydrochim. Hydrobiol. 29, 227–241.

Adlercreutz, H., Jarvenpaa, P., 1982. Assay of estrogens in human feces. J. Steroid Biochem. Mol. Biol. 17, 639–645.

Agematu, H., Matsumoto, N., Fujii, Y., Kabumoto, H., Doi, S., Machida, K., Ishikawa, J., Arisawa, A., 2006. Hydroxylation of testosterone by bacterial cytochromes P450 using the Escherichia coli expression system. Biosci. Biotechnol. Biochem. 70, 307–311.

Andersen, H., Siegrist, H., Halling-Sorensen, B., Ternes, T.A., 2003. Fate of estrogens in a municipal sewage treatment plant. Environ. Sci. Technol. 37, 4021–4026.

Andersen, H.R., Hansen, M., Kjolholt, J., Stuer-Lauridsen, F., Ternes, T., Halling-Sorensen, B., 2005. Assessment of the importance of sorption for steroid estrogens removal during activated sludge treatment. Chemosphere 61, 139–146.

APHA, AWWA, WEF, 2005. Standard Methods for the Examination of Water & Wastewater, 21st ed. Washington D.C.

Atkinson, S.K., Marlatt, V.L., Kimpe, L.E., Lean, D.R.S., Trudeau, V.L., Blais, J.M., 2012. The occurrence of steroidal estrogens in south-eastern Ontario wastewater treatment plants. Sci. Total Environ. 430, 119–125.

Bagnall, J.P., Ito, A., McAdam, E.J., Soares, A., Lester, I.N., Cartmell, E., 2012. Resource dependent biodegradation of estrogens and the role of ammonia oxidising and heterotrophic bacteria. J. Hazard. Mater. 239, 56–63.

Baronti, C., Curini, R., D'Ascenzo, G., Di Corcia, A., Gentili, A., Samperi, R., 2000. Monitoring natural and synthetic estrogens at activated sludge sewage treatment plants and in a receiving river water. Environ. Sci. Technol. 34, 5059–5066.

Baryshnikova, L., Eroshina, N., Myasoedova, N., Termkhitarova, N., Golovlev, E., 1985. Myxotrophic growth of Rhodococcus minimus in a batch culture. Microbiology 54, 234–239.

Beil, S., Kehrli, H., James, P., Staudenmann, W., Cook, A., Leisinger, T., Kertesz, M., 1995. Purification and characterization of the arylsulfatase synthesized by Pseudomonas aeruginosa Pao during growth in sulfate-free medium and cloning of the arylsulfatase gene (atsa). Eur. J. Biochem. 229, 385–394.

Ben-Dov, E., Brenner, A., Kushmaro, A., 2007. Quantification of sulfate-reducing bacteria in industrial wastewater, by real-time polymerase chain reaction (PCR) using dsrA and apsA genes. Microb. Ecol. 54, 439–451.

Bjerregaard, L.B., Korsgaard, B., Bjerregaard, P., 2006. Intersex in wild roach (Rutilus rutilus) from Danish sewage effluent-receiving streams. Ecotoxicol. Environ. Saf. 64, 321–328.

Bjorkblom, C., Mustamaki, N., Olsson, P.-E., Katsiadaki, I., Wiklund, T., 2013. Assessment of reproductive biomarkers in three-spined stickleback (Gasterosteus aculeatus) from sewage effluent recipients. Environ. Toxicol. 28, 229–237.

Busi da Silva, M.L., Corseuil, H.X., 2012. Groundwater microbial analysis to assess enhanced BTEX biodegradation by nitrate injection at a gasohol-contaminated site. Int. Biodeterior. Biodegrad. 67, 21–27.

Caldwell, D.J., Mastrocco, F., Anderson, P.D., Laenge, R., Sumpter, J.P., 2012. Predicted-no-effect concentrations for the steroid estrogens estrone, 17 beta-estradiol, estriol, and 17 alpha-ethinylestradiol. Environ. Toxicol. Chem. 31, 1396–1406.

Campbell, C.G., Borglin, S.E., Green, F.B., Grayson, A., Wozei, E., Stringfellow, W.T., 2006. Biologically directed environmental monitoring, fate, and transport of estrogenic endocrine disrupting compounds in water: A review. Chemosphere 65, 1265–1280.

Can, Z.S., Firlak, M., Kerc, A., Evcimen, S., 2014. Evaluation of different wastewater treatment techniques in three WWTPs in Istanbul for the removal of selected EDCs in liquid phase. Environ. Monit. Assess. 186, 525–539.

Cargouet, M., Perdiz, D., Mouatassim-Souali, A., Tamisier-Karolak, S., Levi, Y., 2004. Assessment of river contamination by estrogenic compounds in Paris area (France). Sci. Total Environ. 324, 55–66.

Chimchirian, R.F., Suri, R.P.S., Fu, H., 2007. Free synthetic and natural estrogen hormones in influent and effluent of three municipal wastewater treatment plants. Water Environ. Res. 79, 969–974.

Cicek, N., Londry, K., Oleszkiewicz, J.A., Wong, D., Lee, Y., 2007. Removal of selected natural and synthetic estrogenic compounds in a Canadian full-scale municipal wastewater treatment plant. Water Environ. Res. 79, 795–800.

Clara, M., Kreuzinger, N., Strenn, B., Gans, O., Kroiss, H., 2005. The solids retention time - a suitable design parameter to evaluate the capacity of wastewater treatment plants to remove micropollutants. Water Res. 39, 97–106.

Clara, M., Strenn, B., Saracevic, E., Kreuzinger, N., 2004. Adsorption of bisphenol-A, 17 beta-estradiole and 17 alpha-ethinylestradiole to sewage sludge. Chemosphere 56, 843–851.

Combalbert, S., Hernandez-Raquet, G., 2010. Occurrence, fate, and biodegradation of estrogens in sewage and manure. Appl. Microbiol. Biotechnol. 86, 1671–1692.

Cregut, M., Piutti, S., Slezack-Deschaumes, S., Benizri, E., 2013. Compartmentalization and regulation of arylsulfatase activities in Streptomyces sp., Microbacterium sp. and Rhodococcus sp. soil isolates in response to inorganic sulfate limitation. Microbiol. Res. 168, 12–21.

D'Ascenzo, G., Di Corcia, A., Gentili, A., Mancini, R., Mastropasqua, R., Nazzari, M., Samperi, R., 2003. Fate of natural estrogen conjugates in municipal sewage transport and treatment facilities. Sci. Total Environ. 302, 199–209.

Dabbs, E.R., Naidoo, S., Lephoto, C., Nikitina, N., 2003. Pathogenic Nocardia, Rhodococcus, and related organisms are highly susceptible to imidazole antifungals. Antimicrob. Agents Chemother. 47, 1476–1478.

Donova, M.V., Egorova, O.V., Nikolayeva, V.M., 2005. Steroid 17 beta-reduction by microorganisms - a review. Process Biochem. 40, 2253–2262.

Drewes, J.E., Hemming, J., Ladenburger, S.J., Schauer, J., Sonzogni, W., 2005. An assessment of endocrine disrupting activity changes during wastewater treatment through the use of bioassays and chemical measurements. Water Environ. Res. 77, 12–23.

Driscoll, M.D., McLean, K.J., Cheesman, M.R., Jowitt, T.A., Howard, M., Carroll, P., Parish, T., Munro, A.W., 2011. Expression and characterization of Mycobacterium tuberculosis CYP144: Common themes and lessons learned in the M. tuberculosis P450 enzyme family. Biochim. Biophys. Acta-Proteins Proteomics 1814, 76–87.

Dytczak, M.A., Londry, K.L., Oleszkiewicz, J.A., 2008. Biotransformation of estrogens in nitrifying activated sludge under aerobic and alternating anoxic/aerobic conditions. Water Environ. Res. 80, 47–52.

Ekama, G.A., Wentzel, M.C., 2004. A predictive model for the reactor inorganic suspended solids concentration in activated sludge systems. Water Res. 38, 4093–4106.

Estrada-Arriaga, E.B., Mijaylova, N.P., 2010. A comparison of biodegradation kinetic models applied to estrogen removal with nitrifying activated sludge. Water Sci. Technol. 62, 2183–2189.

Fahrbach, M., Kuever, J., Meinke, R., Kaempfer, P., Hollender, J., 2006. Denitratisoma oestradiolicum gen. nov., sp nov., a 17 beta-oestradiol-degrading, denitrifying betaproteobacterium. Int. J. Syst. Evol. Microbiol. 56, 1547–1552.

Fahrbach, M., Kuever, J., Remesch, M., Huber, B.E., Kaempfer, P., Dott, W., Hollender, J., 2008. Steroidobacter denitrificans gen. nov., sp nov., a steroidal hormone-degrading gammaproteobacterium. Int. J. Syst. Evol. Microbiol. 58, 2215–2223.

Fernandez, M.P., Buchanan, I.D., Ikonomou, M.G., 2008. Seasonal variability of the reduction in estrogenic activity at a municipal WWTP. Water Res. 42, 3075–3081.

Fujii, K., Kikuchi, S., Satomi, M., Ushio-Sata, N., Morita, N., 2002. Degradation of 17 beta-estradiol by a gram-negative bacterium isolated from activated sludge in a sewage treatment plant in Tokyo, Japan. Appl. Environ. Microbiol. 68, 2057–2060.

Gaulke, L.S., Strand, S.E., Kalhorn, T.F., Stensel, H.D., 2008. 17 alpha-ethinylestradiol transformation via abiotic nitration in the presence of ammonia oxidizing bacteria. Environ. Sci. Technol. 42, 7622–7627.

Gaulke, L.S., Strand, S.E., Kalhorn, T.F., Stensel, H.D., 2009. Estrogen biodegradation kinetics and estrogenic activity reduction for two biological wastewater treatment methods. Environ. Sci. Technol. 43, 7111–7116.

Geets, J., de Cooman, M., Wittebolle, L., Heylen, K., Vanparys, B., De Vos, P., Verstraete, W., Boon, N., 2007. Real-time PCR assay for the simultaneous quantification of nitrifying and denitrifying bacteria in activated sludge. Appl. Microbiol. Biotechnol. 75, 211–221.

Gentili, A., Perret, D., Marchese, S., Mastropasqua, R., Curini, R., Di Corcia, A., 2002. Analysis of free estrogens and their conjugates in sewage and river waters by solid-phase extraction then liquid chromatography-electrospray-tandem mass spectrometry. Chromatographia 56, 25–32.

Gomes, R.L., Birkett, J.W., Scrimshaw, M.D., Lester, J.N., 2005. Simultaneous determination of natural and synthetic steroid estrogens and their conjugates in aqueous matrices by liquid chromatography/mass spectrometry. Int. J. Environ. Anal. Chem. 85, 1–14.

Gomes, R.L., Scrimshaw, M.D., Cartmell, E., Lester, J.N., 2011. The fate of steroid estrogens: partitioning during wastewater treatment and onto river sediments. Environ. Monit. Assess. 175, 431–441.

Gomes, R.L., Scrimshaw, M.D., Lester, J.N., 2009. Fate of conjugated natural and synthetic steroid estrogens in crude sewage and activated sludge batch studies. Environ. Sci. Technol. 43, 3612–3618.

Gujer, W., Henze, M., Mino, T., van Loosdrecht, M., 1999. Activated Sludge Model No. 3. Water Sci. Technol. 39, 183–193.

Gunatilake, S.R., Craver, S., Kwon, J.-W., Xia, K., Armbrust, K., Rodriguez, J.M., Mlsna, T.E., 2013. Analysis of estrogens in wastewater using solid-phase extraction, QuEChERS

144

cleanup, and liquid chromatography/tandem mass spectrometry. J. Aoac Int. 96, 1440–1447.

Gutendorf, B., Westendorf, J., 2001. Comparison of an array of in vitro assays for the assessment of the estrogenic potential of natural and synthetic estrogens, phytoestrogens and xenoestrogens. Toxicology 166, 79–89.

Haiyan, R., Shulan, J., Ahmad, N. ud din, Dao, W., Chengwu, C., 2007. Degradation characteristics and metabolic pathway of 17 alpha-ethynylestradiol by Sphingobacterium sp JCR5. Chemosphere 66, 340–346.

Harris, C.A., Hamilton, P.B., Runnalls, T.J., Vinciotti, V., Henshaw, A., Hodgson, D., Coe, T.S., Jobling, S., Tyler, C.R., Sumpter, J.P., 2011. The consequences of feminization in breeding groups of wild fish. Environ. Health Perspect. 119, 306–311.

Hashimoto, S., Bessho, H., Hara, A., Nakamura, M., Iguchi, T., Fujita, K., 2000. Elevated serum vitellogenin levels and gonadal abnormalities in wild male flounder (Pleuronectes yokohamae) from Tokyo Bay, Japan. Mar. Environ. Res. 49, 37–53.

Hashimoto, T., Murakami, T., 2009. Removal and degradation characteristics of natural and synthetic estrogens by activated sludge in batch experiments. Water Res. 43, 573–582.

Hashimoto, T., Onda, K., Morita, T., Luxmy, B.S., Tada, K., Miya, A., Murakami, T., 2010. Contribution of the estrogen-degrading bacterium Novosphingobium sp strain JEM-1 to estrogen removal in wastewater treatment. J. Environ. Eng.-Asce 136, 890–896.

Henze, M., Grady Jr., C.P.L., Gujer, W., Marais, G.V.R., Matsuo, T., 1987. Activated Sludge Model No.1. IAWPRC Scientific and Technical Report No. 1. IAWPRC, London.

Henze, M., Gujer, W., Mino, T., Matsuo, T., Wentzel, M.C., Marais, G.V.R., Van Loosdrecht, M.C.M., 1999. Activated Sludge Model No.2d, ASM2d. Water Sci. Technol. 39, 165–182.

Jiang, L., Yang, J., Chen, J., 2010. Isolation and characteristics of 17 beta-estradiol-degrading Bacillus spp. strains from activated sludge. Biodegradation 21, 729–736.

Jobling, S., Coey, S., Whitmore, J.G., Kime, D.E., Van Look, K.J.W., McAllister, B.G., Beresford, N., Henshaw, A.C., Brighty, G., Tyler, C.R., Sumpter, J.P., 2002. Wild intersex roach (Rutilus rutilus) have reduced fertility. Biol. Reprod. 67, 515–524.

Jobling, S., Williams, R., Johnson, A., Taylor, A., Gross-Sorokin, M., Nolan, M., Tyler, C.R., van Aerle, R., Santos, E., Brighty, G., 2006. Predicted exposures to steroid estrogens in UK rivers correlate with widespread sexual disruption in wild fish populations. Environ. Health Perspect. 114, 32–39.

Johnson, A.C., Belfroid, A., Di Corcia, A., 2000. Estimating steroid oestrogen inputs into activated sludge treatment works and observations on their removal from the effluent. Sci. Total Environ. 256, 163–173.

Johnson, A.C., Williams, R.J., 2004. A model to estimate influent and effluent concentrations of estradiol, estrone, and ethinylestradiol at sewage treatment works. Environ. Sci. Technol. 38, 3649–3658.

Joss, A., Andersen, H., Ternes, T., Richle, P.R., Siegrist, H., 2004. Removal of estrogens in municipal wastewater treatment under aerobic and anaerobic conditions: Consequences for plant optimization. Environ. Sci. Technol. 38, 3047–3055.

Joss, A., Zabczynski, S., Gobel, A., Hoffmann, B., Loffler, D., McArdell, C.S., Ternes, T.A., Thomsen, A., Siegrist, H., 2006. Biological degradation of pharmaceuticals in municipal wastewater treatment: Proposing a classification scheme. Water Res. 40, 1686–1696.

145

Kaelin, D., Manser, R., Rieger, L., Eugster, J., Rottermann, K., Siegrist, H., 2009. Extension of ASM3 for two-step nitrification and denitrification and its calibration and validation with batch tests and pilot scale data. Water Res. 43, 1680–1692.

Kelly, S.L., Kelly, D.E., 2013. Microbial cytochromes P450: biodiversity and biotechnology. Where do cytochromes P450 come from, what do they do and what can they do for us? Philos. Trans. R. Soc. B-Biol. Sci. 368, 20120476.

Khunjar, W.O., Mackintosh, S.A., Skotnicka-Pitak, J., Baik, S., Aga, D.S., Love, N.G., 2011. Elucidating the relative roles of ammonia oxidizing and heterotrophic bacteria during the biotransformation of 17 alpha-ethinylestradiol and trimethoprim. Environ. Sci. Technol. 45, 3605–3612.

Knauff, U., Schulz, M., Scherer, H.W., 2003. Arylsufatase activity in the rhizosphere and roots of different crop species. Eur. J. Agron. 19, 215–223.

Koch, G., Kuhni, M., Gujer, W., Siegrist, H., 2000. Calibration and validation of Activated Sludge Model No. 3 for Swiss municipal wastewater. Water Res. 34, 3580–3590.

Koh, Y.K.K., Chiu, T.Y., Boobis, A., Cartmell, E., Lester, J.N., Scrimshaw, M.D., 2007. Determination of steroid estrogens in wastewater by high performance liquid chromatography - tandem mass spectrometry. J. Chromatogr. A 1173, 81–87.

Koh, Y.K.K., Chiu, T.Y., Boobis, A.R., Scrimshaw, M.D., Bagnall, J.P., Soares, A., Pollard, S., Cartmell, E., Lester, J.N., 2009. Influence of operating parameters on the biodegradation of steroid estrogens and nonylphenolic compounds during biological wastewater treatment processes. Environ. Sci. Technol. 43, 6646–6654.

Koike, I., Hattori, A., 1975. Energy yield of denitrification - Estimate from growth yield in continuous cultures of Pseudomonas denitrificans under nitrate-limited, nitrite-limited and nitrous oxide-limited conditions. J. Gen. Microbiol. 88, 11–19.

Komori, K., Tanaka, H., Okayasu, Y., Yasojima, M., Sato, C., 2004. Analysis and occurrence of estrogen in wastewater in Japan. Water Sci. Technol. 50, 93–100.

Korner, W., Spengler, P., Bolz, U., Schuller, W., Hanf, V., Metzger, J.W., 2001. Substances with estrogenic activity in effluents of sewage treatment plants in southwestern Germany. 2. Biological analysis. Environ. Toxicol. Chem. 20, 2142–2151.

Koronelli, T., Nesterova, E., 1990. Ecological strategies of bacteria utilizing hydrophobic substrates. Microbiology 59, 691–694.

Kumar, V., Johnson, A., Nakada, N., Yamashita, N., Yasojima, M., Tanaka, H., 2009a. De-conjugation fate of the conjugated estrogens in the raw wastewater. Proceedings of the 82nd Annual WEF Technical Exhibition & Conference 590–602.

Kumar, V., Johnson, A.C., Nakada, N., Yamashita, N., Tanaka, H., 2012. De-conjugation behavior of conjugated estrogens in the raw sewage, activated sludge and river water. J. Hazard. Mater. 227, 49–54.

Kumar, V., Nakada, N., Yasojima, M., Yamashita, N., Johnson, A.C., Tanaka, H., 2009b. Rapid determination of free and conjugated estrogen in different water matrices by liquid chromatography-tandem mass spectrometry. Chemosphere 77, 1440–1446.

Kumar, V., Nakada, N., Yasojima, M., Yamashita, N., Johnson, A.C., Tanaka, H., 2011. The arrival and discharge of conjugated estrogens from a range of different sewage treatment plants in the UK. Chemosphere 82, 1124–1128.

Kurisu, F., Ogura, M., Saitoh, S., Yamazoe, A., Yagi, O., 2010. Degradation of natural estrogen and identification of the metabolites produced by soil isolates of Rhodococcus sp and Sphingomonas sp. J. Biosci. Bioeng. 109, 576–582.

Lai, K.M., Johnson, K.L., Scrimshaw, M.D., Lester, J.N., 2000. Binding of waterborne steroid estrogens to solid phases in river and estuarine systems. Environ. Sci. Technol. 34, 3890–3894.

Lange, A., Paull, G.C., Hamilton, P.B., Iguchi, T., Tyler, C.R., 2011. Implications of persistent exposure to treated wastewater effluent for breeding in wild roach (Rutilus rutilus) populations. Environ. Sci. Technol. 45, 1673–1679.

Larcher, S., Yargeau, V., 2013. Biodegradation of 17 alpha-ethinylestradiol by heterotrophic bacteria. Environ. Pollut. 173, 17–22.

Lee, H.B., Liu, D., 2002. Degradation of 17 beta-estradiol and its metabolites by sewage bacteria. Water. Air. Soil Pollut. 134, 353–368.

Lewis, D.F.V., Wiseman, A., 2005. A selective review of bacterial forms of cytochrome P450 enzymes - Review. Enzyme Microb. Technol. 36, 377–384.

Li, Y.M., Zeng, Q.L., Yang, S.J., 2011. Removal and fate of estrogens in an anaerobic-anoxic-oxic activated sludge system. Water Sci. Technol. 63, 51–56.

Li, Z., Nandakumar, R., Madayiputhiya, N., Li, X., 2012. Proteomic analysis of 17 beta-estradiol degradation by Stenotrophomonas maltophilia. Environ. Sci. Technol. 46, 5947–5955.

Liu, Z., Kanjo, Y., Mizutani, S., 2011. Removal of natural free estrogens and their conjugates in a municipal wastewater treatment plant. Clean-Soil Air Water 39, 128–135.

Lopez, C., Pons, M.N., Morgenroth, E., 2006. Endogenous processes during long-term starvation in activated sludge performing enhanced biological phosphorus removal. Water Res. 40, 1519–1530.

Lust, M., Makinia, J., Stensel, H.D., 2012. A mechanistic model for fate and removal of estrogens in biological nutrient removal activated sludge systems. Water Sci. Technol. 65, 1130–1136.

Maeng, S.K., Choi, B.G., Lee, K.T., Song, K.G., 2013. Influences of solid retention time, nitrification and microbial activity on the attenuation of pharmaceuticals and estrogens in membrane bioreactors. Water Res. 47, 3151–3162.

Makinia, J., Rosenwinkel, K.H., Spering, V., 2005. Long-term simulation of the activated sludge process at the Hanover-Gummerwald pilot WWTP. Water Res. 39, 1489–1502.

Mangan, M.W., Meijer, W.G., 2001. Random insertion mutagenesis of the intracellular pathogen Rhodococcus equi using transposomes. Fems Microbiol. Lett. 205, 243–246.

Martinkova, L., Uhnakova, B., Patek, M., Nesvera, J., Kren, V., 2009. Biodegradation potential of the genus Rhodococcus. Environ. Int. 35, 162–177.

McAdam, E.J., Bagnall, J.P., Koh, Y.K.K., Chiu, T.Y., Pollard, S., Scrimshaw, M.D., Lester, J.N., Cartmell, E., 2010. Removal of steroid estrogens in carbonaceous and nitrifying activated   sludge processes. Chemosphere 81, 1–6.

McLean, K.J., Marshall, K.R., Richmond, A., Hunter, I.S., Fowler, K., Kieser, T., Gurcha, S.S., Besra, G.S., Munro, A.W., 2002. Azole antifungals are potent inhibitors of cytochrome P450 mono-oxygenases and bacterial growth in mycobacteria and streptomycetes. Microbiol.-Sgm 148, 2937–2949.

Mes, T.Z.D. des, Kujawa-Roeleveld, K., Zeeman, G., Lettinga, G., 2008. Anaerobic biodegradation of estrogens - hard to digest. Water Sci. Technol. 57, 1177–1182.

Miege, C., Karolak, S., Gabet, V., Jugan, M.-L., Oziol, L., Chevreuil, M., Levi, Y., Coquery, M., 2009. Evaluation of estrogenic disrupting potency in aquatic environments and urban wastewaters by combining chemical and biological analysis. Trac-Trends Anal. Chem. 28, 186–195.

147

Mills, L.J., Chichester, C., 2005. Review of evidence: Are endocrine-disrupting chemicals in the aquatic environment impacting fish populations? Sci. Total Environ. 343, 1–34.

Monteith, H., Andres, H., Snowling, S., Schraa, O., 2008. Modeling the fate of estrogenic hormones in municipal wastewater treatment. Proceedings of the 81st Annual WEF Technical Exhibition & Conference 3477–3495.

Muller, M., Patureau, D., Godon, J.-J., Delgenes, J.-P., Hernandez-Raquet, G., 2010. Molecular and kinetic characterization of mixed cultures degrading natural and synthetic estrogens. Appl. Microbiol. Biotechnol. 85, 691–701.

Muller, M., Rabenoelina, F., Balaguer, P., Patureau, D., Lemenach, K., Budzinski, H., Barcelo, D., De Alda, M.L., Kuster, M., Delgenes, J.-P., Hernandez-Raquet, G., 2008. Chemical and biological analysis of endocrine-disrupting hormones and estrogenic activity in an advanced sewage treatment plant. Environ. Toxicol. Chem. 27, 1649–1658.

Munz, G., Lubello, C., Oleszkiewicz, J.A., 2011. Factors affecting the growth rates of ammonium and nitrite oxidizing bacteria. Chemosphere 83, 720–725.

Murk, A.J., Legler, J., van Lipzig, M.M.H., Meerman, J.H.N., Belfroid, A.C., Spenkelink, A., van der Burg, B., Rijs, G.B.J., Vethaak, D., 2002. Detection of estrogenic potency in wastewater and surface water with three in vitro bioassays. Environ. Toxicol. Chem. 21, 16–23.

Murooka, Y., Ishibashi, K., Yasumoto, M., Sasaki, M., Sugino, H., Azakami, H., Yamashita, M., 1990. A sulfur-regulated and tyramine-regulated Klebsiella-Aerogenes operon containing the arylsulfatase (atsa) gene and the Atsb gene. J. Bacteriol. 172, 2131–2140.

Nakada, N., Nyunoya, H., Nakamura, M., Hara, A., Iguchi, T., Takada, H., 2004. Identification of estrogenic compounds in wastewater effluent. Environ. Toxicol. Chem. 23, 2807–2815.

Nelder, J., Mead, R., 1965. A simplex-method for function minimization. Comput. J. 7, 308–313.

Ng, H., 1969. Effect of decreasing growth temperature on cell yield of Escherichia Coli. J. Bacteriol. 98, 232–237.

Nie, Y., Qiang, Z., Zhang, H., Ben, W., 2012. Fate and seasonal variation of endocrine-disrupting chemicals in a sewage treatment plant with A/A/O process. Sep. Purif. Technol. 84, 9–15.

O'Grady, D., Evangelista, S., Yargeau, V., 2009. Removal of aqueous 17 alpha-ethinylestradiol by Rhodococcus species. Environ. Eng. Sci. 26, 1393–1400.

Omura, T., 2010. Structural diversity of cytochrome P450 enzyme system. J. Biochem. (Tokyo) 147, 297–306.

Pauwels, B., Noppe, H., De Brabander, H., Verstraete, W., 2008. Comparison of steroid hormone concentrations in domestic and hospital wastewater treatment plants. J. Environ. Eng.-Asce 134, 933–936.

Pauwels, B., Wille, K., Noppe, H., De Brabander, H., van de Wiele, T., Verstraete, W., Boon, N., 2008. 17 alpha-ethinylestradiol cometabolism by bacteria degrading estrone, 17 beta-estradiol and estriol. Biodegradation 19, 683–693.

Purdom, C.E., Hardiman, P.A., Bye, V.J., Eno, N.C., Tyler, C.R., Sumpter, J.P., 1994. Estrogenic effects of effluents from sewage treatment works. Chem. Ecol. 8, 275–285.

Racz, L., Muller, J.G., Goel, R.K., 2012. Fate of selected estrogens in two laboratory scale sequencing batch reactors fed with different organic carbon sources under varying solids retention times. Bioresour. Technol. 110, 35–42.

148

Reddy, S., Iden, C.R., Brownawell, B.J., 2005. Analysis of steroid conjugates in sewage influent and effluent by liquid chromatography-tandem mass spectrometry. Anal. Chem. 77, 7032–7038.

Ren, Y.-X., Nakano, K., Nomura, M., Chiba, N., Nishimura, O., 2007. A thermodynamic analysis on adsorption of estrogens in activated sludge process. Water Res. 41, 2341–2348.

Rieger, L., Koch, G., Kuhni, M., Gujer, W., Siegrist, H., 2001. The EAWAG Bio-P module for activated sludge model No. 3. Water Res. 35, 3887–3903.

Routledge, E.J., Sumpter, J.P., 1996. Estrogenic activity of surfactants and some of their degradation products assessed using a recombinant yeast screen. Environ. Toxicol. Chem. 15, 241–248.

Salem, S., Moussa, M.S., van Loosdrecht, M.C.M., 2006. Determination of the decay rate of nitrifying bacteria. Biotechnol. Bioeng. 94, 252–262.

Schluesener, M.P., Bester, K., 2008. Behavior of steroid hormones and conjugates during wastewater treatment - A comparison of three sewage treatment plants. Clean-Soil Air Water 36, 25–33.

Servos, M.R., Bennie, D.T., Burnison, B.K., Jurkovic, A., McInnis, R., Neheli, T., Schnell, A., Seto, P., Smyth, S.A., Ternes, T.A., 2005. Distribution of estrogens, 17 beta-estradiol and estrone, in Canadian municipal wastewater treatment plants. Sci. Total Environ. 336, 155–170.

Shackleton, C., 1986. Profiling steroid-hormones and urinary steroids. J. Chromatogr. 379, 91–156.

Shi, J., Fujisawa, S., Nakai, S., Hosomi, M., 2004. Biodegradation of natural and synthetic estrogens by nitrifying activated sludge and ammonia-oxidizing bacterium Nitrosomonas europaea. Water Res. 38, 2323–2330.

Siegrist, H., Brunner, I., Koch, G., Phan, L.C., Le, V.C., 1999. Reduction of biomass decay rate under anoxic and anaerobic conditions. Water Sci. Technol. 39, 129–137.

Silva, C.P., Otero, M., Esteves, V., 2012. Processes for the elimination of estrogenic steroid hormones from water: A review. Environ. Pollut. 165, 38–58.

Smolders, G., Vandermeij, J., Vanloosdrecht, M., Heijnen, J., 1994. Stoichiometric model of the aerobic metabolism of the biological phosphorus removal process. Biotechnol. Bioeng. 44, 837–848.

Snyder, S.A., Villeneuve, D.L., Snyder, E.M., Giesy, J.P., 2001. Identification and quantification of estrogen receptor agonists in wastewater effluents. Environ. Sci. Technol. 35, 3620–3625.

Sokolovska, I., Rozenberg, R., Riez, C., Rouxhet, P.G., Agathos, S.N., Wattiau, P., 2003. Carbon source-induced modifications in the mycolic acid content and cell wall permeability of Rhodococcus erythropolis E1. Appl. Environ. Microbiol. 69, 7019–7027.

Suarez, S., Lema, J.M., Omil, F., 2010. Removal of pharmaceutical and personal care products (PPCPs) under nitrifying and denitrifying conditions. Water Res. 44, 3214–3224.

Tan, D.T., Arnold, W.A., Novak, P.J., 2013. Impact of organic carbon on the biodegradation of estrone in mixed culture systems. Environ. Sci. Technol. 47, 12359–12365.

Tchobanoglous, G., Stensel, H.D., Tsuchihashi, R., Burton, F., 2014. Wastewater Engineering: Treatment and Resource Recovery, Fifth Edition. New York: McGraw-Hill Education.

Ternes, T.A., Joss, A., Siegrist, H., 2004. Scrutinizing pharmaceuticals and personal care products in wastewater treatment. Environ. Sci. Technol. 38, 392A–399A.

149

Ternes, T.A., Kreckel, P., Mueller, J., 1999a. Behaviour and occurrence of estrogens in municipal sewage treatment plants - II. Aerobic batch experiments with activated sludge. Sci. Total Environ. 225, 91–99.

Ternes, T.A., Stumpf, M., Mueller, J., Haberer, K., Wilken, R.D., Servos, M., 1999b. Behavior and occurrence of estrogens in municipal sewage treatment plants - I. Investigations in Germany, Canada and Brazil. Sci. Total Environ. 225, 81–90.

Tetreault, G.R., Bennett, C.J., Shires, K., Knight, B., Servos, M.R., McMaster, M.E., 2011. Intersex and reproductive impairment of wild fish exposed to multiple municipal wastewater discharges. Aquat. Toxicol. 104, 278–290.

Thayanukul, P., Zang, K., Janhom, T., Kurisu, F., Kasuga, I., Furumai, H., 2010. Concentration-dependent response of estrone-degrading bacterial community in activated sludge analyzed by microautoradiography-fluorescence in situ hybridization. Water Res. 44, 4878–4887.

Urase, T., Kikuta, T., 2005. Separate estimation of adsorption and degradation of pharmaceutical substances and estrogens in the activated sludge process. Water Res. 39, 1289–1300.

Vajda, A.M., Barber, L.B., Gray, J.L., Lopez, E.M., Woodling, J.D., Norris, D.O., 2008. Reproductive disruption in fish downstream from an estrogenic wastewater effluent. Environ. Sci. Technol. 42, 3407–3414.

Van den Belt, K., Berckmans, P., Vangenechten, C., Verheyen, R., Witters, H., 2004. Comparative study on the in vitro in vivo estrogenic potencies of 17 beta-estradiol, estrone, 17 alpha-ethynylestradiol and nonylphenol. Aquat. Toxicol. 66, 183–195.

Vaneldere, J., Depauw, G., Eyssen, H., 1987. Steroid sulfatase activity in a Peptococcus-Niger strain from the human intestinal microflora. Appl. Environ. Microbiol. 53, 1655–1660.

Vaneldere, J., Parmentier, G., Asselberghs, S., Eyssen, H., 1991. Partial characterization of the steroidsulfatases in Peptococcus-Niger H4. Appl. Environ. Microbiol. 57, 69–76.

Vaneldere, J., Robben, J., Depauw, G., Merckx, R., Eyssen, H., 1988. Isolation and identification of intestinal steroid-desulfating bacteria from rats and humans. Appl. Environ. Microbiol. 54, 2112–2117.

Vega-Morales, T., Sosa-Ferrera, Z., Santana-Rodriguez, J.J., 2013. Evaluation of the presence of endocrine-disrupting compounds in dissolved and solid wastewater treatment plant samples of Gran Canaria Island (Spain). Biomed Res. Int. 790570.

Vethaak, A.D., Lahr, J., Schrap, S.M., Belfroid, A.C., Rijs, G.B.J., Gerritsen, A., de Boer, J., Bulder, A.S., Grinwis, G.C.M., Kuiper, R.V., Legler, J., Murk, T. a. J., Peijnenburg, W., Verhaar, H.J.M., de Voogt, P., 2005. An integrated assessment of estrogenic contamination and biological effects in the aquatic environment of The Netherlands. Chemosphere 59, 511–524.

Wick, L.Y., Wattiau, P., Harms, H., 2002. Influence of the growth substrate on the mycolic acid profiles of mycobacteria. Environ. Microbiol. 4, 612–616.

Woodling, J.D., Lopez, E.M., Maldonado, T.A., Norris, D.O., Vajda, A.M., 2006. Intersex and other reproductive disruption of fish in wastewater effluent dominated Colorado streams. Comp. Biochem. Physiol. Part C Toxicol. Pharmacol. 144, 10–15.

Xie, Y.-P., Fang, Z.-Q., Hou, L.-P., Ying, G.-G., 2010. Altered development and reproduction in western mosquitofish (Gambusia affinis) found in the Hanxi River, southern China. Environ. Toxicol. Chem. 29, 2607–2615.

150

Xu, K., Harper Jr, W.F., Zhao, D., 2008. 17α-Ethinylestradiol sorption to activated sludge biomass: Thermodynamic properties and reaction mechanisms. Water Res. 42, 3146–3152.

Xu, N., Johnson, A.C., Juergens, M.D., Llewellyn, N.R., Hankins, N.P., Darton, R.C., 2009. Estrogen concentration affects its biodegradation rate in activated sludge. Environ. Toxicol. Chem. 28, 2263–2270.

Yamada, T., Murooka, Y., Harada, T., 1978. Comparative immunological studies on arylsulfatase in bacteria of the family Enterobacteriaceae: Occurrence of latent arylsulfatase protein regulated by sulfur compounds and tyramine. J. Bacteriol. 133, 536–541.

Ye, X., Guo, X., Cui, X., Zhang, X., Zhang, H., Wang, M.K., Qiu, L., Chen, S., 2012. Occurrence and removal of endocrine-disrupting chemicals in wastewater treatment plants in the Three Gorges Reservoir area, Chongqing, China. J. Environ. Monit. 14, 2204–2211.

Yi, T., Harper, W.F., 2007. The link between nitrification and biotransformation of 17 alpha-ethinylestradiol. Environ. Sci. Technol. 41, 4311–4316.

Yoshimoto, T., Nagai, F., Fujimoto, J., Watanabe, K., Mizukoshi, H., Makino, T., Kimura, K., Saino, H., Sawada, H., Omura, H., 2004. Degradation of estrogens by Rhodococcus zopfii and Rhodococcus equi isolates from activated sludge in wastewater treatment plants. Appl. Environ. Microbiol. 70, 5283–5289.

Yu, C.-P., Roh, H., Chu, K.-H., 2007. 17 beta-estradiol-degrading bacteria isolated from activated sludge. Environ. Sci. Technol. 41, 486–492.

Zeng, Q., Li, Y., Gu, G., 2009. Nitrate-dependent degradation of 17 alpha-ethinylestradiol by acclimated activated sludge under anaerobic conditions. J. Chem. Technol. Biotechnol. 84, 1841–1847.

Zeng, Q., Li, Y., Yang, S., 2013. Sludge retention time as a suitable operational parameter to remove both estrogen and nutrients in an anaerobic-anoxic-aerobic activated sludge system. Environ. Eng. Sci. 30, 161–169.

Zhang, Z., Feng, Y., Gao, P., Wang, C., Ren, N., 2011. Occurrence and removal efficiencies of eight EDCs and estrogenicity in a STP. J. Environ. Monit. 13, 1366–1373.

Zheng, W., Li, X., Yates, S.R., Bradford, S.A., 2012. Anaerobic transformation kinetics and mechanism of steroid estrogenic hormones in dairy lagoon water. Environ. Sci. Technol. 46, 5471–5478.

Zhou, X., Oleszkiewicz, J.A., 2010. Biodegradation of oestrogens in nitrifying activated sludge. Environ. Technol. 31, 1263–1269.

Zhou, Y., Zha, J., Wang, Z., 2012. Occurrence and fate of steroid estrogens in the largest wastewater treatment plant in Beijing, China. Environ. Monit. Assess. 184, 6799–6813.

Ziels, R., 2013. Influence of kinetic and metabolic selection on 17α-ethinylestradiol biodegradation in activated sludge wastewater treatment systems (Master's thesis), University of Washington.

Appendix I: A Mechanistic Model for Fate and Removal of Estrogens in Biological Nutrient Removal Activated Sludge Systems

I.1 Abstract

Two estrogen fate and transformation models were integrated with a comprehensive activated sludge model (ASM) to predict estrogen removal based on biomass and solids production. Model predictions were evaluated against published full-scale plant data as well as results from a lab-scale sequencing batch reactor (SBR) fed synthetic wastewater. The estrogen fate model relating the rate of total estrogen degradation to soluble estrogen concentrations successfully predicted estrogen removals when compared to measured concentrations. Model fit 17α-ethinylestradiol (EE2) biodegradation rate constant was 19 to 43 percent of the estrone (E1) value and 31 to 72 percent of the 17β-estradiol (E2) value.

I.2 Introduction

Wastewater treatment plant (WWTP) effluents are a primary source of endocrine-disrupting compounds in the environment. The majority of their endocrine-disrupting activity is from anthropogenic estrogen compounds, including synthetic estrogen, 17α-ethinylestradiol (EE2), and the natural estrogens, estrone (E1) and 17β-estradiol (E2). Influent wastewater concentrations may be in the range of 50-200 $\mu g/m^3$, and there is a need to understand design and operating conditions that can lead to minimal effluent concentrations as significant endocrine disruptor effects on fish have been found at EE2 concentrations below 1 $\mu g/m^3$ (Purdom et al., 1994). Numerous literature sources show that estrogen biodegradation occurs in full-scale biological

nutrient removal (BNR) systems, but the removal efficiencies vary widely (10-98%), with EE2 being the most resistant to biodegradation and having the greatest endocrine disruptor activity (Combalbert and Hernandez-Raquet, 2010; Muller et al., 2010).

Two conceptual models for the fate and transformation of estrogens in activated sludge treatment have been proposed by Joss et al. (2004) and Urase and Kikuta (2005). Both conceptual models based estrogen removals on biodegradation and sorption to solids; however, Joss et al. proposed sorption and biodegradation may occur in parallel while Urase and Kikuta proposed these processes occur sequentially with sorption followed by biodegradation. Joss et al. also included cleavage of conjugated estrogens in their model resulting in production of free estrogens. Both Urase and Kikuta (2005) and Joss et al. (2004) applied the conceptual models to predict the fate of estrogens during batch experiments. In addition, Joss et al. modeled estrogen removals across full-scale WWTPs using Aquasim software. Integration of an estrogen fate model with a comprehensive activated sludge model (ASM) was performed by Monteith et al. (2008) using GPS-X software. Simulations predicted the fate of estrogens across a WWTP consisting of primary sedimentation and secondary activated sludge treatment (anaerobic, anoxic and aerobic bioreactors in series) and were based on estrogen biodegradation and sorption occurring in parallel. Biodegradation was modeled based on volatile suspended solids (VSS) concentrations.

In this paper, these modeling efforts have been extended by integrating estrogen removal mechanisms into a comprehensive ASM, which is important for two reasons. First, estrogen degraders are grown primarily on influent wastewater substrates as the amount of influent estrogen is too low to support a sufficient biomass to account for observed estrogen removal

rates. Second, the amount of estrogen removed by solids partitioning is a function of the solids produced from site specific influent wastewater characteristics and operating conditions. Therefore, the aim of this work was (1) a comparison of the reported conceptual models for estrogen removal based on the reported results of experimental studies, (2) review of kinetic expressions and parameter values for estrogen removal, and (3) development of a mechanistically-based mathematical model coupled with the IWA Activated Sludge Model No. 1 (ASM1) and its evaluation based on available data. An additional important advancement with this model effort is that the model accounts for the fact some of the estrogens in the influent wastewater can be in a conjugated form and deconjugation with the production of free estrogen can occur in the activated sludge process.

I.3 Methods

Model development

Removal of micropollutant compounds from the liquid phase can be achieved through four possible pathways: biotic and abiotic degradation, adsorption onto solids and volatilization to the gas phase. Due to physico-chemical properties of the estrogens, their removal mainly occurs by adsorption/biosorption onto activated sludge flocs and biodegradation. Biodegradation of E1, E2 and EE2 by activated sludge comprise degradation of E1 and EE2 to unknown products and oxidation of E2 to E1 (fully or partially, with the remaining to an unknown product). Two conceptual models based on sorption and biodegradation occurring either in parallel (Figure I-1a) or sequentially (Figure I-1b) were considered. Biodegradation based on the parallel model related total estrogen degradation rates to soluble estrogen concentrations while the sequential model related total estrogen degradation rates to sorbed estrogen concentrations. Cleavage of

154

conjugated estrogens to free estrogens was also incorporated in the estrogen fate model (but is
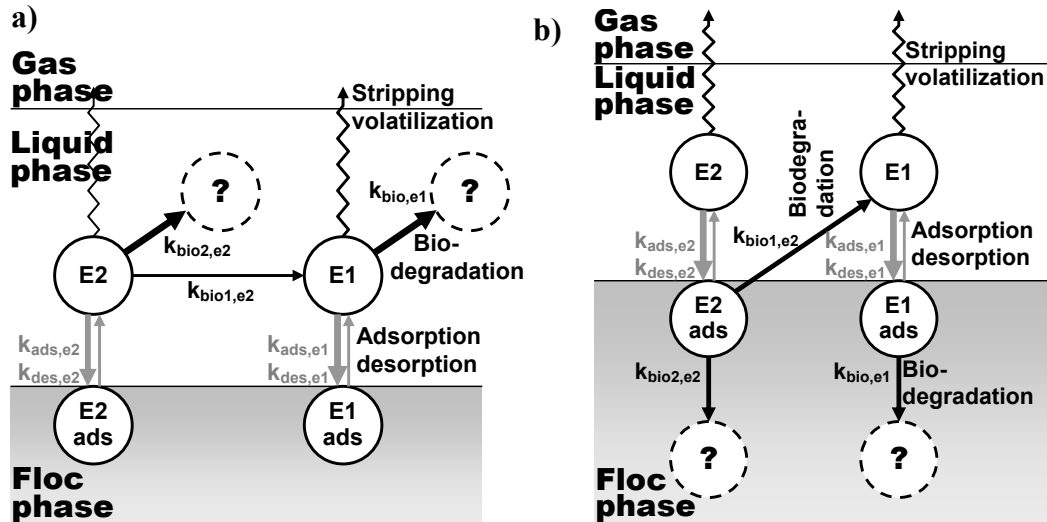
not shown in Figure I-1).

Figure I-1. Conceptual models of free estrogen (E1 and E2) removals in activated sludge systems based on (a) sorption and biodegradation occurring in parallel or (b) sorption and biodegradation occurring sequentially (EE2 model is similar to E1 except for not having any generation source)

The two conceptual models of the estrogen fate were written as a set of mathematical

expressions and implemented in the GPS-X simulation software as an expansion of the ASM1.

General kinetic expressions for the processes incorporated in the new models are presented in

Table I-1.

155

Table I-1. General kinetic expressions for the processes incorporated in the new models

Process	Parallel model
Cleavage	$k_{cle}S_{CE}X_H$
Adsorption	$k_{ads}\left(\dfrac{K_{S,a}}{K_{S,a}+S_S}\right)S_E X_{VSS}$
Desorption	$k_{des}\left(\dfrac{S_S}{K_{S,d}+S_S}\right)X_E X_{VSS}$
Aerobic biodegradation	$k_{bio}\left(\dfrac{K_{S,b}}{K_{S,b}+S_S}\right)\left(\dfrac{S_O}{K_O+S_O}\right)S_E X_H$
Anoxic biodegradation	$\eta_{bio}k_{bio}\left(\dfrac{K_{S,b}}{K_{S,b}+S_S}\right)\left(\dfrac{K_O}{K_O+S_O}\right)\left(\dfrac{S_{NO}}{K_{NO}+S_{NO}}\right)S_E X_H$

The equations for the sequential model are the same except for biodegradation where S_E is replaced by X_E.

Definitions for terms shown in Table I-1 are as follows: k_{cle} is the cleavage rate for conjugated estrogens (m^3/gCOD·d), S_{CE} is the conjugated estrogen concentration (μg/m^3), X_H is the active heterotrophic biomass concentration (gCOD/m^3), X_{VSS} is the volatile suspended solids concentration (g/m^3), S_S is the readily biodegradable substrate concentration (gCOD/m^3), S_E is the soluble estrogen concentration (μg/m^3), X_E is the sorbed estrogen concentration (μg/m^3), S_O is the dissolved oxygen concentration (gO$_2$/m^3), and S_{NO} is the sum of nitrite and nitrate concentrations (gN/m^3). All other terms are described in Table I-3.

Model calibration and validation

Model predictions were evaluated based on published data of a full-scale plant (Andersen et al., 2003) as well as our results from a lab-scale SBR. Descriptions of the WWTP and SBR operation and model calibration are provided below.

Full-scale WWTP in Wiesbaden (Germany). The total volume of the activated sludge bioreactor was 63,000 m^3 (1/3 and 2/3 occupied by the anoxic and aerobic compartments, respectively) and

156

the process temperature was 16-17 ºC. The influent flow rate to the WWTP was 66,000 m^3/d, whereas the return activated sludge (RAS) and mixed liquor recirculation (MLR) were about 50% and 200% of the inlet flow rate, respectively. During a 2-day measurement campaign, total estrogen concentrations were measured in samples of wastewater withdrawn as 24-h flow-proportional composite samples from the primary and secondary effluents. Sorbed and soluble estrogen concentrations were also measured in three grab samples withdrawn in the sampling points located inside the bioreactor including the anoxic zones (ANOX1 and ANOX2) and aerobic zone (AER2). The studied models were calibrated based on these measurements. The operating parameters (SRT, MLSS and WAS load) are presented in Figure I-2a. More information about the studied WWTP can be found in Andersen et al. (2003) and Joss et al. (2004). Conjugated estrogens were not measured during the sampling campaign and were therefore not modeled for the full-scale WWTP.

Lab-scale SBR at the University of Washington, Seattle (USA). A lab-scale SBR was operated at 20 ºC at a 10-day aerobic SRT (13-day total SRT) with four cycles per day. Each six hour cycle consisted of a one hour anoxic period followed by a 4.5 hour aeration period. Feeding occurred during the first five minutes of the anoxic period. Acetate, propionic acid, peptone and casein were the main components of the synthetic wastewater feed to which 330 μg/m^3 of E1 and E2 and 280 μg/m^3 of EE2 were added. No conjugated estrogens were added to the synthetic feed. Estrogen concentrations in the feed and effluent were measured in duplicate as described by Gaulke et al. (2008) using LC-MS-MS analysis. Following operation to steady state, an in situ estrogen degradation test was conducted where the SBR was spiked to an initial concentration of

157

200 µg/m^3 E1, E2 and EE2 and the total estrogen concentrations measured throughout the cycle. The data collected during this test were used for calibration of the studied models.

Simulation environment

GPS-X ver. 5.0.2 (Hydromantis, Canada) was used as a simulator environment for implementing the developed models and running simulations. For model calibration, a special utility called "Optimizer" was used (parameters were estimated based on the Nelder-Mead simplex method with the maximum likelihood as an objective function).

I.4 Results and Discussion

Full-scale WWTP

Figure I-2a shows the operating and effluent quality parameters and their predictions obtained with the calibrated ASM1 for the Wiesbaden WWTP (Andersen et al., 2003). Figure I-2b-d illustrates the parallel model results predicting E1, E2 and EE2 concentration profiles in both liquid and floc phases for the same full-scale plant data of Andersen et al. (2003). Predictions by Joss et al. (2004) based on the same sampling campaign have also been included. Predicted sorbed estrogen concentrations based on the parallel model were similar to measured values; however, predicted soluble estrogen concentrations in the second anoxic zone (ANOX2) were relatively high for both E1 and E2 (the model could not explain these discrepancies). Model results showed most of the estrogen removed was via biodegradation (>90%).
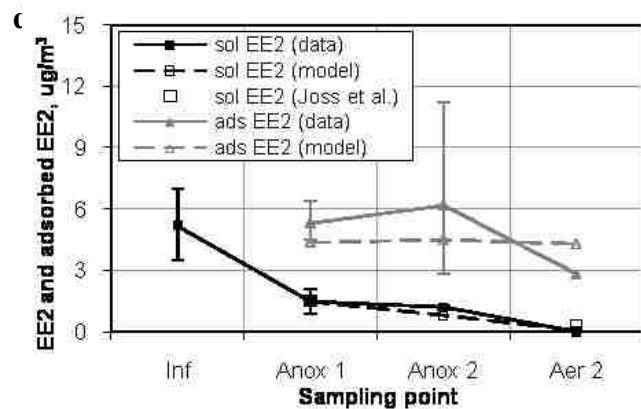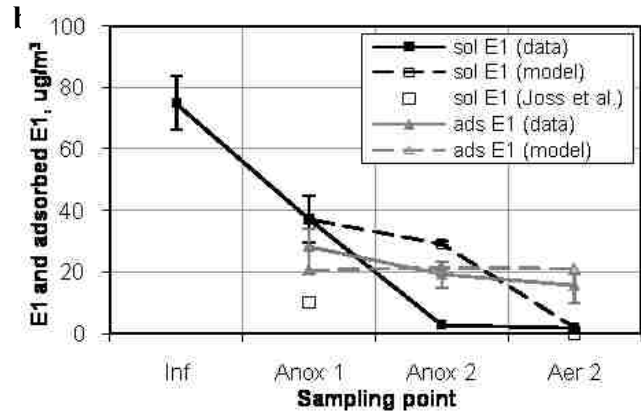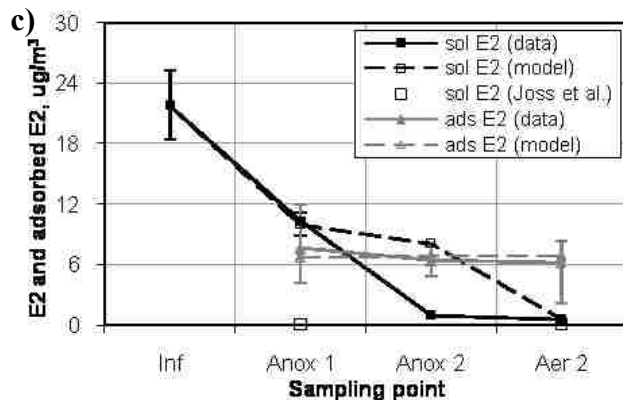
158

Figure I-2. Measured values versus steady-state model predictions for the published data from the Wiesbaden WWTP: (a) operating parameters and effluent concentrations and (b) E1, (c) E2 and (d) EE2 concentrations across the system. Soluble and sorbed estrogen concentrations are shown in black and gray, respectively. Measured values by Andersen et al. (2003) indicated by solid lines; predicted values based on parallel model indicated by dashed lines. Predictions of Joss et al. (2004) also shown for E1, E2 and EE2.

Figure I-3 compares the results from the calibrated estrogen fate models (parallel and sequential) for the Wiesbaden WWTP (Andersen et al., 2003). The two estrogen fate models produced similar predictions of soluble and sorbed E1, E2 and EE2 in the first anoxic zone (ANOX1) and aeration zone (AER2). However, the detailed analysis of mass balances revealed a different level of importance of the sorption process. For the sequential model, for which the mass balance is presented in Figure I-4b, the sorption rate is an order of magnitude higher compared to the parallel model (Figure I-4a).
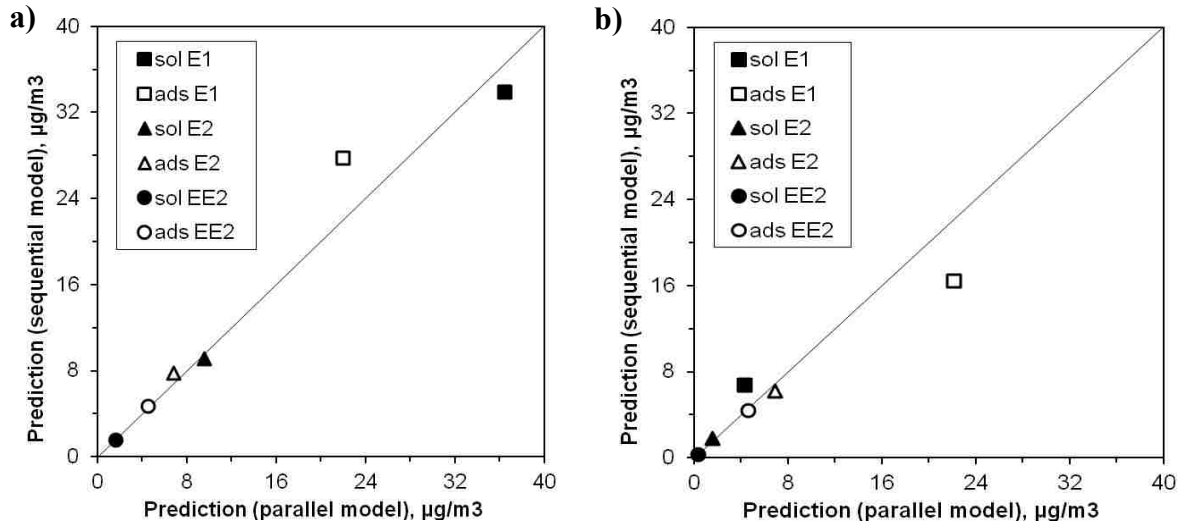
159

Figure I-3. Comparison of predicted estrogen concentrations in (a) the first anoxic zone (ANOX1) and (b) the aeration zone (AER2) of the Wiesbaden WWTP according to the sequential model versus the parallel model.
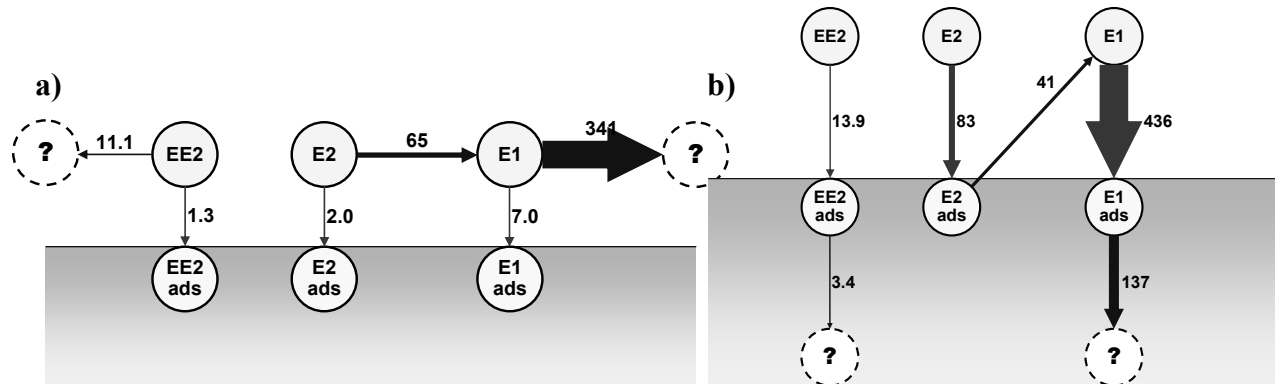

Figure I-4. Predicted estrogen mass flows ($\mu g/(m^3 \cdot d)$) in the first anoxic zone (ANOX1) of the Wiesbaden WWTP according to (a) the parallel model and (b) the sequential model.

Lab-scale SBR

Batch simulations of the in situ SBR estrogen degradation test using the same modelling parameters used for the full-scale WWTP with the exception of modified η_{bio} values are shown in Figure I-5 for the two estrogen models (parallel and sequential). The two models produced significantly different predictions. The parallel model provided the best fit to actual measurements and was therefore selected as the model to use for future simulations.
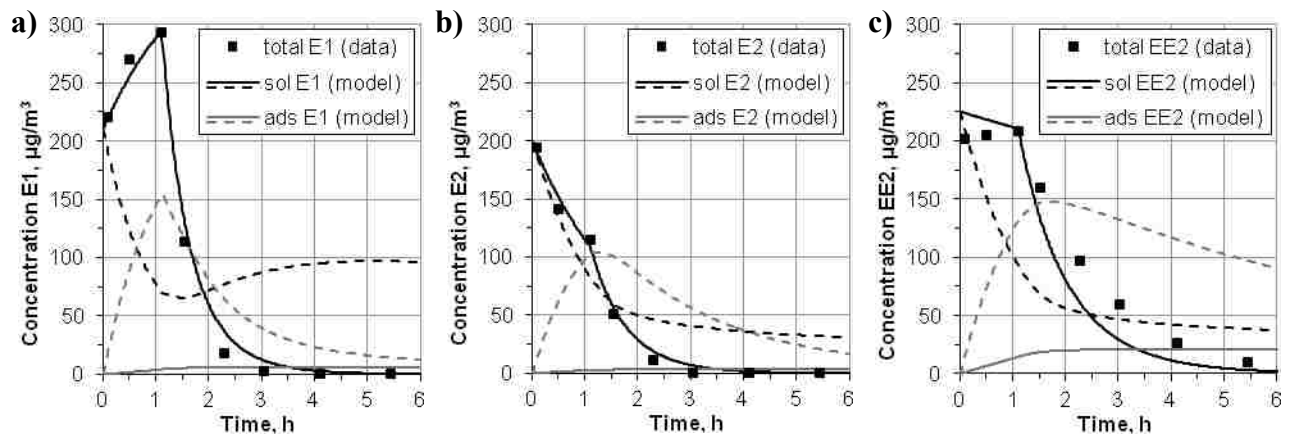
160

Figure I-5. Measured data versus model predictions for the anoxic/aerobic in situ SBR tests with one hour anoxic followed by 4.5 hours aeration: (a) E1, (b) E2, (c) EE2 (solid line – predictions of the parallel model, dashed line – predictions of the sequential model).

A dynamic SBR simulation was performed with the parallel model over ten days under steady-state operating conditions after which the estrogen feed concentrations were increased to model spiking of the in situ estrogen degradation test. Different estrogen modelling parameters were used for the dynamic SBR simulation than for the full-scale WWTP. The k_{ads}, k_{des} and $K_{S,a}$ values used for the full-scale WWTP resulted in predicted adsorbed estrogen concentrations being greater than the total measured estrogen concentrations when applied to the lab-scale SBR. The operating and effluent quality parameters and their predictions based on the dynamic SBR simulation are shown in Table I-2. Figure I-6 shows the modeled estrogen performance of the SBR along with the data from the in situ estrogen degradation test. A mass balance on model predictions showed biodegradation accounted for over 97 percent of the fate of the incoming estrogens.

www.manaraa.com

Table I-2. Comparison of measured versus predicted operating parameters for lab-scale anoxic/aerobic SBR. Measured data (± one standard deviation) taken from period of one SRT prior to in situ estrogen degradation test.

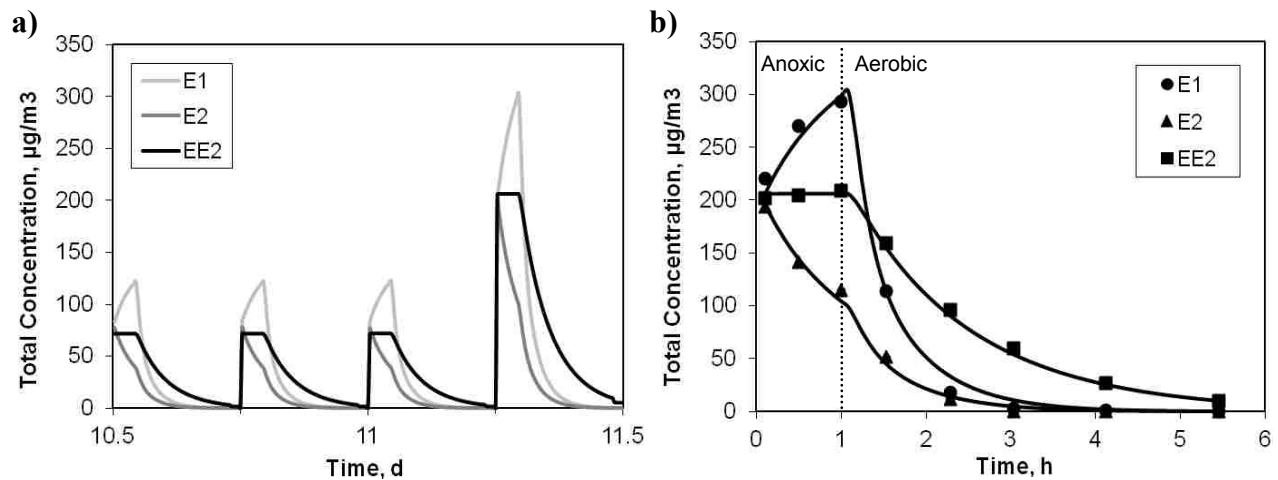| Parameter	Unit	Data	Prediction
Aerobic SRT	d	10	10
MLSS	g/m^3	1185 ± 61	1193
MLVSS	g/m^3	1056 ± 54	1062
Effluent quality			
NH_4-N	gN/m^3	<1	<1
NO_3-N	gN/m^3	10.8 ± 3.4	10.7

Adjusted parameter: $b_H = 0.28$ d^{-1}

Figure I-6. Modeled estrogen performance of SBR (a) after 10 days of dynamic simulation followed by an increase in estrogen feed concentration to simulate estrogen spiking of the in situ estrogen degradation test (b) fitted to measured data. Markers correspond to estrogen measurements taken after spiking SBR to initial concentration of 200 µg/m^3. Solid lines indicate predicted estrogen concentrations based on selection of k$_{bio}$ values to fit in situ estrogen degradation test measurements.

Modelling Parameters

Table I-3 lists the values used in the simulations conducted on both the Wiesbaden WWTP and

lab-scale SBR. The only temperature dependent parameter was the biodegradation rate constant,

k$_{bio}$, and the temperature correction factor, θ, was set to 1.03 for k$_{bio}$.

162

Table I-3. List of kinetic parameters and their values at T = 20 °C in the ASM1 extension for modeling estrogen removal (parallel model)

Symbol	Definition	Unit	Wiesbaden WWTP[*]			Lab-scale SBR		
			E1	E2	EE2	E1	E2	EE2
k_{ads}	Adsorption rate constant	$m^3/(g \cdot d)$	0.0048	0.0053	0.002	0.021	0.021	0.021
k_{des}	Desorption rate constant	$m^3/(g \cdot d)$	0.0002	0.0002	0.0002	0.044	0.044	0.044
$K_{S,a}$	Substrate half-saturation constant for adsorption	$gCOD/m^3$	10	10	10	1000	1000	1000
$K_{S,d}$	Substrate half-saturation constant for desorption	$gCOD/m^3$	0	0	0	0	0	0
$K_{S,b}$	Substrate half-saturation constant for biodegradation	$gCOD/m^3$	1000	1000	1000	1000	1000	1000
k_{bio}	Biodegradation rate constant	$m^3/(gCOD \cdot d)$	0.077	0.046	0.033	0.126	0.078	0.024
η_{bio}	Anoxic factor for biodegradation	-	0.19	0.29	0.5	0	0.24	0
K_O	Oxygen half-saturation constant for biodegradation	gO_2/m^3	0.2	0.2	0.2	0.2	0.2	0.2
K_{NO}	Nitrate half-saturation constant for biodegradation	gN/m^3	0.1	0.1	0.1	0.1	0.1	0.1

[*] - the simulations were run at T = 16.5 °C

Fitting of the model to estrogen measurements from the lab-scale SBR in situ degradation test resulted in k_{bio} coefficients (normalized to biomass concentration) of 0.126, 0.078 and 0.024 $m^3/(gCOD \cdot d)$ for E1, E2 and EE2, respectively. A lower but similar EE2 k_{bio} value of 0.020 $m^3/(gCOD \cdot d)$ was determined based on fitting the model to measured EE2 effluent concentrations prior to spiking the SBR for the in situ test. All k_{bio} values were based on a 1:1 conversion of E2 to E1. Partial conversion of E2 to E1 would reduce the production of E1 and result in a lower estimated E1 k_{bio} value.

Adsorption and desorption rate constants of 0.021 m^3/g-d and 0.044 m^3/g-d were applied to all estrogens for the lab-scale SBR model, achieving sorption near equilibrium within 0.5 hours and reaching an equilibrium solid/liquid partitioning (K_D) coefficient of 0.45 m^3/kg VSS within five hours. This is in agreement with Andersen et al. (2005) who showed E1, E2 and EE2 sorption to

163

activated sludge reached near equilibrium within 0.5 hours with K_D coefficients of 0.40, 0.48 and 0.58 m^3/kg solids, respectively.

Selection of $K_{S,a}$ of 10 gCOD/m^3 for the Wiesbaden WWTP simulations effectively reduced the adsorption rates by greater than 70 percent. Predicted solid/liquid partitioning (m^3/kg solids) of estrogens in the first anoxic zone (ANOX1) were 0.2, 0.3 and 1.0 for E1, E2 and EE2, respectively. These respective values increased to 1.9, 1.6 and 4.8 in the aeration zone (AER2). For the lab-scale SBR simulations, predicted solid/liquid partitioning (m^3/kg solids) of estrogens during the anoxic cycle ranged from 0.03 to 0.3 for E1, 0.03 to 0.5 for E2 and 0.04 to 0.4 for EE2. During the aerobic cycle, these respective values increased to 1.7, 1.5 and 0.6 m^3/kg solids. Reported equilibrium solid/liquid partitioning coefficients (m^3/kg solids), given as 95 percent confidence intervals, are 0.40 ± 0.13 for E1, 0.48 ± 0.19 for E2 and 0.58 ± 0.14 for EE2 (Andersen et al., 2005). Greatest deviation from equilibrium was predicted during aerobic treatment when estrogen concentrations were low and biodegradation rates were high indicating adsorption and desorption rates are important in predicting estrogen partitioning under these conditions.

Conjugated estrogens were not modeled for the full-scale WWTP as these were not measured during the WWTP sampling campaign by Andersen et al. (2003). Sampling of WWTPs in Germany showed conjugated estrogens comprised up to 50 percent of the total influent steroids (Adler et al., 2001). Therefore, larger k_{bio} values would likely have been used in the model had production of free estrogens from deconjugation been included for the full-scale WWTP.

Model limitations and future research needs

Simulations conducted with the estrogen fate and transformation model highlighted many areas needing additional research. Model limitations and future research needs are summarized below.

- Estrogen degrader kinetics – An understanding of variations in estrogen degrading populations and kinetics due to different activated sludge process designs is needed to model biodegradation.

- Sorption and desorption rates – Sorption and desorption rates are needed to accurately model estrogen removals due to solids sorption.

- Substrate inhibition – Presence of readily biodegradable substrates may reduce sorption sites and/or binding sites of enzymes available to the estrogens. The model currently has the ability to account for substrate inhibition of both sorption and biodegradation, however, substrate half-saturation constants are unknown.

- Deconjugation rates – Continuation of research addressing cleavage rates of conjugated estrogens under different operating conditions will lead to improvements in modelling production of free estrogens from deconjugation.

- Conversion fraction of E2 to E1 – Knowledge of the fraction of E2 removed via oxidation to E1 is needed to appropriately model the production and fate of E1.

- Temperature effects – A better understanding of the effects of temperature on sorption/desorption, biodegradation and deconjugation rates are needed to appropriately use the temperature correction factors included in the model.

- Calibration and WWTP sampling – Calibration of the model to a WWTP would require measurements of both free and conjugated estrogens at multiple points along the

165

treatment train, preferably between staged reactors. Dynamic simulations would also require multiple samples to be taken over the course of a day. The feasibility associated with this sampling demand requires development of a careful sampling protocol.

I.5 Conclusions

Two estrogen fate and transformation models based on sorption and biodegradation occurring either in parallel or sequentially were integrated into the IWA ASM1. Both models were applied to published full-scale plant data as well as results from a lab-scale SBR, and the parallel model was selected as providing the best fit to measured estrogen concentrations. This model may also be applied for predicting the fate and removal of other micropollutants. Although this modeling effort lays a foundation for a prediction tool that may be used to evaluate different scenarios to optimize estrogen removals, many limitations of the model need to be addressed with further research.

Acknowledgements

166

Appendix II: Equation for Estrogen Biodegradation during Exponential Growth

Estrogen biodegradation during exponential growth was described in Chapter 5, "Degradation, Inhibition, and Transposome Mutagenesis Experiments with an EE2-degrading Isolate," by Equation 2 as follows:

$$\frac{dE_T}{dt} = \frac{-k_b E_T X_o e^{\mu t}}{1 + K_P X_o e^{\mu t}}$$

The differential equation was solved using separation of variables.

$$\int_{E_T=E_{T,o}}^{E_T=E_{T,t}} \frac{1}{E_T} dE_T = \int_{t=0}^{t=t} \frac{-k_b X_o e^{\mu t}}{1 + K_P X_o e^{\mu t}} dt$$

The following substitutions were made,

$$u = 1 + K_P X_o e^{\mu t}$$
$$du = K_P X_o \mu e^{\mu t} dt$$

resulting in the integrals:

$$\int_{E_T=E_{T,o}}^{E_T=E_{T,t}} \frac{1}{E_T} dE_T = \int_{u=1+K_P X_o}^{u=1+K_P X_o e^{\mu t}} \frac{-k_b}{K_P \mu} \frac{1}{u} du$$

Integration produces the solution:

$$ln|E_T|\Big|_{E_T=E_{T,o}}^{E_T=E_{T,t}} = \frac{-k_b}{K_P \mu} ln|u|\Big|_{u=1+K_P X_o}^{u=1+K_P X_o e^{\mu t}}$$

$$ln|E_{T,t}| - ln|E_{T,o}| = \frac{-k_b}{K_P \mu}(ln|1 + K_P X_o e^{\mu t}| - ln|1 + K_P X_o|)$$

$$ln\left|\frac{E_{T,t}}{E_{T,o}}\right| = \frac{-k_b}{K_P \mu} ln\left|\frac{1 + K_P X_o e^{\mu t}}{1 + K_P X_o}\right|$$

167

$$ln\left|\frac{E_{T,t}}{E_{T,o}}\right| = ln\left(\left|\frac{1 + K_P X_o e^{\mu t}}{1 + K_P X_o}\right|^{-\frac{k_b}{K_P \mu}}\right)$$

$$\left|\frac{E_{T,t}}{E_{T,o}}\right| = \left|\frac{1 + K_P X_o e^{\mu t}}{1 + K_P X_o}\right|^{-\frac{k_b}{K_P \mu}}$$

The absolute value signs are not needed since $E_{T,t}$, $E_{T,o}$, K_P, and X_o are all greater than zero, resulting in the following solution:

$$E_{T,t} = E_{T,o}\left(\frac{1 + K_P X_o e^{\mu t}}{1 + K_P X_o}\right)^{-\frac{k_b}{K_P \mu}}$$